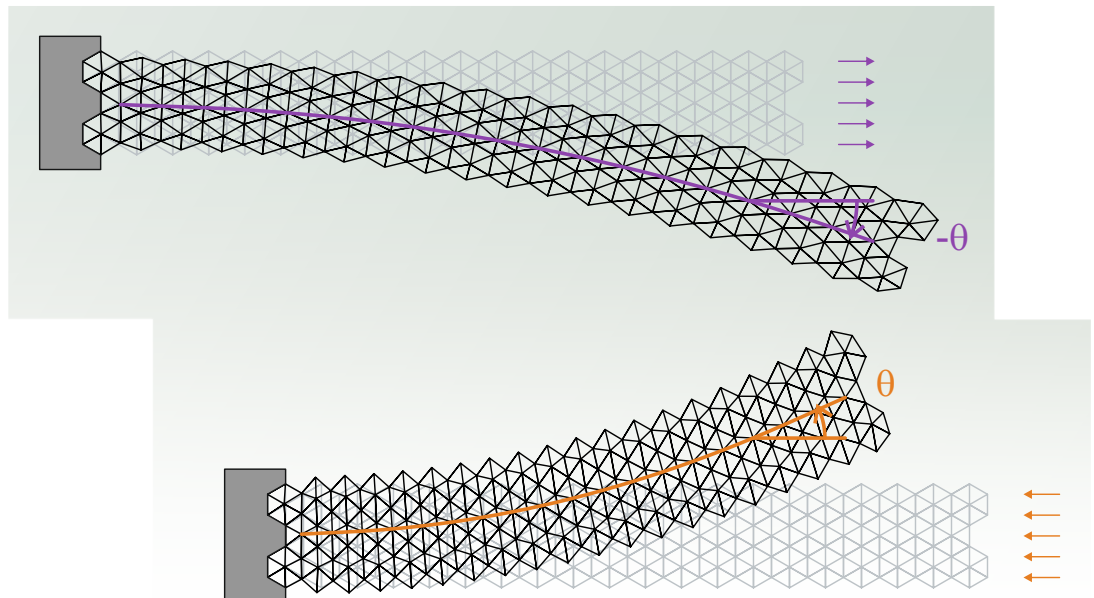
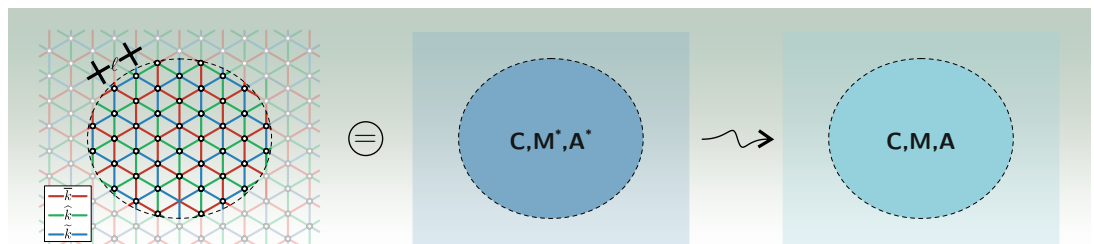


Gianluca Rizzi

Strain-gradient effects in the discrete/continuum transition via homogenization





Doctoral School in Civil, Environmental and Mechanical Engineering
Topic 3. Modelling and Simulation - XXXI cycle 2015/2018

Doctoral Thesis - March 2019

Gianluca Rizzi

Strain-gradient effects in
the discrete/continuum transition
via homogenization

Supervisors

Prof. Davide Bigoni, University of Trento
Dr. Francesco Dal Corso, University of Trento



Except where otherwise noted, contents on this book are licensed under a Creative
Common Attribution - Non Commercial - No Derivatives
4.0 International License

University of Trento
Doctoral School in Civil, Environmental and Mechanical Engineering
<http://web.unitn.it/en/dricam>
Via Mesiano 77, I-38123 Trento
Tel. +39 0461 282670 / 2611 - dicamphd@unitn.it

Declaration of Authorship

I, Gianluca RIZZI, declare that this thesis titled, “Strain-gradient effects in the discrete/continuum transition via homogenization” and the work presented in it are my own. I confirm that:

- This work was done wholly or mainly while in candidature for a research degree at this University.
- Where any part of this thesis has previously been submitted for a degree or any other qualification at this University or any other institution, this has been clearly stated.
- Where I have consulted the published work of others, this is always clearly attributed.
- Where I have quoted from the work of others, the source is always given. With the exception of such quotations, this thesis is entirely my own work.
- I have acknowledged all main sources of help.
- Where the thesis is based on work done by myself jointly with others, I have made clear exactly what was done by others and what I have contributed myself.

Signed:

Date:

"It is during our darkest moments that we must focus to see the light."

Aristotle

UNIVERSITY OF TRENTO

Abstract

Department of Civil, Environmental and Mechanical Engineering (DICAM)

Doctor of Philosophy

Strain-gradient effects in the discrete/continuum transition via homogenization

by Gianluca RIZZI

A second-gradient elastic material has been identified as the equivalent homogeneous material of an hexagonal lattice made up of three different orders of linear elastic bars (hinged at each junction). In particular, the material equivalent to the lattice exhibits: (i.) non-locality, (ii.) non-centrosymmetry, and (iii.) anisotropy (even if the hexagonal geometry leads to isotropy at first-order). A Cauchy elastic equivalent solid is only recovered in the limit of vanishing length of the lattice's bars. The identification of the second-gradient elastic material is complemented by analyses of positive definiteness and symmetry of the constitutive operators. Solutions of specific mechanical problems in which the lattice response is compared to the corresponding response of an equivalent boundary value problem for the homogeneous second-gradient elastic material are presented. These comparisons show the efficacy of the proposed identification procedure.

Acknowledgements

I would like to express my most sincere gratitude to my advisors, Prof. Davide Bigoni and Dr. Francesco Dal Corso, whose enthusiasm as well as their contribution in stimulating suggestions, encouragement and remarks, helped me to throughout all my Ph.D..

I am grateful to all my colleagues, the wonderful Costanza, I do not want to imagine how my Ph.D. would have been without her; Diana and Gabriel, we started together and we will finish together, what a great story; Giovanni, Nicola, Alessandro, Marco, Andrea, Mirko and L.K. for the unforgettable discussions, those series and those less but all beautiful; thanks also to Alice, Ilaria, both Luigi, Riccardo, Piotr and all the people that worked at my department in these years. A special thanks for Dr. Diego Misseroni, for guiding me throughout the meanders of teaching and supporting me with his expertise as well as with his irony.

Last but certainly not the least, my biggest and deepest gratitude goes to C.d. Ing. Dr. Daniele Veber for his immeasurable support. It has been a privilege as well as a great pleasure to have the possibility to work with him.

Finally, I am particularly indebted to my family and all my friends for supporting me and been my relief.

Support from the ERC Advanced Grant “Instabilities and non-local multiscale modelling of materials” 340561-FP7-PEOPLE-IDEAS-ERC-2013-AdG (2014-2019) is gratefully acknowledged.

Published papers

The main results presented in this thesis have been summarized in the following papers:

- 1) G. Rizzi, D. Veber, F. Dal Corso and D. Bigoni, “Homogenisation of planar hexagonal lattices yields a Mindlin elastic material. Part I: Analytical expressions for the identified equivalent model”, (*In preparation*).
- 2) G. Rizzi, D. Veber, F. Dal Corso and D. Bigoni, “Homogenisation of planar hexagonal lattices yields a Mindlin elastic material. Part II: Properties and capability of the identified equivalent model”, (*In preparation*).
- 3) G. Rizzi, D. Veber, F. Dal Corso and D. Bigoni, “Extreme non-local materials from hexagonal lattice structures”, (*In preparation*).

Contents

Declaration of Authorship	iii
Abstract	vii
Acknowledgements	ix
1 Introduction	1
2 Strain gradient elasticity formulation	5
2.1 Constitutive equation	7
2.2 Derivation of transformation matrices	8
3 Second-gradient material equivalent to the lattice structure	11
3.1 Preliminaries: the periodic structure and its elastic equilibrium	11
3.2 Definition of an average operator for the displacement gradient	14
3.3 Second-order displacement boundary condition	16
3.4 Identification of the higher-order solid equivalent to the lattice structure	22
3.5 Energy stored in the lattice structure	23
3.6 Energy stored in a second-gradient elastic solid	24
3.7 The equivalent second-gradient material	27
3.8 A note on the quadratic displacement condition.	29
4 Derivation of the constitutive law for the equivalent SGE	33
4.1 The equivalent second-gradient elastic material	33
4.2 From the solid in the ‘condensed form’ to the full SGE: symmetries and positive definiteness	34
4.3 Anisotropy characterization	38
4.3.1 Isotropy of the first-order equivalent material \mathbf{C}	38
4.3.2 The condensed transformation matrix and the characterization of \mathbf{M}^* and \mathbf{A}^*	38
4.3.3 Anisotropy characterization of \mathbf{M}^*	39
4.3.4 Anisotropy characterization of \mathbf{A}^*	40
4.3.5 Isotropic and centrosymmetric second-gradient equivalent ma- terial	40
4.4 The directional properties of the elastic energy for the SGE material . .	41
4.5 Positive definiteness	43
4.5.1 Variation of the elastic energy with the characteristic length. . .	44
4.6 Derivation of the constitutive law for the equivalent second-gradient elastic material	46
5 Capability of the SGE solid to be equivalent to the hexagonal lattice	47
5.1 Simple shear problem	48
5.1.1 Simple shear parallel to the x_1 -axis	50
5.1.2 Simple shear parallel the x_2 -axis	52

5.2	Uniaxial strain problem	53
5.2.1	Uniaxial strain parallel to the x_2 -axis	54
5.2.2	Uniaxial strain parallel to the x_1 -axis	56
5.2.3	An example of extreme reticular structures far from a Cauchy solid	57
5.2.4	A remark on non-centro-symmetric behaviour	59
6	Conclusions	61
A	Components of the matrices $H^{[r]}$ and $G^{[r]}$	63
	Bibliography	77

List of Figures

1.1	(Left) The considered planar lattice obtained as the periodic repetition of an hexagonal unit cell (with side length ℓ) made up of linear elastic bars, characterized by three stiffnesses \bar{k} (red bars), \hat{k} (green bars), and \tilde{k} (blue bars). Reference systems are also reported. (Right) Explosion of the hexagonal lattice highlighting how the perimeter nodes connect adjacent cells.	1
2.1	Three-dimensional continuum body with volume Ω , boundary $\partial\Omega$ and edge $\partial\partial\Omega$ subjected to body forces (F_k), traction (P_k), double-traction (R_k) and edge forces (E_k).	5
2.2	(left) Normal to the surface and (right) decomposition of the variation $\delta u_{k,j}$ towards the normal to the surface.	6
3.1	Hexagonal lattice (left) and its exploded drawing, highlighting the definitions of the cells (right), which correspond to the representative volume elements (RVEs) of an equivalent continuum. The red, green and blue bars have stiffness \bar{k} , \hat{k} and \tilde{k} , respectively.	12
3.2	Resultant forces $\mathbf{R}^{(m,n i)}$ (left) and corrective displacements $\Delta \mathbf{u}^{(m,n i)}$ (right) associated with the node i belonging to the cell $\{m,n\}$ within the lattice drawn in its undeformed configuration.	18
3.3	(Upper part) Deformed configuration for a lattice with bars of stiffness $\bar{k} = \hat{k} = 10\tilde{k}$ subject to (left) a purely linear displacement condition with $\{\alpha_{11}, \alpha_{22}, \alpha_{12}\} = \{0, 0, 1/5\}$, (center) its corrective field, and (right) the sum of these two. (Lower part) As in the upper part, but for a purely quadratic displacement condition with $\{\beta_{111}, \beta_{221}, \beta_{112}, \beta_{222}, \beta_{211}^{\text{lat}}, \beta_{122}^{\text{lat}}\} = \{-1, 1, 1, -1, 1, 1\}1/(80\ell)$	22
3.4	Nonlocal constitutive parameters M_{13}^* (left) and M_{14}^* (right) as functions of the bar stiffness ratios \hat{k}/\bar{k} and \tilde{k}/\bar{k} . The red lines represent the stiffness ratios pairs for which a centrosymmetric response is attained, while in all the other cases the solid equivalent to the hexagonal bars' lattice displays a non-centrosymmetric mechanical behaviour.	30
3.5	Nonlocal constitutive parameters M_{13}^* (left) and M_{14}^* (right) as functions of the bar stiffness ratios \hat{k}/\bar{k} and \tilde{k}/\bar{k} . The red lines represent the stiffness ratios pairs for which a centrosymmetric response is attained, while in all the other cases the solid equivalent to the hexagonal bars' lattice displays a non-centrosymmetric mechanical behaviour.	31

4.1	The second-gradient elastic material in the ‘condensed form’ (center) characterized by the matrices \mathbf{C} , \mathbf{M}^* , and \mathbf{A}^* (identified in Part I of this study) as the solid energetically equivalent to the hexagonal lattice microstructure (left) with elastic bars characterized by the three values of axial stiffness \bar{k} , \tilde{k} and \hat{k} (distinguished through different colours). The second-gradient elastic material (right) characterized by matrices \mathbf{C} , \mathbf{M} , and \mathbf{A} obtained from a relaxation of the solid in the ‘condensed form’.	35
4.2	Polar diagrams of the curvature energy density $\mathcal{U}_{\mathbf{A}^*}$ stored within a ‘condensed’ SGE material, equivalent to a lattice with stiffness bar ratios $\hat{k}/\bar{k} = 10$, $\tilde{k}/\bar{k} = 100$, when subject to a specific curvature input $\mathbf{q}^{*[j]}$ ($j = 1, \dots, 4$), Eq. (4.38). The diagrams show the $\pi/3$ symmetry (green coloured curve part) in the constitutive response related to curvature through the matrix \mathbf{A}^* . The energy density with varying the rotation angle θ of the related kinematic input $\mathbf{q}^{*[j]}$ ($j = 1, \dots, 4$) is reported along the radial coordinate normalized through division by its maximum value.	41
4.3	As for Fig. 4.2, but for the total energy density $\mathcal{U}_{\text{SGE}^*}$ considering the specific kinematic input $\mathbf{t}^{*[j]}$ ($j = 1, \dots, 7$), Eq. (4.43). The diagrams show different periodicity in the response: the $2\pi/3$ symmetry in the mutual constitutive response for $\mathbf{t}^{*[1]}$, $\mathbf{t}^{*[2]}$, and $\mathbf{t}^{*[3]}$, the $\pi/3$ symmetry in the curvature only constitutive response, as evident for $\mathbf{t}^{*[4]}$, $\mathbf{t}^{*[5]}$ as counterpart of kinematic input $\mathbf{q}^{*[2]}$, $\mathbf{q}^{*[4]}$, and the <i>isotropic</i> behaviour, provided by the symmetry in Cauchy constitutive response, for null curvature inputs $\mathbf{t}^{*[6]}$ and $\mathbf{t}^{*[7]}$.	43
4.4	The values of bar stiffnesses corresponding to a positive definite equivalent second-gradient elastic material correspond to the green zone; in the red zone the equivalent material is indefinite.	44
4.5	Parameter \mathcal{R} , Eq. (4.45) versus the ratio ρ/ℓ for non-null components of the tensor β given by $\beta_{222} = -\beta_{112} = -\beta_{211} = 1$. Curves are reported for different pairs of stiffness bars ratio $\{\hat{k}/\bar{k}, \tilde{k}/\bar{k}\}$, given by $\{4.5, 3.5\}$ (green), $\{5, 0.2\}$ (purple) and $\{10, 0.1\}$ (orange).	45
5.1	Upper row from left to right: Undeformed lattice and equivalent SGE material; simple shear parallel to the horizontal direction; uniaxial strain in the vertical direction. Lower row from left to right: Undeformed lattice and equivalent SGE material; simple shear parallel to the vertical direction; uniaxial strain in the horizontal direction. The deformed configurations for the lattice are displayed for the three bars having the same stiffness, $\hat{k}/\bar{k} = \tilde{k}/\bar{k} = 1$.	47
5.2	Simple shear aligned parallel the x_1 -axis. From left to right: Deformed configuration, displacement field $u_1(x_2)$, and strain energy density $\mathcal{U}(x_2)$ for the three cases Ex1 (upper part), Ex2 (central part), and Ex3 (lower part) as defined in Table 5.1. Mechanical fields within the equivalent Cauchy and SGE solids are reported as dashed and purple lines, respectively, while the values averaged within the lattice (at the same coordinate x_2) are reported as yellow dots.	52

5.3	From top to bottom: deformed configuration, displacement field $u_2(x_1)$, and strain energy density $\mathcal{U}(x_1)$ for the stiffness ratios Ex1, Ex2, and Ex3 as defined by Table 5.1 from left to right. In purple it is portrayed the solution for the SGE material, in black-dashed the solution for a classic Cauchy material, and the yellow dots the quantities related to the lattice.	53
5.4	Uniaxial strain aligned parallel to the x_2 -axis. From left to right: Deformed configuration, displacement field $u_2(x_2)$, and strain energy density $\mathcal{U}(x_2)$ for the three stiffness ratios Ex1, Ex4, and Ex5 defined in Table 5.1 from top to bottom. In purple it is portrayed the solution for the SGE material, in black-dashed the solution for a classic Cauchy material, and the yellow dots the quantities related to the lattice.	56
5.5	Uniaxial strain aligned parallel to the x_1 -axis. From top to bottom: Deformed configuration, displacement field $u_1(x_1)$, and strain energy density \mathcal{U} for the three stiffness ratios corresponding to Ex1, Ex4, and Ex5 defined in Table 5.1 (from left to right). In purple it is portrayed the solution for the SGE material, in black-dashed the solution for a classic Cauchy material, and the yellow dots the quantities related to the lattice.	57
5.6	From top to bottom: deformed configuration, displacement field $u_1(x_1)$, displacement field $u_2(x_1)$, and strain energy density $\mathcal{U}(x_1)$ for the following stiffness bars ratios $\tilde{k}/\bar{k} = \{1, 2.5 \cdot 10^4, 5 \cdot 10^4\}$. In purple it is portrayed the solution for the SGE material, in black-dashed the solution for a classic Cauchy material, and the yellow dots the quantities related to the lattice.	58
5.7	Deformed configurations and dimensionless transversal displacement $u_2(x_1)/U_1$ for lattice (and corresponding equivalent SGE solid) of properties Ex5 and Ex6 (one is the permutation in the non-perimeter springs of the other, Table 5.1) subject to compressive ($U_1 < 0$) and tensile ($U_1 > 0$) uniaxial strain aligned parallel to the x_1 -axis. Different geometries are reported, $H = \{4\sqrt{3} + 1/2, 8\sqrt{3} + 1/2, 16\sqrt{3} + 1/2\}\ell$. . .	60

List of Tables

5.1	The six stiffness ratios pairs \hat{k}/\bar{k} and $\hat{\bar{k}}/\bar{k}$ and the corresponding equivalent constitutive parameters μ , λ , m_{13} , a_{11} , a_{22} , a_{33} , and a_{44} (made dimensionless through division by the bar stiffness \bar{k}) used for the comparisons reported in Figs. 5.2-5.5.	48
5.2	Errors in the energy matching and in the resultant shear force between the lattice and the equivalent Cauchy solid and the equivalent strain-gradient solid for the simple shear problem parallel to x_1 and x_2 axis considering stiffness ratios Ex1, Ex2, and Ex3 as defined by Table 5.1. .	50
5.3	Errors in the energy matching and in the resultant normal force between the lattice and the equivalent Cauchy solid and the equivalent strain-gradient solid for the uniaxial problem parallel to x_1 and x_2 axis considering stiffness ratios Ex1, Ex4, and Ex5 as defined by Table 5.1. .	54
5.4	Evaluation of the discrepancy between the dimensionless energy of both the equivalent Cauchy (U_{Cau}) and the equivalent second-gradient elastic (U_{SGE}) solids and the dimensionless energy of the lattice (U_{lat}) for the two uniaxial problems.	59

To my Mother and my Brother.

Chapter 1

Introduction

An hexagonal lattice of linearly elastic bars with three different stiffnesses (as shown in Fig. 1.1) is analyzed in the present thesis, with the aim of identifying an equivalent, homogeneous elastic material.

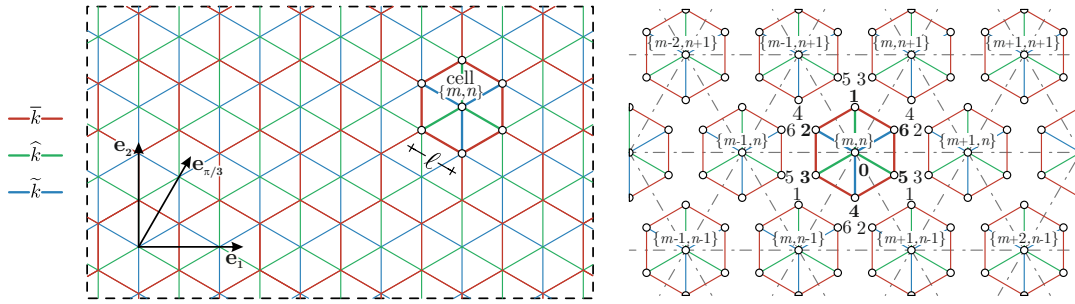


FIGURE 1.1: (Left) The considered planar lattice obtained as the periodic repetition of an hexagonal unit cell (with side length ℓ) made up of linear elastic bars, characterized by three stiffnesses \bar{k} (red bars), \hat{k} (green bars), and \tilde{k} (blue bars). Reference systems are also reported. (Right) Explosion of the hexagonal lattice highlighting how the perimeter nodes connect adjacent cells.

Research on the equivalence between spring networks and continuous bodies initiates with Cauchy [18] and was refined by Born [16], to determine the elastic properties of a crystalline solid subject to small strain. Here, the interactions between atoms are treated as linear, so that the solid is modelled as a three-dimensional linear elastic lattice, where the elements are subject to purely axial deformation. This is the so-called ‘Cauchy–Born Rule’, which yields the ‘rari-constant’ theory of elasticity, relating the elastic property of a solid to the interactions between its atoms or molecules.

Over the years, mechanical characteristics such as the Young modulus, Poisson’s ratio and normal modes of vibration have been evaluated for a number of geometrically different networks [21, 24, 25, 27, 35]. With reference to the hexagonal lattice considered in the present thesis (Fig. 1.1), Day et al. [20, 40] have shown that the overall behaviour of the lattice may be modelled as an equivalent isotropic Cauchy linear elastic solid with elastic bulk and shear moduli, respectively K and μ , given by

$$K = \frac{1}{\sqrt{12}} (\bar{k} + \hat{k} + \tilde{k}), \quad \mu = \sqrt{\frac{27}{16}} \left(\frac{1}{\bar{k}} + \frac{1}{\hat{k}} + \frac{1}{\tilde{k}} \right)^{-1} \quad (1.1)$$

where \bar{k} , \hat{k} and \tilde{k} are the stiffnesses of the three lattice bars.

Our goal is to generalize the theory developed by Day et al. [20, 40], to show that at an higher-order of approximation the elastic material equivalent to the hexagonal lattice displays nonlocal effects that can be related to the properties of the bars forming the lattice, which, in a sense, represents a micro-scale.

Phenomenological constitutive models, used to model materials of engineering relevance, are usually local, or in other words, lack an internal characteristic length. Mechanical behaviours at the micro- and nano-scale, shown as size-effects in experiments [14, 17, 26, 44, 45] cannot be described by local constitutive models, so that they fail when large strain gradient are involved, as when shear band are formed [19, 22, 23, 30, 31, 34, 39].

Various authors [1, 2, 7, 8, 9, 10, 11, 12, 28, 36, 37, 38, 41, 43] have proposed non-classical continuum model to describe the behaviour of non-simple lattice structures, namely, involving beam-type interactions. The non-local effects in these models emerge as the response to non simple interactions between material points, generated, for example when rotational springs are used [42].

The second gradient elastic (**SGE**) model proposed by Mindlin [32, 33] is presented in *Chapter 2*, introducing the constitutive equations, kinematic entities and their static conjugate quantities. The balance equations and the boundary conditions are derived via principle of virtual work, within a linear theory framework. The constitutive law is definite through tensors \mathbf{C} (local component), \mathbf{M} (non-centrosymmetric component), and \mathbf{A} (purely curvature non-local component) and their symmetry properties are addressed. These tensors are also represented in a matrix form by using the Voigt notation.

In *Chapter 3*, the infinite hexagonal lattice shown in Fig. 1.1 is investigated. The bars composing the unit cell are pinned to each other and characterised by three different values of stiffness. Closed-form expressions are derived for the properties of an homogeneous second-gradient elastic material (**SGE**) equivalent to the lattice. These are obtained through an energy match under boundary conditions representing a generic (but self-equilibrated) quadratic displacement field. As related to the constraint of having a self-equilibrated boundary conditions, only a ‘condensed form’ of the constitutive tensor is defined. It is noted that the ‘self-equilibrated’ constraint can be interpreted as a lack of a sufficient number of independent tests to characterise a standard strain gradient elastic material.

The homogenization technique shows that the equivalent material displays non-local behaviour, anisotropy and non-centrosymmetry, even if the first-order homogenization, leading to the constants Eqs. (1.1) play these effects. The equivalent material is shown to lack of positive definiteness of the elastic energy for certain values of the bar’s stiffnesses (\hat{k}/\bar{k} and \tilde{k}/\bar{k}) and this lack of positive definiteness is analyzed in detail. The developed elastic model always reduces to the isotropic Cauchy material defined by the constants Eqs. (1.1) when the internal characteristic lengths are set to zero.

In *Chapter 4*, the simplest approach is proposed to extrapolate from the ‘condensed form’ of the equivalent material a standard **SGE** material, which corresponds to imposing from the beginning the equivalence between the elastic energies of the lattice and of the equivalent material, thus neglecting the equilibrium constraint. The proposed approach preserves the symmetry properties of the ‘condensed’ material and leaves its positive definiteness domain unchanged.

In *Chapter 5*, a comparison is provided between lattice structures (subject to overall conditions of simple shear and uniaxial strain), which can be analytically solved with Mathematica and their equivalent material counterparts, for which analytical

solutions have been derived. It is shown that the lattice structures and their continuous counterparts behave in excellent agreement, a result which provides a validation to our homogenization technique.

Finally, conclusions of this thesis are drawn in *Chapter 6*.

Chapter 2

Strain gradient elasticity formulation

The equilibrium equation for a strain gradient material can be obtained by using the Principle of Virtual Work as shown in [32]. In Mindlin theory the work done by the

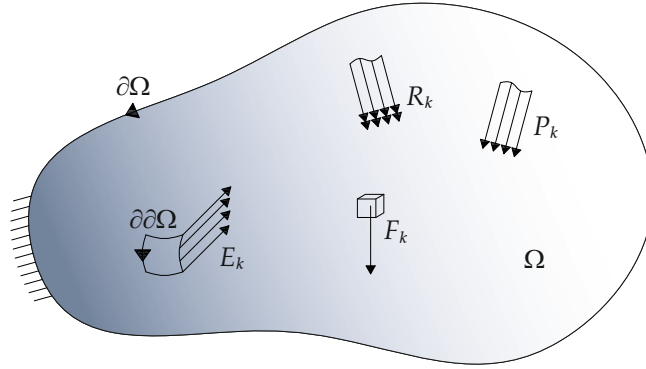


FIGURE 2.1: Three-dimensional continuum body with volume Ω , boundary $\partial\Omega$ and edge $\partial\partial\Omega$ subjected to body forces (F_k), traction (P_k), double-traction (R_k) and edge forces (E_k).

internal forces (W^i) is a function of both the strain (ϵ_{jk}) and the curvature (χ_{ijk}):

$$W^i = W^i(\epsilon_{jk}, \chi_{ijk}), \quad (2.1)$$

where

$$\epsilon_{jk} = \frac{1}{2}(u_{k,j} + u_{j,k}) \quad \text{and} \quad \chi_{ijk} = u_{k,ij} \text{ (Form I)}. \quad (2.2)$$

In the *Form I* the curvature is taken as the second gradient of the displacement. The stress (σ_{jk}) and the double stress (τ_{ijk}) are respectively conjugate with the strain and the curvature as

$$\sigma_{jk} = \frac{\partial W^i}{\partial \epsilon_{jk}} \quad \text{and} \quad \tau_{ijk} = \frac{\partial W^i}{\partial \chi_{ijk}}. \quad (2.3)$$

The internal work and his first variation in a domain Ω are:

$$W^i = \int_{\Omega} (\sigma_{jk}\epsilon_{jk} + \tau_{ijk}\chi_{ijk}) dV, \quad (2.4)$$

$$\delta W^i = \int_{\Omega} (\sigma_{jk}\delta\epsilon_{jk} + \tau_{ijk}\delta\chi_{ijk}) dV = \int_{\Omega} (\sigma_{jk}\delta u_{k,j} + \tau_{ijk}\delta u_{k,ij}) dV. \quad (2.5)$$

It is possible to rewrite the two term on the right side of Eq. (2.5) as:

$$\sigma_{jk}\delta u_{k,j} = (\sigma_{jk}\delta u_k)_{,j} - \sigma_{jk,j}\delta u_k, \quad (2.6)$$

$$\tau_{ijk} \delta u_{k,ij} = (\tau_{ijk} \delta u_{k,j})_{,i} - \tau_{ijk,i} \delta u_{k,j}. \quad (2.7)$$

The second term on the right side of Eq. (2.7) can be written as:

$$\tau_{ijk,i} \delta u_{k,j} = (\tau_{ijk,i} \delta u_k)_{,j} - \tau_{ijk,ij} \delta u_k. \quad (2.8)$$

It is now possible to rewrite the Eq. (2.5) as:

$$\delta W^i = \int_{\Omega} \left([(\sigma_{jk} - \tau_{ijk,i}) \delta u_k]_{,j} - (\sigma_{jk} - \tau_{ijk,i})_{,j} \delta u_k + (\tau_{ijk} \delta u_{k,j})_{,i} \right) dV. \quad (2.9)$$

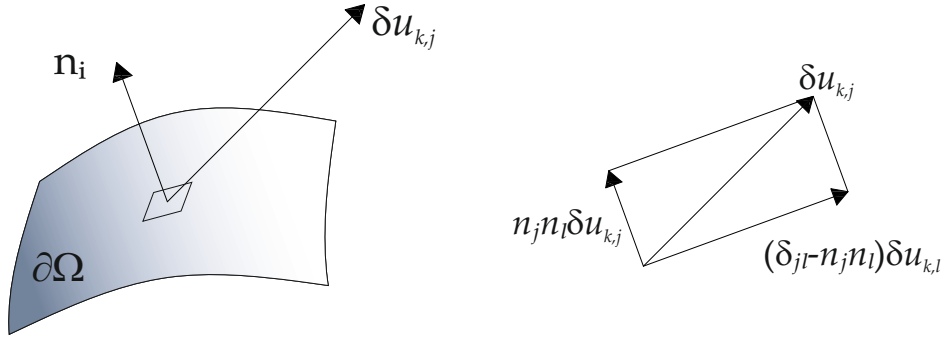


FIGURE 2.2: (left) Normal to the surface and (right) decomposition of the variation $\delta u_{k,j}$ towards the normal to the surface.

Applying directly the divergence theorem it is possible to rewrite the first and the third term of the Eq. (2.9):

$$\delta W^i = \int_{\partial\Omega} n_j (\sigma_{jk} - \tau_{ijk,i}) \delta u_k dS - \int_{\Omega} (\sigma_{jk} - \tau_{ijk})_{,j} \delta u_k dV + \int_{\partial\Omega} n_i \tau_{ijk} \delta u_{k,j} dS. \quad (2.10)$$

The variation $\delta u_{k,j}$ in the latter term on the right of the Eq. (2.10) is not independent of the virtual displacement δu_k , but its normal component. The components of $\delta u_{k,j}$ are:

$$\delta u_{k,j} = [\delta u_{k,j} - (n_\ell \delta u_{k,\ell}) n_j] + (n_\ell \delta u_{k,\ell}) n_j = (\delta_{jl} - n_j n_\ell) \delta u_{k,\ell} + n_j n_\ell \delta u_{k,\ell}. \quad (2.11)$$

Calling

$$D_j(\cdot) = (\delta_{jl} - n_j n_\ell)(\cdot)_{,\ell} \quad \text{and} \quad D(\cdot) = n_\ell(\cdot)_{,\ell}, \quad (2.12)$$

it is possible to rewrite the latter term of the Eq. (2.10):

$$n_i \tau_{ijk} \delta u_{k,j} = n_i \tau_{ijk} D_j(\delta u_k) + n_i \tau_{ijk} n_j D(\delta u_k). \quad (2.13)$$

The first term on the right side of the Eq. (2.13) can be written as:

$$n_i \tau_{ijk} D_j(\delta u_k) = D_j(n_i \tau_{ijk} \delta u_k) - n_i D_j(\tau_{ijk}) \delta u_k - D_j(n_i) \tau_{ijk} \delta u_k, \quad (2.14)$$

and the first term on the right side of Eq. (2.14) can be written as:

$$D_j(n_i \tau_{ijk} \delta u_k) = D_\ell(n_\ell) n_j n_i \tau_{ijk} \delta u_k + n_q e_{qpm} (e_{mlj} n_\ell n_i \tau_{ijk} \delta u_k)_{,p}. \quad (2.15)$$

The second term on the right side of Eq. (2.15), on $\partial\Omega$, is zero if the surface $\partial\Omega$ is smooth. If the surface $\partial\Omega$ has an edge $\partial\partial\Omega$, formed by the intersection of $\partial\Omega_1$ and $\partial\Omega_2$ (two portion of $\partial\Omega$), then:

$$\int_{\partial\Omega} n_q e_{qpm} (e_{mlj} n_\ell n_i \tau_{ijk} \delta u_k) , p \, dS = \oint_{\partial\partial\Omega} \llbracket n_i m_j \tau_{ijk} \rrbracket \delta u_k \, ds. \quad (2.16)$$

The double brackets indicate that the enclosed quantity is the difference between the value on $\partial\Omega_1$ and $\partial\Omega_2$.

Considering that:

$$n_j \tau_{ijk,i} = n_j D_i (\tau_{ijk}) + n_i n_j D (\tau_{ijk}) , \quad (2.17)$$

it is finally possible to write:

$$\begin{aligned} \delta W^i = & - \int_{\Omega} (\sigma_{jk} - \tau_{ijk,i})_{,j} \delta u_k dV \\ & + \int_{\partial\Omega} [n_j \sigma_{jk} - n_i n_j D (\tau_{ijk}) - 2n_j D_i (\tau_{ijk}) + (n_i n_j D_\ell n_\ell - D_j n_i) \tau_{ijk}] \delta u_k dS \\ & + \int_{\partial\Omega} n_i n_j \tau_{ijk} D (\delta u_k) dS + \oint_{\partial\partial\Omega} \llbracket n_i m_j \tau_{ijk} \rrbracket \delta u_k ds, \end{aligned} \quad (2.18)$$

where $m_j = e_{mlj} s_m n_\ell$ and s_m in the unit vector tangent to $\partial\partial\Omega$

The work of external forces is accordingly:

$$\delta W^e = \int_{\Omega} F_k \delta u_k dV + \int_{\partial\Omega} P_k \delta u_k dS + \int_{\partial\Omega} R_k D (\delta u_k) dS + \oint_{\partial\partial\Omega} E_k \delta u_k ds, \quad (2.19)$$

where

$$\begin{aligned} F_k &= \text{body forces per unit volume,} \\ P_k &= \text{traction per unit area,} \\ R_k &= \text{double traction per unit area,} \\ E_k &= \text{line load along sharp edge.} \end{aligned} \quad (2.20)$$

Since the internal work as to be equal to the external work on Ω , $\partial\Omega$ and $\partial\partial\Omega$ independently and for every variation δu_k and $D (\delta u_k)$, we obtain the following stress-equation and the boundary condition:

$$\begin{aligned} (\sigma_{jk} - \tau_{ijk,i})_{,j} + F_k &= 0 & \text{in } V \\ \sigma_{jk} n_j + n_i n_j D (\tau_{ijk}) - 2n_j D_i (\tau_{ijk}) + (n_i n_j D_\ell n_\ell - D_j n_i) \tau_{ijk} &= P_k & \text{on } S \\ n_i n_j \tau_{ijk} &= R_k & \text{on } S \\ \llbracket n_i m_j \tau_{ijk} \rrbracket &= E_k & \text{on } C \end{aligned} \quad (2.21)$$

2.1 Constitutive equation

The strain energy is chosen to be a quadratic form written as

$$\mathcal{U}_{\text{SGE}} (\epsilon, \chi) = \frac{1}{2} \mathbb{E}_{ijkl} \epsilon_{ij} \epsilon_{kl} + \frac{1}{2} \mathbb{A}_{ijklmn} \chi_{ijk} \chi_{lmn} + \mathbb{M}_{ijkmn} \chi_{ijk} \epsilon_{mn} \quad (2.22)$$

where \mathbb{E} is the classic constitutive 4th order tensor, \mathbb{A} is a constitutive 6th order tensor linked only to the curvature and \mathbb{M} is a 5th order tensor which takes into account the mixed energy (non-centrosymmetric) due to the coupling between the strain and the curvature.

The stress and the double stress can be expressed as:

$$\sigma_{jk} = \frac{\partial U(\epsilon, \chi)}{\partial \epsilon_{jk}} = \mathbb{E}_{ijkl} \epsilon_{ij} + \mathbb{M}_{ijkmn} \chi_{ijk}, \quad (2.23)$$

$$\tau_{ijk} = \frac{\partial U(\epsilon, \chi)}{\partial \chi_{ijk}} = \mathbb{A}_{ijklmn} \chi_{ijk} + \mathbb{M}_{ijkmn} \epsilon_{mn}. \quad (2.24)$$

From these equations we can deduce the following symmetries

$$\begin{aligned} \mathbb{E}_{ijkl} &= \mathbb{E}_{jikl} = \mathbb{E}_{ijlk} = \mathbb{E}_{klij}, \\ \mathbb{A}_{ijklmn} &= \mathbb{A}_{jiklmn} = \mathbb{A}_{ijkmln} = \mathbb{A}_{lmnijk}, \\ \mathbb{M}_{ijkmn} &= \mathbb{M}_{jikmn} = \mathbb{M}_{ijmkn}. \end{aligned} \quad (2.25)$$

2.2 Derivation of transformation matrices

Using the orthogonal matrix \mathbf{D} to introduce a rotation or reflection of a reference system, the transformations for the components of strain ϵ_{ij} and curvature tensors χ_{ijk} are

$$\epsilon_{ij}^{\#} = \epsilon_{kl} D_{ik} D_{jl}, \quad \chi_{ijk}^{\#} = \chi_{lmn} D_{il} D_{jm} D_{kn}. \quad (2.26)$$

and $\mathbf{D}\mathbf{D}^T = \mathbf{D}^T\mathbf{D} = \mathbf{I}$. The reflection \mathbf{S} and rotation $\mathbf{R}(\theta)$ restricted to a two-dimensional space are

$$\mathbf{S} = \begin{pmatrix} 1 & 0 \\ 0 & -1 \end{pmatrix}, \quad \mathbf{R} = \begin{pmatrix} c(\theta) & -s(\theta) \\ s(\theta) & c(\theta) \end{pmatrix}, \quad (2.27)$$

with $s(\theta) = \sin \theta$ and $c(\theta) = \cos \theta$. Condensing the transformation matrices into higher-dimension tensors in Eqs. (2.26) it is possible to write

$$\epsilon_{ij}^{\#} = \epsilon_{kl} \tilde{D}_{ikjl}, \quad \chi_{ijk}^{\#} = \chi_{lmn} \hat{D}_{iljmn}. \quad (2.28)$$

In order to obtain more manageable expressions, the two tensors \tilde{D} and \hat{D} will be expressed in a matrix form [3, 4]. In order to do that, it is necessary to collect the strain and the curvature tensors in vectors as follow

$$\mathbf{p}^{\diamond} = \begin{bmatrix} \epsilon_{11} \\ \epsilon_{22} \\ \epsilon_{12} \\ \epsilon_{12} \end{bmatrix}, \quad \mathbf{q}^{\diamond} = \begin{bmatrix} \chi_{111} \\ \chi_{221} \\ \chi_{112} \\ \chi_{222} \\ \chi_{211} \\ \chi_{122} \\ \chi_{211} \\ \chi_{122} \end{bmatrix}. \quad (2.29)$$

Giving the specific order of the strain and the curvature components in Eqs. (2.29), the matrix form of \tilde{D} and \hat{D} results to be

$$\tilde{\mathbf{D}}^\diamond = \begin{pmatrix} \begin{array}{cc|cc} \tilde{\mathbf{D}}_{1111} & \tilde{\mathbf{D}}_{1212} & \tilde{\mathbf{D}}_{1112} & \tilde{\mathbf{D}}_{1211} \\ \tilde{\mathbf{D}}_{2121} & \tilde{\mathbf{D}}_{2222} & \tilde{\mathbf{D}}_{2122} & \tilde{\mathbf{D}}_{2221} \\ \hline \tilde{\mathbf{D}}_{1121} & \tilde{\mathbf{D}}_{1222} & \tilde{\mathbf{D}}_{1122} & \tilde{\mathbf{D}}_{1221} \\ \tilde{\mathbf{D}}_{2111} & \tilde{\mathbf{D}}_{2212} & \tilde{\mathbf{D}}_{2112} & \tilde{\mathbf{D}}_{2211} \end{array} \end{pmatrix}$$

$$\hat{\mathbf{D}}^\diamond = \begin{pmatrix} \begin{array}{cccc|cc|cc} \hat{\mathbf{D}}_{111111} & \hat{\mathbf{D}}_{121211} & \hat{\mathbf{D}}_{111112} & \hat{\mathbf{D}}_{121212} & \hat{\mathbf{D}}_{121111} & \hat{\mathbf{D}}_{111212} & \hat{\mathbf{D}}_{111211} & \hat{\mathbf{D}}_{121112} \\ \hat{\mathbf{D}}_{212111} & \hat{\mathbf{D}}_{222211} & \hat{\mathbf{D}}_{212112} & \hat{\mathbf{D}}_{222212} & \hat{\mathbf{D}}_{222111} & \hat{\mathbf{D}}_{212212} & \hat{\mathbf{D}}_{212211} & \hat{\mathbf{D}}_{222112} \\ \hat{\mathbf{D}}_{111121} & \hat{\mathbf{D}}_{121221} & \hat{\mathbf{D}}_{111122} & \hat{\mathbf{D}}_{121222} & \hat{\mathbf{D}}_{121121} & \hat{\mathbf{D}}_{111222} & \hat{\mathbf{D}}_{111221} & \hat{\mathbf{D}}_{121122} \\ \hat{\mathbf{D}}_{212121} & \hat{\mathbf{D}}_{222221} & \hat{\mathbf{D}}_{212122} & \hat{\mathbf{D}}_{222222} & \hat{\mathbf{D}}_{222121} & \hat{\mathbf{D}}_{212222} & \hat{\mathbf{D}}_{212221} & \hat{\mathbf{D}}_{222122} \\ \hline \hat{\mathbf{D}}_{211111} & \hat{\mathbf{D}}_{221211} & \hat{\mathbf{D}}_{211112} & \hat{\mathbf{D}}_{221212} & \hat{\mathbf{D}}_{221111} & \hat{\mathbf{D}}_{211212} & \hat{\mathbf{D}}_{211211} & \hat{\mathbf{D}}_{221112} \\ \hat{\mathbf{D}}_{112121} & \hat{\mathbf{D}}_{122221} & \hat{\mathbf{D}}_{112122} & \hat{\mathbf{D}}_{122222} & \hat{\mathbf{D}}_{122121} & \hat{\mathbf{D}}_{112222} & \hat{\mathbf{D}}_{112221} & \hat{\mathbf{D}}_{122122} \\ \hline \hat{\mathbf{D}}_{112111} & \hat{\mathbf{D}}_{122211} & \hat{\mathbf{D}}_{112112} & \hat{\mathbf{D}}_{122212} & \hat{\mathbf{D}}_{122111} & \hat{\mathbf{D}}_{112212} & \hat{\mathbf{D}}_{112211} & \hat{\mathbf{D}}_{122112} \\ \hat{\mathbf{D}}_{211121} & \hat{\mathbf{D}}_{221221} & \hat{\mathbf{D}}_{211122} & \hat{\mathbf{D}}_{221222} & \hat{\mathbf{D}}_{221121} & \hat{\mathbf{D}}_{211222} & \hat{\mathbf{D}}_{211221} & \hat{\mathbf{D}}_{221122} \end{array} \end{pmatrix}$$

and Eqs. (2.26) can be written in the following matrix form

$$\mathbf{p}_i^\diamond = \tilde{\mathbf{D}}_{ij}^\diamond \mathbf{p}_j^\diamond, \quad \mathbf{q}_i^\diamond = \hat{\mathbf{D}}_{ij}^\diamond \mathbf{q}_j^\diamond. \quad (2.30)$$

Introducing now the Voigt notation, the vector \mathbf{p}^\diamond and \mathbf{q}^\diamond will be condensed as follow

$$\mathbf{p} = \begin{bmatrix} \epsilon_{11} \\ \epsilon_{22} \\ 2\epsilon_{12} \end{bmatrix}, \quad \mathbf{q} = \begin{bmatrix} \chi_{111} \\ \chi_{221} \\ \chi_{112} \\ \chi_{222} \\ 2\chi_{211} \\ 2\chi_{122} \end{bmatrix} \quad (2.31)$$

while the matrices $\tilde{\mathbf{D}}^\diamond$ and $\hat{\mathbf{D}}^\diamond$ are reduced as follow

$$\mathbf{D}_{[\mathbf{p}]} = \begin{pmatrix} \tilde{\mathbf{A}}^\diamond & \frac{\tilde{\mathbf{B}}^\diamond + \tilde{\mathbf{C}}^\diamond}{2} \\ \tilde{\mathbf{D}}^\diamond + \tilde{\mathbf{E}}^\diamond & \frac{\tilde{\mathbf{F}}^\diamond + \tilde{\mathbf{G}}^\diamond + \tilde{\mathbf{H}}^\diamond + \tilde{\mathbf{I}}^\diamond}{2} \end{pmatrix}, \quad \mathbf{D}_{[\mathbf{q}]} = \begin{pmatrix} \hat{\mathbf{A}}^\diamond & \frac{\hat{\mathbf{B}}^\diamond + \hat{\mathbf{C}}^\diamond}{2} \\ \hat{\mathbf{D}}^\diamond + \hat{\mathbf{E}}^\diamond & \frac{\hat{\mathbf{F}}^\diamond + \hat{\mathbf{G}}^\diamond + \hat{\mathbf{H}}^\diamond + \hat{\mathbf{I}}^\diamond}{2} \end{pmatrix}. \quad (2.32)$$

where the colours are introduced in order to explain in an easy and visual way how to perform the contraction.

The dimensions of $\mathbf{D}_{[\mathbf{p}]}$ is 3×3 while that of $\mathbf{D}_{[\mathbf{q}]}$ is 6×6 . These transformation matrices will be taken in the following to coincide respectively with $\mathbf{S}_{[\mathbf{p}]}$ or $\mathbf{R}_{[\mathbf{p}]}$ and

$\mathbf{S}_{[\mathbf{q}]}$ or $\mathbf{R}_{[\mathbf{q}]}$ defined as

$$\mathbf{S}_{[\mathbf{p}]} = \begin{pmatrix} 1 & 0 & 0 \\ 0 & 1 & 0 \\ 0 & 0 & -1 \end{pmatrix}, \quad \mathbf{S}_{[\mathbf{q}]} = \begin{pmatrix} 1 & 0 & 0 & 0 & 0 & 0 \\ 0 & 1 & 0 & 0 & 0 & 0 \\ 0 & 0 & -1 & 0 & 0 & 0 \\ 0 & 0 & 0 & -1 & 0 & 0 \\ 0 & 0 & 0 & 0 & -1 & 0 \\ 0 & 0 & 0 & 0 & 0 & 1 \end{pmatrix}, \quad \mathbf{R}_{[\mathbf{p}]}(\theta) = \begin{pmatrix} c^2(\theta) & s^2(\theta) & -c(\theta)s(\theta) \\ s^2(\theta) & c^2(\theta) & c(\theta)s(\theta) \\ s(2\theta) & -2c(\theta)s(\theta) & c(2\theta) \end{pmatrix},$$

$$\mathbf{R}_{[\mathbf{q}]}(\theta) = \begin{pmatrix} c^3(\theta) & s^2(\theta)c(\theta) & -s(\theta)c^2(\theta) & -s^3(\theta) & -s(\theta)c^2(\theta) & s^2(\theta)c(\theta) \\ s^2(\theta)c(\theta) & c^3(\theta) & -s^3(\theta) & -s(\theta)c^2(\theta) & s(\theta)c^2(\theta) & -s^2(\theta)c(\theta) \\ s(\theta)c^2(\theta) & s^3(\theta) & c^3(\theta) & s^2(\theta)c(\theta) & -s^2(\theta)c(\theta) & -s(\theta)c^2(\theta) \\ s^3(\theta) & s(\theta)c^2(\theta) & s^2(\theta)c(\theta) & c^3(\theta) & s^2(\theta)c(\theta) & s(\theta)c^2(\theta) \\ 2s(\theta)c^2(\theta) & -2s(\theta)c^2(\theta) & -2s^2(\theta)c(\theta) & s(\theta)s(2\theta) & (c(\theta) + c(3\theta))/2 & (s(\theta) - s(3\theta))/2 \\ s(\theta)s(2\theta) & -2s^2(\theta)c(\theta) & 2s(\theta)c^2(\theta) & -2s(\theta)c^2(\theta) & s(\theta)c(2\theta) & (c(\theta) + c(3\theta))/2. \end{pmatrix} \quad (2.33)$$

namely, the reflection and rotation matrices, respectively.

Chapter 3

Second-gradient material equivalent to the lattice structure

An infinite hexagonal lattice is analyzed when subject to a linear and quadratic nodal displacement field, with the final purpose of determining an equivalent elastic continuum.

3.1 Preliminaries: the periodic structure and its elastic equilibrium

An infinite periodic lattice is considered as the repetition of an hexagonal unit cell (as shown in Fig. 3.1 with reference to the orthonormal basis \mathbf{e}_1 – \mathbf{e}_2), which will eventually be considered as representative volume element (RVE) of an equivalent continuum. The hexagonal cell is regular and has edge of length ℓ , it is characterized by linear elastic bars with three different values of axial stiffnesses \bar{k}, \hat{k} , and \tilde{k} , distributed according to the scheme reported in Fig. 3.1. Within the lattice, each hinge node, where three bars of different elastic stiffness converge, can be identified through three indexes: the node index i and the cell indexes m and n .

There are three possible tessellations, equivalent from the geometric point of view, the one is chosen in which the centre is defined by the convergence of the bars of stiffness \hat{k} and \tilde{k} , while the other bars of stiffness \bar{k} are perimetric.

Each node of the cell is defined by an index $i = \{0, 1, 2, 3, 4, 5, 6\}$ and each cell is singled out by the integers $\{m, n\} \in \mathbb{Z}$, which determine the cell position with reference respectively to the non-orthogonal direction \mathbf{e}_1 and $\mathbf{e}_{\pi/3} = 1/2\mathbf{e}_1 + \sqrt{3}/2\mathbf{e}_2$. It follows that the position $\mathbf{x}^{(m,n|i)}$ of the perimetral i -th node of the $\{m, n\}$ cell can be described with reference to the position $\mathbf{x}^{(m,n|0)}$ of the cell's central node ($i = 0$), through the following expression

$$\mathbf{x}^{(m,n|i)} = \mathbf{x}^{(m,n|0)} + \ell \mathbf{g}^{(i)}, \quad (3.1)$$

where $\mathbf{g}^{(i)}$ defines the direction spanning from the central node to the i -th node,

$$\mathbf{g}^{(i)} = (1 - \delta_{i0}) \left\{ -\sin \left[\frac{\pi(i-1)}{3} \right] \mathbf{e}_1 + \cos \left[\frac{\pi(i-1)}{3} \right] \mathbf{e}_2 \right\}, \quad (3.2)$$

in which the index is not summed and δ_{i0} is the Kronecker delta defined to include the null index value, so that $\delta_{00} = 1$ while $\delta_{i0} = 0$ for every $i \neq 0$. From the definition expressed by Eq. (3.2), it follows that the vector $\mathbf{g}^{(i)}$ has unit modulus for every $i \neq 0$, while it vanishes when $i = 0$ (central node),

$$\mathbf{g}^{(0)} = \mathbf{0}, \quad |\mathbf{g}^{(i)}| = 1, \quad \text{for } i = 1, 2, 3, 4, 5, 6. \quad (3.3)$$

Furthermore, due to the RVE symmetry, the unit vectors $\mathbf{g}^{(i)}$ satisfy the following property

$$\mathbf{g}^{(i)} = -\mathbf{g}^{(i+3)}, \quad i = 1, 2, 3, \quad (3.4)$$

and the following combination of the unit vectors $\mathbf{g}^{(1)}$, $\mathbf{g}^{(5)}$, and $\mathbf{g}^{(6)}$ provides the unit vectors \mathbf{e}_1 and $\mathbf{e}_{\pi/3}$

$$\mathbf{e}_1 = \frac{\mathbf{g}^{(5)} + \mathbf{g}^{(6)}}{\sqrt{3}}, \quad \mathbf{e}_{\pi/3} = \frac{\mathbf{g}^{(1)} + \mathbf{g}^{(6)}}{\sqrt{3}}. \quad (3.5)$$

Considering the definition of the unit vector $\mathbf{g}^{(i)}$, Eq. (3.2), the position $\mathbf{x}^{(m,n|0)}$ of the central node of the cell $\{m, n\}$ can be expressed with reference to the position $\mathbf{x}^{(0,0|0)}$ of the central node of the cell $\{m, n\} = \{0, 0\}$ as

$$\mathbf{x}^{(m,n|0)} = \mathbf{x}^{(0,0|0)} + \ell \left[m \left(\mathbf{g}^{(5)} + \mathbf{g}^{(6)} \right) + n \left(\mathbf{g}^{(1)} + \mathbf{g}^{(6)} \right) \right], \quad (3.6)$$

so that the position $\mathbf{x}^{(m,n|i)}$ of each node i of every $\{m, n\}$ cell, expressed by Eq.(3.1), can be finally reduced to

$$\mathbf{x}^{(m,n|i)} = \mathbf{x}^{(0,0|0)} + \ell \left[\mathbf{g}^{(i)} + m \left(\mathbf{g}^{(5)} + \mathbf{g}^{(6)} \right) + n \left(\mathbf{g}^{(1)} + \mathbf{g}^{(6)} \right) \right]. \quad (3.7)$$

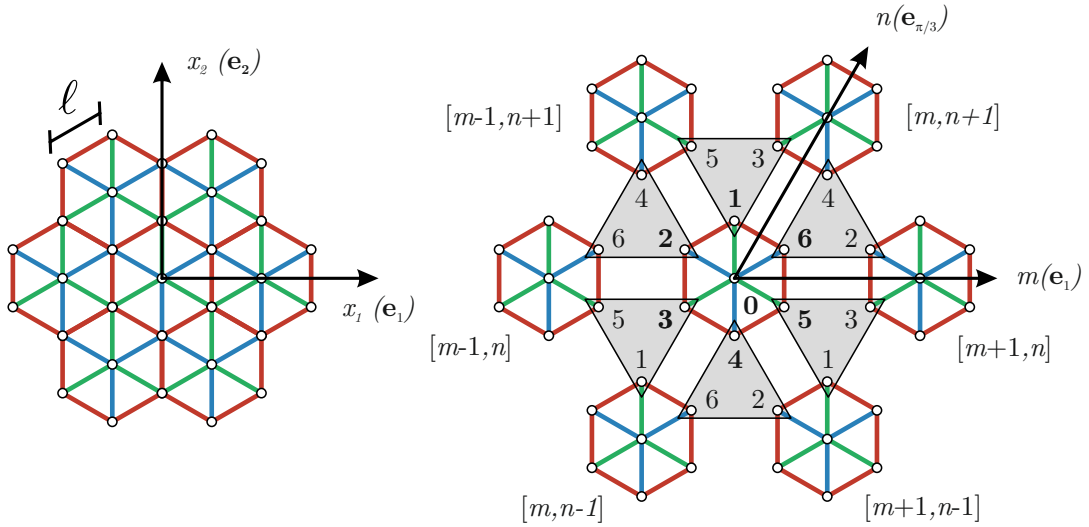


FIGURE 3.1: Hexagonal lattice (left) and its exploded drawing, highlighting the definitions of the cells (right), which correspond to the representative volume elements (RVEs) of an equivalent continuum.

The red, green and blue bars have stiffness \bar{k} , \hat{k} and \tilde{k} , respectively.

It is also noted that all the perimetric nodes ($i = \{1, 2, 3, 4, 5, 6\}$) are shared between three adjacent hexagonal cells (associated to three different pairs $\{m, n\}$),

Fig. 3.1, so that the following relations hold

$$\begin{aligned}
 \mathbf{x}^{(m,n|1)} &= \mathbf{x}^{(m,n+1|3)} = \mathbf{x}^{(m-1,n+1|5)}, \\
 \mathbf{x}^{(m,n|2)} &= \mathbf{x}^{(m-1,n+1|4)} = \mathbf{x}^{(m-1,n|6)}, \\
 \mathbf{x}^{(m,n|3)} &= \mathbf{x}^{(m-1,n|5)} = \mathbf{x}^{(m,n-1|1)}, \\
 \mathbf{x}^{(m,n|4)} &= \mathbf{x}^{(m,n-1|6)} = \mathbf{x}^{(m+1,n-1|2)}, \\
 \mathbf{x}^{(m,n|5)} &= \mathbf{x}^{(m+1,n-1|1)} = \mathbf{x}^{(m+1,n|3)}, \\
 \mathbf{x}^{(m,n|6)} &= \mathbf{x}^{(m+1,n|2)} = \mathbf{x}^{(m,n+1|4)}.
 \end{aligned} \tag{3.8}$$

Introducing $\mathbf{u}^{(m,n|i)}$ as the small displacement of the i -th node belonging to the cell $\{m, n\}$, which according to Eqs. (3.8) satisfies the following relations

$$\begin{aligned}
 \mathbf{u}^{(m,n|1)} &= \mathbf{u}^{(m,n+1|3)} = \mathbf{u}^{(m-1,n+1|5)}, \\
 \mathbf{u}^{(m,n|2)} &= \mathbf{u}^{(m-1,n+1|4)} = \mathbf{u}^{(m-1,n|6)}, \\
 \mathbf{u}^{(m,n|3)} &= \mathbf{u}^{(m-1,n|5)} = \mathbf{u}^{(m,n-1|1)}, \\
 \mathbf{u}^{(m,n|4)} &= \mathbf{u}^{(m,n-1|6)} = \mathbf{u}^{(m+1,n-1|2)}, \\
 \mathbf{u}^{(m,n|5)} &= \mathbf{u}^{(m+1,n-1|1)} = \mathbf{u}^{(m+1,n|3)}, \\
 \mathbf{u}^{(m,n|6)} &= \mathbf{u}^{(m+1,n|2)} = \mathbf{u}^{(m,n+1|4)}.
 \end{aligned} \tag{3.9}$$

the elongation $E^{(m,n|i,j)}$ of the bar connecting the nodes i and j (with $i \neq j$) is given by

$$E^{(m,n|i,j)} = \left(\mathbf{u}^{(m,n|i)} - \mathbf{u}^{(m,n|j)} \right) \cdot \left(\mathbf{g}^{(i)} - \mathbf{g}^{(j)} \right), \quad i \neq j, \tag{3.10}$$

showing that the permutation between the indexes i and j (referred to the involved nodes) does not vary this measure,

$$E^{(m,n|i,j)} = E^{(m,n|j,i)}. \tag{3.11}$$

Considering a linear elastic response for the bars, the corresponding force $\mathbf{F}^{(m,n|i,j)}$ acting on the i -th node of the cell $\{m, n\}$ is given by

$$\mathbf{F}^{(m,n|i,j)} = -k^{(i,j)} E^{(m,n|i,j)} \left(\mathbf{g}^{(i)} - \mathbf{g}^{(j)} \right), \tag{3.12}$$

while the respective force acting at the j -th node of the same cell, according to the second Newton's law, has reversed sign,

$$\mathbf{F}^{(m,n|j,i)} = -\mathbf{F}^{(m,n|i,j)}. \tag{3.13}$$

The usual convention is assumed that tensile forces are positive, while a negative sign denotes compression. In Eq. (3.12), the stiffness $k^{(i,j)}$ is defined as (Fig. 3.1)

$$k^{(i,j)} = \begin{cases} \bar{k}, & i \neq 0 \text{ and } j \neq 0, \\ \tilde{k}, & i = 0 \text{ and } j \text{ even} \quad \text{or} \quad i \text{ even and } j = 0, \\ \hat{k}, & i = 0 \text{ and } j \text{ odd} \quad \text{or} \quad i \text{ odd and } j = 0. \end{cases} \tag{3.14}$$

The sum of all the forces $\mathbf{F}^{(m,n|i,j)}$ applied to the node i (belonging to the cell $\{m, n\}$) and generated by the elongation of all the jointed bars, provide the resultant $\mathbf{R}^{(m,n|i)}$. Considering properties expressed by Eq. (3.8), the resultant forces at all the lattice nodes may be described through the three primary resultants $\mathbf{R}^{(m,n|0)}$, $\mathbf{R}^{(m,n|1)}$, $\mathbf{R}^{(m,n|2)}$ as

$$\begin{aligned}\mathbf{R}^{(m,n|0)} &= \sum_{j=1}^6 \mathbf{F}^{(m,n|0,j)}, \\ \mathbf{R}^{(m,n|1)} &= \mathbf{F}^{(m,n|1,0)} + \mathbf{F}^{(m,n|1,2)} + \mathbf{F}^{(m,n|1,6)} + \mathbf{F}^{(m,n+1|3,0)} + \mathbf{F}^{(m-1,n+1|5,6)} + \mathbf{F}^{(m-1,n+1|5,0)}, \\ \mathbf{R}^{(m,n|2)} &= \mathbf{F}^{(m,n|2,0)} + \mathbf{F}^{(m,n|2,1)} + \mathbf{F}^{(m,n|2,3)} + \mathbf{F}^{(m-1,n|6,0)} + \mathbf{F}^{(m-1,n+1|4,3)} + \mathbf{F}^{(m-1,n+1|4,0)}.\end{aligned}\quad (3.15)$$

Assuming quasi-static response, Eqs. (3.8) imply that equilibrium is satisfied for the whole lattice when the three primary resultants $\mathbf{R}^{(m,n|0)}$, $\mathbf{R}^{(m,n|1)}$, and $\mathbf{R}^{(m,n|2)}$ vanish for every cell $\{m, n\}$

$$\mathbf{R}^{(m,n|0)} = \mathbf{R}^{(m,n|1)} = \mathbf{R}^{(m,n|2)} = \mathbf{0}, \quad \forall \{m, n\}. \quad (3.16)$$

The elastic energy stored in the cell $\{m, n\}$ (that will be interpreted later as the microstructure of a continuum) is provided by

$$U_{lat}^{(m,n)} = \frac{1}{2} \sum_{i=1}^6 k^{(i,0)} \left[E^{(m,n|i,0)} \right]^2 + \frac{1}{4} \sum_{i=1}^6 k^{(i,i+1-6\delta_{i6})} \left[E^{(m,n|i,i+1-6\delta_{i6})} \right]^2, \quad (3.17)$$

where only one half of the energy accumulated within the perimetric bars has been considered, so that the total energy of the infinite lattice is obtained by summing the energy of each cell

$$U_{lat} = \sum_{m,n \in A \subseteq \mathbb{Z}} U_{lat}^{(m,n)}, \quad (3.18)$$

where A is a mono-connected compact set of \mathbb{Z} .

3.2 Definition of an average operator for the displacement gradient

With reference to a generic field $\mathbf{f}(x_1, x_2)$ over a domain Ω of a continuous body, its gradient and the related average are respectively given by

$$f_{j,k}(x_1, x_2) = \frac{\partial f_j(x_1, x_2)}{\partial x_k}, \quad \langle f_{j,k} \rangle = \frac{1}{||\Omega||} \int_{\Omega} f_{j,k} d\Omega, \quad (3.19)$$

where $||\Omega||$ is the measure of Ω . By means of the divergence theorem, the gradient average can be rewritten as

$$\langle f_{j,k} \rangle = \frac{1}{||\Omega||} \int_{\partial\Omega} f_j n_k ds, \quad (3.20)$$

where only the evaluation of the field $\mathbf{f}(x_1, x_2)$ along the cell perimeter is needed. In order to compute the displacement gradient average, the displacement field along

the cell perimeter can be linearly interpolated as

$$\mathbf{u}(s) = \mathbf{u}^{(m,n|i)} + \left(\mathbf{u}^{(m,n|i+1-6\delta_{i6})} - \mathbf{u}^{(m,n|i)} \right) \frac{s}{\ell}. \quad (3.21)$$

where s is the curvilinear coordinate along the bar connecting the node i to node $i + 1 - 6\delta_{i6}$ and measuring the distance from the former. Considering this interpolating field and identifying Ω with the hexagonal domain, the average of the displacement gradient for the lattice structure (identified with the subscript 'lat' to highlight its relation with the lattice, and not with the continuum) can be obtained by substituting Eq. (3.21) into Eq. (3.20) as

$$\langle u_{j,k} \rangle_{\text{lat}}^{(m,n)} = \frac{1}{3\sqrt{3}\ell} \sum_{i=1}^6 \left(u_j^{(m,n|i)} + u_j^{(m,n|i+1-6\delta_{i6})} \right) n_k^{(i)}, \quad (3.22)$$

which, when the normal vectors $n_k^{(i)}$ are related to the unit vectors $g_k^{(i)}$, reduces to

$$\langle u_{j,k} \rangle_{\text{lat}}^{(m,n)} = \frac{1}{9\ell} \sum_{i=1}^6 \left(u_j^{(m,n|i)} + u_j^{(m,n|i+1-6\delta_{i6})} \right) \left(g_k^{(i)} + g_k^{(i+1-6\delta_{i6})} \right). \quad (3.23)$$

More specifically, the four components of $\langle u_{j,k} \rangle_{\text{lat}}^{(m,n)}$ can be expressed in the reference system \mathbf{e}_1 – \mathbf{e}_2 as

$$\begin{aligned} \langle \nabla \mathbf{u}(\mathbf{x}) \rangle_{\text{lat}}^{(m,n)} = \\ \frac{1}{\ell} \begin{bmatrix} \frac{-u_1^{(m,n|2)} - u_1^{(m,n|3)} + u_1^{(m,n|5)} + u_1^{(m,n|6)}}{2\sqrt{3}} & \frac{2u_1^{(m,n|1)} + u_1^{(m,n|2)} - u_1^{(m,n|3)} - 2u_1^{(m,n|4)} - u_1^{(m,n|5)} + u_1^{(m,n|6)}}{6} \\ \frac{-u_2^{(m,n|2)} - u_2^{(m,n|3)} + u_2^{(m,n|5)} + u_2^{(m,n|6)}}{2\sqrt{3}} & \frac{2u_2^{(m,n|1)} + u_2^{(m,n|2)} - u_2^{(m,n|3)} - 2u_2^{(m,n|4)} - u_2^{(m,n|5)} + u_2^{(m,n|6)}}{6} \end{bmatrix}. \end{aligned} \quad (3.24)$$

An alternative but equivalent way to that described above to derive the average of the displacement gradient, Eq. (3.24), can be obtained with reference to the piecewise description of the displacement field along each one of the six equilateral triangles, subdomains of the hexagonal cells and enclosed by the three different bars. Such a piecewise description of the displacement field $\mathbf{u}^{(m,n,j)}(\mathbf{x})$ follows from the linear interpolation of the displacements between the three nodes $(0, j, j + 1 - 6\delta_{j6})$, with $j = 1, \dots, 6$ which are the vertices of the triangles defining the $\{m, n\}$ hexagonal cell, as

$$\mathbf{u}^{(m,n,j)}(\mathbf{x}) = \mathbf{A}^{(m,n,j)} \mathbf{x} + \mathbf{c}^{(m,n,j)} \quad \text{with} \quad j = 1, \dots, 6 \quad m, n \in \mathbb{Z} \quad (3.25)$$

where matrix $\mathbf{A}^{(m,n,j)}$ and the vector $\mathbf{c}^{(m,n,j)}$ are

$$\begin{aligned} A_{11}^{(m,n,j)} &= \frac{2 \cos\left(\frac{\pi j}{3}\right) (u_1^{(m,n|j)} - u_1^{(m,n|0)}) + 2 \cos\left(\frac{\pi(j-1)}{3}\right) (u_1^{(m,n|0)} - u_1^{(m,n|j+1)})}{\sqrt{3}\ell}, \\ A_{12}^{(m,n,j)} &= \frac{2 \cos\left(\frac{\pi j}{3}\right) (u_2^{(m,n|j)} - u_2^{(m,n|0)}) + 2 \cos\left(\frac{\pi(j-1)}{3}\right) (u_2^{(m,n|0)} - u_2^{(m,n|j+1)})}{\sqrt{3}\ell}, \end{aligned}$$

$$\begin{aligned}
A_{21}^{(m,n,j)} &= \frac{2 \sin\left(\frac{\pi j}{3}\right) (u_1^{(m,n|j)} - u_1^{(m,n|0)}) + 2 \sin\left(\frac{\pi(i-1)}{3}\right) (u_1^{(m,n|0)} - u_1^{(m,n|j+1)})}{\sqrt{3}\ell}, \\
A_{22}^{(m,n,j)} &= \frac{2 \sin\left(\frac{\pi j}{3}\right) (u_2^{(m,n|j)} - u_2^{(m,n|0)}) + 2 \sin\left(\frac{\pi(j-1)}{3}\right) (u_2^{(m,n|0)} - u_2^{(m,n|j+1)})}{\sqrt{3}\ell}, \\
c_1^{(m,n,j)} &= u_1^{(m,n|0)}, \quad c_2^{(m,n,j)} = u_2^{(m,n|0)}.
\end{aligned} \tag{3.26}$$

The average of the displacement gradient within the unit cell $\{m, n\}$ follows from Eq. (3.19) as

$$\langle \nabla \mathbf{u}(\mathbf{x}) \rangle_{\text{lat}}^{(m,n)} = \frac{1}{||\Omega||} \sum_{j=1}^6 \int_{\Omega^{(m,n,j)}} \nabla \mathbf{u}^{(m,n,j)}(\mathbf{x}) d\Omega. \tag{3.27}$$

Considering the piecewise description of displacement (3.25), Eq. (3.27) can be rewritten as

$$\langle \nabla \mathbf{u}(\mathbf{x}) \rangle_{\text{lat}}^{(m,n)} = \frac{1}{6} \sum_{j=0}^6 \begin{bmatrix} A_{11}^{(m,n,j)} & A_{12}^{(m,n,j)} \\ A_{21}^{(m,n,j)} & A_{22}^{(m,n,j)} \end{bmatrix}, \tag{3.28}$$

which, recalling Eq. (3.26), reduces to the same expression given by Eq. (3.23).

3.3 Second-order displacement boundary condition

The key to the homogenization scheme that will be developed in the next Section is the imposition to the infinite lattice of a linear and a quadratic nodal displacement fields (as in [5], [6], [13], [15]), together with a ‘correction field’ $\Delta \mathbf{u}^{(m,n|i)}$, namely,

$$u_r^{(m,n|i)} = \alpha_{sr} x_s^{(m,n|i)} + \beta_{str} x_s^{(m,n|i)} x_t^{(m,n|i)} + \Delta u_r^{(m,n|i)}, \quad \text{with} \quad r, s, t = 1, 2 \tag{3.29}$$

where α_{sr} and β_{str} are tensors modulating the fields and satisfying the symmetry properties $\alpha_{sr} = \alpha_{rs}$ and $\beta_{str} = \beta_{tsr}$. The presence of the correction term $\Delta u_r^{(m,n|i)}$ is necessary (as will be shown later) for the quasi-static equilibrium, to hold for every α_{sr} and β_{str} as defined by Eqs. (3.16). The displacement field expressed through Eq. (3.29) can equivalently be written as

$$\mathbf{u}^{(m,n|i)} = \boldsymbol{\alpha} \mathbf{x}^{(m,n|i)} + \left(\mathbf{x}^{(m,n|i)} \otimes \mathbf{x}^{(m,n|i)} \right) : \boldsymbol{\beta} + \Delta \mathbf{u}^{(m,n|i)}, \tag{3.30}$$

where the second-order tensor $\boldsymbol{\alpha}$ and the third-order tensor $\boldsymbol{\beta}$ have components $\alpha_{sr} = (\boldsymbol{\alpha})_{sr}$ and $\beta_{str} = (\boldsymbol{\beta})_{str}$. In Eq. (3.30), the dyadic product \otimes and double scalar product $:$ are introduced, respectively defined as $(\mathbf{a} \otimes \mathbf{b})_{st} = a_s b_t$ and $(\mathbf{A} : \mathbf{B})_r = A_{st} B_{str}$. With reference to the displacement field, Eq. (3.30), and using Eq. (3.10), the bars elongations are computed as

$$\begin{aligned}
E^{(m,n|i,j)} &= \ell \left\{ \boldsymbol{\alpha} \left(\mathbf{g}^{(i)} - \mathbf{g}^{(j)} \right) + 2 \left[\mathbf{x}^{(m,n|0)} \otimes \left(\mathbf{g}^{(i)} - \mathbf{g}^{(j)} \right) \right] : \boldsymbol{\beta} \right. \\
&\quad \left. + \ell \left[\left(\mathbf{g}^{(i)} + \mathbf{g}^{(j)} \right) \otimes \left(\mathbf{g}^{(i)} - \mathbf{g}^{(j)} \right) \right] : \boldsymbol{\beta} \right\} \cdot \left(\mathbf{g}^{(i)} - \mathbf{g}^{(j)} \right) + \Delta E^{(m,n|i,j)}, \quad i \neq j,
\end{aligned} \tag{3.31}$$

from which Eq. (3.12) yields the corresponding force at the i -th node

$$\mathbf{F}^{(m,n|i,j)} = -k^{(i,j)} \ell \mathbf{G}^{(i,j)} \left\{ \boldsymbol{\alpha} \left(\mathbf{g}^{(i)} - \mathbf{g}^{(j)} \right) + 2 \left[\mathbf{x}^{(m,n|0)} \otimes \left(\mathbf{g}^{(i)} - \mathbf{g}^{(j)} \right) \right] : \boldsymbol{\beta} \right. \\ \left. + \ell \left[\left(\mathbf{g}^{(i)} + \mathbf{g}^{(j)} \right) \otimes \left(\mathbf{g}^{(i)} - \mathbf{g}^{(j)} \right) \right] : \boldsymbol{\beta} \right\} + \Delta \mathbf{F}^{(m,n|i,j)}, \quad i \neq j, \quad (3.32)$$

with

$$\Delta E^{(m,n|i,j)} = \left(\Delta \mathbf{u}^{(m,n|i)} - \Delta \mathbf{u}^{(m,n|j)} \right) \cdot \left(\mathbf{g}^{(i)} - \mathbf{g}^{(j)} \right), \quad i \neq j, \quad (3.33)$$

$$\Delta \mathbf{F}^{(m,n|i,j)} = -k^{(i,j)} \Delta E^{(m,n|i,j)} \left(\mathbf{g}^{(i)} - \mathbf{g}^{(j)} \right), \quad i \neq j. \quad (3.34)$$

$$\mathbf{G}^{(i,j)} = \left(\mathbf{g}^{(i)} - \mathbf{g}^{(j)} \right) \otimes \left(\mathbf{g}^{(i)} - \mathbf{g}^{(j)} \right), \quad (3.35)$$

In combination with Eqs. (3.32) and (3.34), Eqs. (3.15) allows to write the resultant acting on the node i of the cell $\{m, n\}$ as

$$\mathbf{R}^{(m,n|0)} = \left(\widehat{k} - \widetilde{k} \right) \ell \sum_{i=1,3,5} \left(\mathbf{g}^{(i)} \cdot \boldsymbol{\alpha} \mathbf{g}^{(i)} \right) \mathbf{g}^{(i)} + \left(\widehat{k} + \widetilde{k} \right) \ell^2 \sum_{i=1,3,5} \left[\left(\mathbf{g}^{(i)} \otimes \mathbf{g}^{(i)} \right) : \boldsymbol{\beta} \cdot \mathbf{g}^{(i)} \right] \mathbf{g}^{(i)} \\ + 2 \left(\widehat{k} - \widetilde{k} \right) \ell \sum_{i=1,3,5} \left[\left(\mathbf{x}^{(m,n|0)} \otimes \mathbf{g}^{(i)} \right) : \boldsymbol{\beta} \cdot \mathbf{g}^{(i)} \right] \mathbf{g}^{(i)} \\ + \sum_{j=1}^6 k^{(0,j)} \mathbf{G}^{(0,j)} \left(\Delta \mathbf{u}^{(m,n|0)} - \Delta \mathbf{u}^{(m,n|j)} \right), \quad (3.36)$$

$$\mathbf{R}^{(m,n|1)} = \left(\bar{k} - \widehat{k} \right) \ell \sum_{i=1,3,5} \left(\mathbf{g}^{(i)} \cdot \boldsymbol{\alpha} \mathbf{g}^{(i)} \right) \mathbf{g}^{(i)} \\ + \left(\bar{k} + \widehat{k} \right) \ell^2 \sum_{i=1,3,5} \left[\left(\mathbf{g}^{(i)} \otimes \mathbf{g}^{(i)} \right) : \boldsymbol{\beta} \cdot \mathbf{g}^{(i)} \right] \mathbf{g}^{(i)} \\ + 2 \left(\bar{k} - \widehat{k} \right) \ell \sum_{i=1,3,5} \left[\left(\mathbf{x}^{(m,n|0)} \otimes \mathbf{g}^{(i)} \right) : \boldsymbol{\beta} \cdot \mathbf{g}^{(i)} \right] \mathbf{g}^{(i)} \\ + 2 \left(\bar{k} - \widehat{k} \right) \ell^2 \sum_{i=1,3,5} \left[\left(\mathbf{g}^{(1)} \otimes \mathbf{g}^{(i)} \right) : \boldsymbol{\beta} \cdot \mathbf{g}^{(i)} \right] \mathbf{g}^{(i)} \\ + \bar{k} \left[\mathbf{G}^{(1,0)} \left(\Delta \mathbf{u}^{(m,n|1)} - \Delta \mathbf{u}^{(m,n|0)} \right) + \mathbf{G}^{(5,0)} \left(\Delta \mathbf{u}^{(m,n|1)} - \Delta \mathbf{u}^{(m-1,n+1|0)} \right) \right. \\ \left. + \mathbf{G}^{(3,0)} \left(\Delta \mathbf{u}^{(m,n|1)} - \Delta \mathbf{u}^{(m,n+1|0)} \right) \right] - \widehat{k} \left[\mathbf{G}^{(3,0)} \left(\Delta \mathbf{u}^{(m,n|1)} - \Delta \mathbf{u}^{(m,n|2)} \right) \right. \\ \left. + \mathbf{G}^{(5,0)} \left(\Delta \mathbf{u}^{(m,n|1)} - \Delta \mathbf{u}^{(m,n|6)} \right) + \mathbf{G}^{(1,0)} \left(\Delta \mathbf{u}^{(m,n|1)} - \Delta \mathbf{u}^{(m,n+1|2)} \right) \right], \quad (3.37)$$

$$\begin{aligned}
\mathbf{R}^{(m,n|2)} = & \left(\tilde{k} - \bar{k} \right) \ell \sum_{i=1,3,5} \left(\mathbf{g}^{(i)} \cdot \boldsymbol{\alpha} \mathbf{g}^{(i)} \right) \mathbf{g}^{(i)} \\
& + \left(\tilde{k} + \bar{k} \right) \ell^2 \sum_{i=1,3,5} \left[\left(\mathbf{g}^{(i)} \otimes \mathbf{g}^{(i)} \right) : \boldsymbol{\beta} \cdot \mathbf{g}^{(i)} \right] \mathbf{g}^{(i)} \\
& + 2 \left(\tilde{k} - \bar{k} \right) \ell \sum_{i=1,3,5} \left[\left(\mathbf{x}^{(m,n|0)} \otimes \mathbf{g}^{(i)} \right) : \boldsymbol{\beta} \cdot \mathbf{g}^{(i)} \right] \mathbf{g}^{(i)} \\
& + 2 \left(\tilde{k} - \bar{k} \right) \ell^2 \sum_{i=1,3,5} \left[\left(\mathbf{g}^{(2)} \otimes \mathbf{g}^{(i)} \right) : \boldsymbol{\beta} \cdot \mathbf{g}^{(i)} \right] \mathbf{g}^{(i)} \\
& + \tilde{k} \left[\mathbf{G}^{(2,0)} \left(\Delta \mathbf{u}^{(m,n|2)} - \Delta \mathbf{u}^{(m,n|0)} \right) + \mathbf{G}^{(4,0)} \left(\Delta \mathbf{u}^{(m,n|2)} - \Delta \mathbf{u}^{(m-1,n+1|0)} \right) \right. \\
& + \left. \mathbf{G}^{(6,0)} \left(\Delta \mathbf{u}^{(m,n|2)} - \Delta \mathbf{u}^{(m-1,n|0)} \right) \right] - \bar{k} \left[\mathbf{G}^{(4,0)} \left(\Delta \mathbf{u}^{(m,n|2)} - \Delta \mathbf{u}^{(m,n|3)} \right) \right. \\
& + \left. \mathbf{G}^{(6,0)} \left(\Delta \mathbf{u}^{(m,n|2)} - \Delta \mathbf{u}^{(m,n|1)} \right) + \mathbf{G}^{(2,0)} \left(\Delta \mathbf{u}^{(m,n|2)} - \Delta \mathbf{u}^{(m-1,n|1)} \right) \right].
\end{aligned} \tag{3.38}$$

Due to the fact that the resultant forces $\mathbf{R}^{(m,n|i)}$ are linear expressions with respect $\mathbf{x}^{(m,n|0)}$ it follows that they may be annihilated only when the correction field $\Delta \mathbf{u}^{(m,n|i)}$ has a linear expression, which under the constraint of satisfying equations (3.9), Fig. 3.2, is given by the general form

$$\Delta \mathbf{u}^{(m,n|i)} = \begin{cases} \Delta \mathbf{a}^{(m,n|0)} = \mathbf{Z} \mathbf{x}^{(m,n|0)} + \mathbf{z}, \\ \Delta \mathbf{b}^{(m,n|i)} = \mathbf{V} \mathbf{x}^{(m,n|i)} + \mathbf{v}, & i \text{ odd}, \\ \Delta \mathbf{c}^{(m,n|i)} = \mathbf{W} \mathbf{x}^{(m,n|i)} + \mathbf{w}, & i \neq 0 \text{ and even.} \end{cases} \tag{3.39}$$

and implying that the mean value (3.23) of the gradient of the second-order displacement field is

$$\langle \nabla \mathbf{u} \rangle_{\text{lat}}^{(m,n)} = \boldsymbol{\alpha} + \ell \boldsymbol{\beta} \cdot \left[\frac{\sqrt{3}(2m+n)}{3n} \right] + \frac{\mathbf{V} + \mathbf{W}}{2}. \tag{3.40}$$

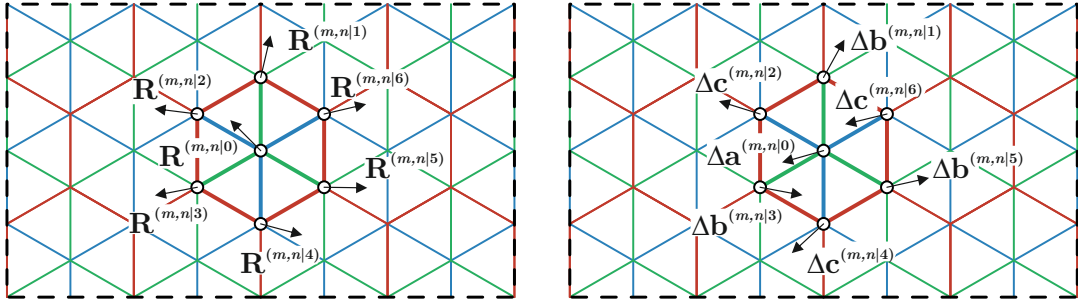


FIGURE 3.2: Resultant forces $\mathbf{R}^{(m,n|i)}$ (left) and corrective displacements $\Delta \mathbf{u}^{(m,n|i)}$ (right) associated with the node i belonging to the cell $\{m, n\}$ within the lattice drawn in its undeformed configuration.

Substituting such a correction field into Eqs. (3.36)–(3.38), the resultant forces at the three nodes reduce to

$$\begin{aligned} \mathbf{R}^{(m,n|0)} = & \left(\widehat{k} - \widetilde{k}\right) \ell \sum_{i=1,3,5} \left(\mathbf{g}^{(i)} \cdot \boldsymbol{\alpha} \mathbf{g}^{(i)}\right) \mathbf{g}^{(i)} + \left(\widehat{k} + \widetilde{k}\right) \ell^2 \sum_{i=1,3,5} \left[\left(\mathbf{g}^{(i)} \otimes \mathbf{g}^{(i)}\right) : \boldsymbol{\beta} \cdot \mathbf{g}^{(i)}\right] \mathbf{g}^{(i)} \\ & + 2 \left(\widehat{k} - \widetilde{k}\right) \ell \sum_{i=1,3,5} \left[\left(\mathbf{x}^{(m,n|0)} \otimes \mathbf{g}^{(i)}\right) : \boldsymbol{\beta} \cdot \mathbf{g}^{(i)}\right] \mathbf{g}^{(i)} + \\ & + \sum_{i=1,3,5} \left(\mathbf{g}^{(i)} \otimes \mathbf{g}^{(i)}\right) \left[\widehat{k} \left(\ell \mathbf{V} \mathbf{g}^{(i)} + (\mathbf{V} - \mathbf{Z}) \mathbf{x}^{(m,n|0)} + \mathbf{v} - \mathbf{z}\right) \right. \\ & \left. + \widetilde{k} \left(-\ell \mathbf{W} \mathbf{g}^{(i)} + (\mathbf{W} - \mathbf{Z}) \mathbf{x}^{(m,n|0)} + \mathbf{w} - \mathbf{z}\right)\right], \end{aligned} \quad (3.41)$$

$$\begin{aligned} \mathbf{R}^{(m,n|1)} = & \left(\bar{k} - \widehat{k}\right) \ell \sum_{i=1,3,5} \left(\mathbf{g}^{(i)} \cdot \boldsymbol{\alpha} \mathbf{g}^{(i)}\right) \mathbf{g}^{(i)} + \left(\bar{k} + \widehat{k}\right) \ell^2 \sum_{i=1,3,5} \left[\left(\mathbf{g}^{(i)} \otimes \mathbf{g}^{(i)}\right) : \boldsymbol{\beta} \cdot \mathbf{g}^{(i)}\right] \mathbf{g}^{(i)} \\ & + 2 \left(\bar{k} - \widehat{k}\right) \ell \sum_{i=1,3,5} \left[\left(\mathbf{x}^{(m,n|0)} \otimes \mathbf{g}^{(i)}\right) : \boldsymbol{\beta} \cdot \mathbf{g}^{(i)}\right] \mathbf{g}^{(i)} \\ & + 2 \left(\bar{k} - \widehat{k}\right) \ell^2 \sum_{i=1,3,5} \left[\left(\mathbf{g}^{(1)} \otimes \mathbf{g}^{(i)}\right) : \boldsymbol{\beta} \cdot \mathbf{g}^{(i)}\right] \mathbf{g}^{(i)} + \\ & + \sum_{i=1,3,5} \left(\mathbf{g}^{(i)} \otimes \mathbf{g}^{(i)}\right) \left[\widehat{k} \left(-\ell \mathbf{V} \mathbf{g}^{(1)} + (\mathbf{Z} - \mathbf{V}) \mathbf{x}^{(m,n|0)} \right. \right. \\ & \left. \left. + \ell \mathbf{Z} \left(\mathbf{g}^{(1)} - \mathbf{g}^{(i)}\right) + \mathbf{z} - \mathbf{v}\right) \right. \\ & \left. + \bar{k} \left(-\ell \mathbf{V} \mathbf{g}^{(1)} + (\mathbf{W} - \mathbf{V}) \mathbf{x}^{(m,n|0)} + \ell \mathbf{W} \left(\mathbf{g}^{(i)} + \mathbf{g}^{(1)}\right) + \mathbf{w} - \mathbf{v}\right)\right], \end{aligned} \quad (3.42)$$

$$\begin{aligned} \mathbf{R}^{(m,n|2)} = & \left(\widetilde{k} - \bar{k}\right) \ell \sum_{i=1,3,5} \left(\mathbf{g}^{(i)} \cdot \boldsymbol{\alpha} \mathbf{g}^{(i)}\right) \mathbf{g}^{(i)} + \left(\widetilde{k} + \bar{k}\right) \ell^2 \sum_{i=1,3,5} \left[\left(\mathbf{g}^{(i)} \otimes \mathbf{g}^{(i)}\right) : \boldsymbol{\beta} \cdot \mathbf{g}^{(i)}\right] \mathbf{g}^{(i)} \\ & + 2 \left(\widetilde{k} - \bar{k}\right) \ell \sum_{i=1,3,5} \left[\left(\mathbf{x}^{(m,n|0)} \otimes \mathbf{g}^{(i)}\right) : \boldsymbol{\beta} \cdot \mathbf{g}^{(i)}\right] \mathbf{g}^{(i)} \\ & + 2 \left(\widetilde{k} - \bar{k}\right) \ell^2 \sum_{i=1,3,5} \left[\left(\mathbf{g}^{(2)} \otimes \mathbf{g}^{(i)}\right) : \boldsymbol{\beta} \cdot \mathbf{g}^{(i)}\right] \mathbf{g}^{(i)} + \\ & + \sum_{i=1,3,5} \left(\mathbf{g}^{(i)} \otimes \mathbf{g}^{(i)}\right) \left[\widetilde{k} \left(-\ell \mathbf{W} \mathbf{g}^{(2)} + (\mathbf{Z} - \mathbf{W}) \mathbf{x}^{(m,n|0)} \right. \right. \\ & \left. \left. + \ell \mathbf{Z} \left(\mathbf{g}^{(i)} + \mathbf{g}^{(2)}\right) + \mathbf{z} - \mathbf{w}\right) \right. \\ & \left. + \bar{k} \left(-\ell \mathbf{W} \mathbf{g}^{(2)} + (\mathbf{V} - \mathbf{W}) \mathbf{x}^{(m,n|0)} - \ell \mathbf{V} \left(\mathbf{g}^{(i)} - \mathbf{g}^{(2)}\right) + \mathbf{v} - \mathbf{w}\right)\right]. \end{aligned} \quad (3.43)$$

The annihilation of the three resultant forces $\mathbf{R}^{(m,n|0)}$, $\mathbf{R}^{(m,n|1)}$, and $\mathbf{R}^{(m,n|2)}$ for every unit cell $\{m, n\}$ is equivalent to a system of 30 linear equations in the 18 unknown components of the vectors \mathbf{v} , \mathbf{w} , and \mathbf{z} , and of the matrices \mathbf{V} , \mathbf{W} , and \mathbf{Z} (Eqs. (3.39)). Solving this system leads to two results, namely, (i.) the determination of 12 out of the 18 additional field components, which depend on the components of \mathbf{z}

and \mathbf{Z} assumed as free parameters as

$$\begin{aligned}\mathbf{v} &= \mathcal{K}^{[1]} \left\{ \begin{bmatrix} \frac{\alpha_{12}}{2} \\ \frac{\alpha_{11} - \alpha_{22}}{2} \end{bmatrix} + \begin{bmatrix} \frac{Z_{12} + Z_{12}}{2} \\ \frac{Z_{11} - Z_{22}}{2} \end{bmatrix} \right\} \ell \\ &\quad + \left\{ \mathcal{K}^{[3]} \begin{bmatrix} \beta_{111} + \beta_{122} \\ \beta_{222} + \beta_{211} \end{bmatrix} + \mathcal{K}^{[5]} \begin{bmatrix} \beta_{221} - \beta_{122} \\ \beta_{112} - \beta_{211} \end{bmatrix} \right\} \ell^2 + \mathbf{z}, \\ \mathbf{w} &= \mathcal{K}^{[2]} \left\{ \begin{bmatrix} \frac{\alpha_{12}}{2} \\ \frac{\alpha_{11} - \alpha_{22}}{2} \end{bmatrix} + \begin{bmatrix} \frac{Z_{12} + Z_{12}}{2} \\ \frac{Z_{11} - Z_{22}}{2} \end{bmatrix} \right\} \ell \\ &\quad + \left\{ \mathcal{K}^{[4]} \begin{bmatrix} \beta_{111} + \beta_{122} \\ \beta_{222} + \beta_{211} \end{bmatrix} + \mathcal{K}^{[6]} \begin{bmatrix} \beta_{221} - \beta_{122} \\ \beta_{112} - \beta_{211} \end{bmatrix} \right\} \ell^2 + \mathbf{z},\end{aligned}\tag{3.44}$$

$$\begin{aligned}\mathbf{V} &= \mathcal{K}^{[1]} \begin{bmatrix} \beta_{112} + \beta_{211} & \beta_{122} + \beta_{221} \\ \beta_{111} - \beta_{122} & \beta_{211} - \beta_{222} \end{bmatrix} \ell + \mathbf{Z}, \\ \mathbf{W} &= \mathcal{K}^{[2]} \begin{bmatrix} \beta_{112} + \beta_{211} & \beta_{122} + \beta_{221} \\ \beta_{111} - \beta_{122} & \beta_{211} - \beta_{222} \end{bmatrix} \ell + \mathbf{Z},\end{aligned}\tag{3.45}$$

and (ii.) two linear equations for the six components of $\boldsymbol{\beta}$.

It follows from these two equations that tensor $\boldsymbol{\beta}$ is constrained to have only four independent components and will be henceforth referred as $\boldsymbol{\beta}^{\text{lat}}$, a symbol defining the set of generic quadratic amplitude tensors $\boldsymbol{\beta}$, for which the lattice structure is in equilibrium in the absence of external nodal forces. Considering $\beta_{111}, \beta_{221}, \beta_{112}, \beta_{222}$ as the four independent components, tensor $\boldsymbol{\beta}^{\text{lat}}$ is defined by the six components $\beta_{111}, \beta_{221}, \beta_{112}, \beta_{222}, \beta_{211}^{\text{lat}},$ and β_{122}^{lat} , where the last two are

$$\begin{bmatrix} \beta_{211}^{\text{lat}} \\ \beta_{122}^{\text{lat}} \end{bmatrix} = - \left(1 + \frac{9I_{[3]}}{2I_{[1]}I_{[2]}} \right) \begin{bmatrix} \beta_{222} \\ \beta_{111} \end{bmatrix} - \frac{9I_{[3]}}{2I_{[1]}I_{[2]}} \begin{bmatrix} \beta_{112} \\ \beta_{221} \end{bmatrix}.\tag{3.46}$$

The superscript ‘lat’ is introduced to highlight that these two components are constrained in order to satisfy the equilibrium in the lattice material. Henceforth, when referred to the lattice material, the generic tensor $\boldsymbol{\beta}$ is considered as the subset $\boldsymbol{\beta}^{\text{lat}}$, satisfying Eq. (3.46). In Eqs. (3.44)-(3.45) and (3.46), the coefficients $\mathcal{K}^{[j]}$ ($j = 1, \dots, 6$) and $I_{[j]}$ ($j = 1, 2, 3$) are introduced, the former are given by

$$\begin{aligned}\mathcal{K}^{[1]} &= \frac{\bar{k}(\hat{k} - \tilde{k}) + \tilde{k}(\hat{k} - \bar{k})}{I_{[2]}}, & \mathcal{K}^{[2]} &= \frac{\hat{k}(\bar{k} - \tilde{k}) + \bar{k}(\hat{k} - \tilde{k})}{I_{[2]}}, & \mathcal{K}^{[3]} &= \frac{3\hat{k}(\bar{k} + \tilde{k}) + 4\bar{k}(\bar{k} + 2\tilde{k})}{4I_{[2]}}, \\ \mathcal{K}^{[4]} &= \frac{3\tilde{k}(k + \hat{k}) + 4\bar{k}(k + 2\hat{k})}{4I_{[2]}}, & \mathcal{K}^{[5]} &= \frac{I_{[2]} + 3\tilde{k}\hat{k}}{4I_{[2]}}, & \mathcal{K}^{[6]} &= \frac{I_{[2]} + 3\tilde{k}\hat{k}}{4I_{[2]}},\end{aligned}\tag{3.47}$$

while the latter are the three invariants of the diagonal matrix \mathbf{K}

$$\mathbf{K} = \begin{bmatrix} \bar{k} & 0 & 0 \\ 0 & \hat{k} & 0 \\ 0 & 0 & \tilde{k} \end{bmatrix},\tag{3.48}$$

so that

$$\begin{aligned} I_{[1]} &= \text{tr} \mathbf{K} = \bar{k} + \hat{k} + \tilde{k}, \\ I_{[2]} &= \frac{1}{2} \left[(\text{tr} \mathbf{K})^2 - \text{tr} \mathbf{K}^2 \right] = \bar{k} \hat{k} + \bar{k} \tilde{k} + \hat{k} \tilde{k}, \\ I_{[3]} &= \det(\mathbf{K}) = \bar{k} \hat{k} \tilde{k}. \end{aligned} \quad (3.49)$$

Imposing that the correction field $\Delta \mathbf{u}$ does not affect the mean value of the displacement gradient $\langle \nabla \mathbf{u} \rangle_{\text{lat}}^{(m,n)}$, Eq. (3.40), leads to the condition

$$\mathbf{V} + \mathbf{W} = \mathbf{0}, \quad (3.50)$$

which, considering their expressions given in Eq. (3.45), is equivalent to the following value of \mathbf{Z}

$$\mathbf{Z} = -\frac{\mathcal{K}^{[1]} + \mathcal{K}^{[2]}}{2} \begin{bmatrix} \beta_{112} + \beta_{211}^{\text{lat}} & \beta_{122}^{\text{lat}} + \beta_{221} \\ \beta_{111} - \beta_{122}^{\text{lat}} & \beta_{211}^{\text{lat}} - \beta_{222} \end{bmatrix} \ell. \quad (3.51)$$

Note that vector \mathbf{z} appearing in Eqs. (3.44) is not present in the above equations, so that it remains indeterminate because it only produces a rigid-body translation.

It is worth noting that:

- in the case of springs with same stiffness ($\bar{k} = \tilde{k} = \hat{k}$), enforcing Eqs.(3.46) automatically provides the equilibrium Eqs.(3.41)–(3.43) for the generic purely quadratic displacement field augmented by a rigid translation \mathbf{z} ,

$$\bar{k} = \tilde{k} = \hat{k} \implies \begin{cases} \mathbf{v} = \mathbf{w} = \mathbf{z} \\ \mathbf{V} = \mathbf{W} = \mathbf{Z} = \mathbf{0} \end{cases} \quad (3.52)$$

so that in this case the correction field is null.

- in the case $\beta = \mathbf{0}$, it follows that $\mathbf{V} = \mathbf{W} = \mathbf{Z} = \mathbf{0}$ but the correction field is in general non-null when two over the three stiffnesses are different from each other. Indeed, the correction field is annihilated only when $\mathbf{g}^{(1)} \cdot \boldsymbol{\alpha} \mathbf{g}^{(1)} = \mathbf{g}^{(3)} \cdot \boldsymbol{\alpha} \mathbf{g}^{(3)} = \mathbf{g}^{(5)} \cdot \boldsymbol{\alpha} \mathbf{g}^{(5)}$ (or equivalently, $\alpha_{11} = \alpha_{22}$ and $\alpha_{12} = 0$), except in the particular case of springs with same stiffness ($\bar{k} = \tilde{k} = \hat{k}$) when the correction field is always null.
- with the permutation of the three stiffnesses κ_1 , κ_2 , and κ_3 , the second-order tensors \mathbf{V} , \mathbf{W} , and \mathbf{Z} of the correction field have the following properties

$$\begin{aligned} \mathbf{V}(\kappa_1, \kappa_2, \kappa_3) &= \mathbf{V}(\kappa_1, \kappa_3, \kappa_2), & \mathbf{W}(\kappa_1, \kappa_2, \kappa_3) &= \mathbf{W}(\kappa_1, \kappa_3, \kappa_2), \\ \mathbf{Z}(\kappa_1, \kappa_2, \kappa_3) &= -\mathbf{Z}(\kappa_1, \kappa_3, \kappa_2), \end{aligned} \quad (3.53)$$

In the case $\beta = \mathbf{0}$, the above equations are also complemented by following properties for the vectors \mathbf{v} , \mathbf{w} of the correction field

$$\mathbf{v}(\kappa_1, \kappa_2, \kappa_3) = \mathbf{v}(\kappa_3, \kappa_2, \kappa_1), \quad \mathbf{w}(\kappa_1, \kappa_2, \kappa_3) = \mathbf{w}(\kappa_2, \kappa_1, \kappa_3), \quad \text{when } \beta = \mathbf{0}. \quad (3.54)$$

At this stage, the additional field $\Delta \mathbf{u}^{(m,n|i)}$, Eq. (3.39), results completely defined through Eqs. (3.44), (3.45), (3.46), and (3.51). With the purpose of highlighting the contribution of the additional field $\Delta \mathbf{u}$ to the considered second-order displacement, Eq. (3.29), three deformed configurations of the lattice are shown in Fig. 3.3.

Looking to the upper row of the figure, the first image on the left shows the displacement produced by a purely linear ($\beta = 0$) displacement, while the second image depicts the corresponding additional field only. Finally the image on the right is the composition of the two. The lower row shows respectively a purely quadratic ($\alpha = 0$) displacement, its additional field $\Delta \mathbf{u}^{(m,n|i)}$, and the composition of the two. In the figure, the following stiffnesses of the lattice have been considered: $\bar{k} = \hat{k} = 10\tilde{k}$.

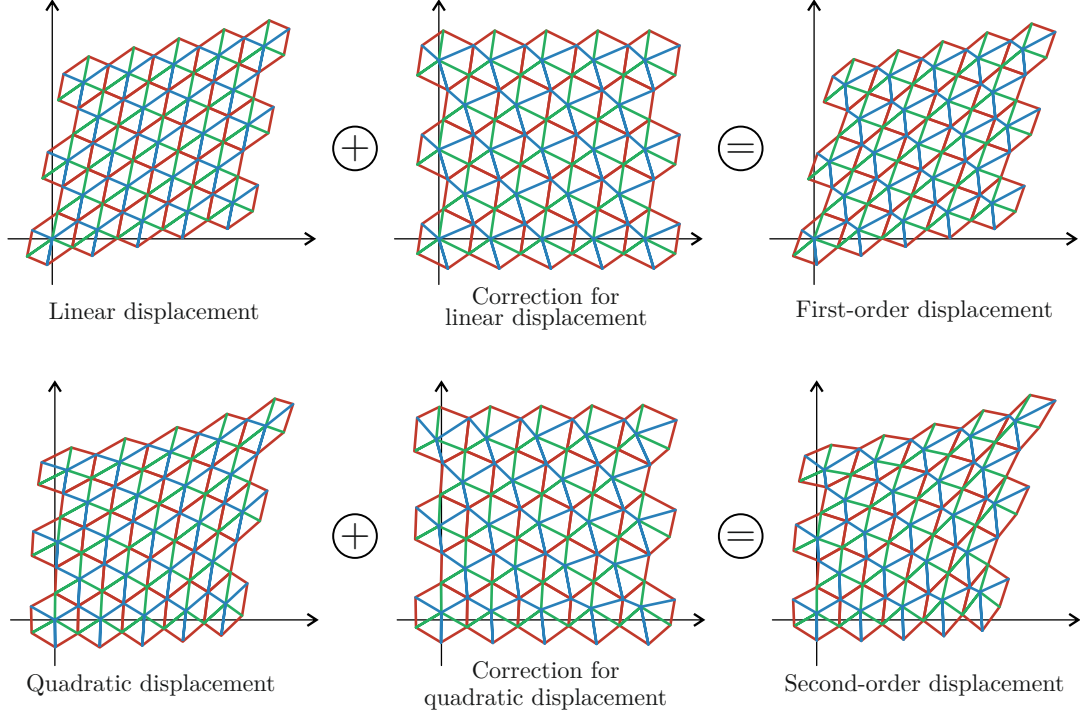


FIGURE 3.3: (Upper part) Deformed configuration for a lattice with bars of stiffness $\bar{k} = \hat{k} = 10\tilde{k}$ subject to (left) a purely linear displacement condition with $\{\alpha_{11}, \alpha_{22}, \alpha_{12}\} = \{0, 0, 1/5\}$, (center) its corrective field, and (right) the sum of these two. (Lower part) As in the upper part, but for a purely quadratic displacement condition with $\{\beta_{111}, \beta_{221}, \beta_{112}, \beta_{222}, \beta_{211}^{\text{lat}}, \beta_{122}^{\text{lat}}\} = \{-1, 1, 1, -1, 1, 1\}1/(80\ell)$.

3.4 Identification of the higher-order solid equivalent to the lattice structure

Considering the second-order displacement field Eq. (3.29) defined by the tensors α and β^{lat} Eqs. (3.46) and by the ‘additional field’ $\Delta \mathbf{u}^{(m,n|i)}$, Eqs. (3.44), (3.45), and Eq. (3.51), the elastic energy stored within the lattice cell $\{m, n\}$ is computed. This elastic energy is shown to display the same mathematical structure of the elastic energy stored within a unit cell made up of an homogeneous elastic strain-gradient solid (SGE) when subject to a quadratic displacement field, defined by the tensors α and β^{SGE} (note that β^{SGE} defines the coefficients of all quadratic fields which generate equilibrated stresses in a second-gradient elastic material without body forces). Therefore, imposing the elastic energy matching between the lattice and the SGE solid leads to $\beta^{\text{lat}} = \beta^{\text{SGE}}$ and allows the identification of the constitutive parameters of the elastic solid equivalent to the lattice structure.

It is instrumental to represent the components of the tensors α and $\beta^{(\cdot)}$ (where the superscript (\cdot) denotes either (lat) or (SGE)) using a vectorial notation through the vectors \mathbf{a} and $\mathbf{b}^{(\cdot)}$ as

$$\mathbf{a} = \begin{bmatrix} \alpha_{11} \\ \alpha_{22} \\ 2\alpha_{12} \end{bmatrix}, \quad \mathbf{b}^{(\cdot)} = \begin{bmatrix} \beta_{111} \\ \beta_{221} \\ \beta_{112} \\ \beta_{222} \\ 2\beta_{211} \\ 2\beta_{122} \end{bmatrix}. \quad (3.55)$$

and to collect the four components of $\beta^{(\cdot)}$ not constrained by the equilibrium Eq. (3.46) in the vector \mathbf{b}^*

$$\mathbf{b}^* = \begin{bmatrix} \beta_{111} \\ \beta_{221} \\ \beta_{112} \\ \beta_{222} \end{bmatrix}, \quad (3.56)$$

so that vector $\mathbf{b}^{(\cdot)}$ can be obtained as

$$\mathbf{b}^{(\cdot)} = \mathbf{T}^{(\cdot)} \mathbf{b}^* \quad (3.57)$$

where matrix $\mathbf{T}^{(\cdot)}$ is the transformation matrix providing the equilibrium conditions in the lattice (in which case will be denoted as \mathbf{T}^{lat}) or in the strain-gradient elastic solid (in which case will be denoted as \mathbf{T}^{SGE}).

3.5 Energy stored in the lattice structure

Considering the second-order displacement field Eq. (3.29) defined by the tensors α and β^{lat} Eqs. (3.46) and by the ‘additional field’ $\Delta \mathbf{u}^{(m,n|i)}$, Eqs. (3.44), (3.45), and Eq. (3.51), the elastic energy stored within the lattice cell $\{m, n\}$ is computed. This elastic energy is shown to display the same mathematical structure of the elastic energy stored within a unit cell made up of an homogeneous elastic strain-gradient solid (SGE) when subject to a quadratic displacement field, defined by the tensors α and β^{SGE} (note that β^{SGE} defines the coefficients of all quadratic fields which generate equilibrated stresses in a second-gradient elastic material without body forces). Therefore, imposing the elastic energy matching between the lattice and the SGE solid leads to $\beta^{\text{lat}} = \beta^{\text{SGE}}$ and allows the identification of the constitutive parameters of the elastic solid equivalent to the lattice structure.

It is instrumental to represent the components of the tensors α and $\beta^{(\cdot)}$ (where the superscript (\cdot) denotes either (lat) or (SGE)) using a vectorial notation through the vectors \mathbf{a} and $\mathbf{b}^{(\cdot)}$ as

$$\mathbf{U}_{\text{lat}}^{(m,n)}(\alpha, \beta^{\text{lat}}) = \mathbf{U}_{\text{lat}}^{(m,n)}(\mathbf{a}, \mathbf{b}^{\text{lat}}) = \mathbf{U}_{\text{lat}}^{(m,n)}(\mathbf{a}, \mathbf{b}^*), \quad (3.58)$$

where $\mathbf{b}^{\text{lat}} = \mathbf{T}^{\text{lat}} \mathbf{b}^*$ with

$$\mathbf{T}^{\text{lat}} = \begin{pmatrix} 1 & 0 & 0 & 0 \\ 0 & 1 & 0 & 0 \\ 0 & 0 & 1 & 0 \\ 0 & 0 & 0 & 1 \\ 0 & 0 & -\frac{9I_{[3]}}{I_{[1]}I_{[2]}} & -\frac{9I_{[3]}}{I_{[1]}I_{[2]}} - 2 \\ -\frac{9I_{[3]}}{I_{[1]}I_{[2]}} - 2 & -\frac{9I_{[3]}}{I_{[1]}I_{[2]}} & 0 & 0 \end{pmatrix}. \quad (3.59)$$

The energy $U_{\text{lat}}^{(m,n)}(\mathbf{a}, \mathbf{b}^*)$ is given by the following quadratic form of \mathbf{a} and \mathbf{b}^*

$$\begin{aligned} U_{\text{lat}}^{(m,n)}(\mathbf{a}, \mathbf{b}^*) = \ell^2 \Big\{ & \mathbf{a} \cdot \mathbf{H}^{[1]}(\bar{k}, \hat{k}, \tilde{k}) \mathbf{a} + 2\ell \mathbf{a} \cdot \left[m\mathbf{H}^{[2]}(\bar{k}, \hat{k}, \tilde{k}) + n\mathbf{H}^{[3]}(\bar{k}, \hat{k}, \tilde{k}) + \mathbf{H}^{[4]}(\bar{k}, \hat{k}, \tilde{k}) \right] \mathbf{b}^* \\ & + \ell^2 \mathbf{b}^* \cdot \left[m^2\mathbf{H}^{[5]}(\bar{k}, \hat{k}, \tilde{k}) + n^2\mathbf{H}^{[6]}(\bar{k}, \hat{k}, \tilde{k}) + m n \mathbf{H}^{[7]}(\bar{k}, \hat{k}, \tilde{k}) + m\mathbf{H}^{[8]}(\bar{k}, \hat{k}, \tilde{k}) + \right. \\ & \left. + n\mathbf{H}^{[9]}(\bar{k}, \hat{k}, \tilde{k}) + \mathbf{H}^{[10]}(\bar{k}, \hat{k}, \tilde{k}) \right] \mathbf{b}^* \Big\}, \end{aligned} \quad (3.60)$$

where the matrices $\mathbf{H}^{[r]}$ ($r = 1, \dots, 10$) depend on the values of the three stiffnesses \bar{k}, \hat{k} , and \tilde{k} . These matrixes have different dimensions (3×3 for $r = 1$, 3×4 for $r = 2, 3, 4$, and 4×4 in the other cases) and their components $H_{ij}^{[r]}$ are reported in Appendix A. From Eq. (3.60) it is evident that the strain energy depends on the cell position whenever $\mathbf{b}^* \neq 0$, so that it becomes independent of indexes m and n only when $\mathbf{b}^* = 0$, a condition corresponding to $\mathbf{b}^{\text{lat}} = 0$ and also implying $\beta^{\text{lat}} = 0$.

3.6 Energy stored in a second-gradient elastic solid

With reference to the ‘form I’ introduced by Mindlin [32, 33], a second-gradient elastic (SGE) solid has a quadratic strain energy density \mathcal{U}_{SGE} in the strain ϵ and curvature χ , which can be derived from the displacement field \mathbf{u} as

$$\epsilon_{ij} = \frac{u_{i,j} + u_{j,i}}{2}, \quad \chi_{ijk} = u_{k,ij}, \quad (3.61)$$

displaying the symmetry properties $\epsilon_{ij} = \epsilon_{ji}$ and $\chi_{ijk} = \chi_{jik}$ as shown in Chapter 2. The quadratic strain energy density \mathcal{U}_{SGE} can be decomposed as

$$\mathcal{U}_{\text{SGE}}(\epsilon, \chi) = \mathcal{U}_{\text{C}}(\epsilon) + \mathcal{U}_{\text{M}}(\epsilon, \chi) + \mathcal{U}_{\text{A}}(\chi), \quad (3.62)$$

where $\mathcal{U}_{\text{C}}(\epsilon)$ is a ‘purely local’ (Cauchy) energy term and $\mathcal{U}_{\text{A}}(\chi)$ a ‘completely non-local’ energy term, while the mutual energy term $\mathcal{U}_{\text{M}}(\epsilon, \chi)$ expresses the coupling between strain and curvature,

$$\mathcal{U}_{\text{C}}(\epsilon) = \frac{1}{2} \mathbb{C}_{ijkl} \epsilon_{ij} \epsilon_{kl}, \quad \mathcal{U}_{\text{M}}(\epsilon, \chi) = \mathbb{M}_{ijklm} \chi_{ijk} \epsilon_{lm}, \quad \mathcal{U}_{\text{A}}(\chi) = \frac{1}{2} \mathbb{A}_{ijklmn} \chi_{ijk} \chi_{lmn}, \quad (3.63)$$

being \mathbb{C} , \mathbb{A} , and \mathbb{M} , the fourth-, sixth-, and fifth-order constitutive tensors, respectively, with the symmetries Eqs. (2.25) reported in Chapter 2.

The work-conjugate quantities of the fundamental kinematic fields ϵ and χ are respectively the stress σ and double stress τ , given by

$$\sigma_{ij} = \mathbb{C}_{ijlm} \epsilon_{lm} + \mathbb{M}_{ijlmn} \chi_{lmn}, \quad \tau_{kji} = \mathbb{A}_{kjlmn} \chi_{lmn} + \mathbb{M}_{lmkji} \epsilon_{lm}, \quad (3.64)$$

The stresses have to satisfy the equilibrium equations in the absence of body-forces

$$\sigma_{ij,j} - \tau_{kji,jk} = 0, \quad (3.65)$$

A vectorial representation of the components of the strain ϵ and the curvature χ tensors as strain \mathbf{p} and curvature \mathbf{q} vectors is introduced (recalling Eqs. (2.31))

$$\mathbf{p} = \begin{bmatrix} \epsilon_{11} \\ \epsilon_{22} \\ 2\epsilon_{12} \end{bmatrix}, \quad \mathbf{q} = \begin{bmatrix} \chi_{111} \\ \chi_{221} \\ \chi_{112} \\ \chi_{222} \\ 2\chi_{211} \\ 2\chi_{122} \end{bmatrix}, \quad (3.66)$$

so that the elastic energy terms (3.63) can be rewritten as

$$\mathcal{U}_{\mathbf{C}}(\epsilon) = \mathcal{U}_{\mathbf{C}}(\mathbf{p}), \quad \mathcal{U}_{\mathbf{M}}(\epsilon, \chi) = \mathcal{U}_{\mathbf{M}}(\mathbf{p}, \mathbf{q}), \quad \mathcal{U}_{\mathbf{A}}(\chi) = \mathcal{U}_{\mathbf{A}}(\mathbf{q}), \quad (3.67)$$

where

$$\mathcal{U}_{\mathbf{C}}(\mathbf{p}) = \frac{1}{2} C_{ij} p_i p_j, \quad \mathcal{U}_{\mathbf{M}}(\mathbf{p}, \mathbf{q}) = M_{jk} p_j q_k, \quad \mathcal{U}_{\mathbf{A}}(\mathbf{q}) = \frac{1}{2} A_{kl} q_k q_l, \quad \begin{cases} i, j = 1, 2, 3 \\ k, l = 1, \dots, 6 \end{cases}. \quad (3.68)$$

The matrices C_{ij} , M_{jk} , and A_{kl} represent a Voigt notation for the constitutive tensors \mathbf{C} , \mathbf{M} , and \mathbf{A} , respectively [3, 4]. Note that matrices C_{ij} and A_{kl} are symmetric and square (the former of order 3 and the latter of order 6), while M_{jk} is a 3×6 rectangular matrix.

Introducing the strain energy density $\mathcal{U}_{\text{SGE}}(\mathbf{p}, \mathbf{q}) = \mathcal{U}_{\mathbf{C}}(\mathbf{p}) + \mathcal{U}_{\mathbf{M}}(\mathbf{p}, \mathbf{q}) + \mathcal{U}_{\mathbf{A}}(\mathbf{q})$, the strain energy can be given in the two equivalent forms

$$\mathcal{U}_{\text{SGE}}(\epsilon, \chi) = \mathcal{U}_{\text{SGE}}(\mathbf{p}(\epsilon), \mathbf{q}(\chi)). \quad (3.69)$$

It is assumed now that the second-gradient elastic material is subject to remote quadratic displacement boundary conditions provided by the second-order displacement field, Eq. (3.29), in the absence of the additional field ($\Delta \mathbf{u}^{(m,n|i)} = \mathbf{0}$, see also Sect. 3.7),

$$\mathbf{u}(\mathbf{x}) = \alpha \mathbf{x} + (\mathbf{x} \otimes \mathbf{x}) : \beta. \quad (3.70)$$

The quadratic displacement field (3.70) is restricted, at first order, by equilibrium,

$$C_{ljk} \beta_{jkh} = 0, \quad (3.71)$$

an equation which introduces two relationships between the coefficients β_{ijk} , so that the independent coefficients remain 4, while the remaining 2 are dependent. Collectively, the coefficients β_{ijk} are re-assembled in the vector β^{SGE} , so that

$$\mathbf{u}(\mathbf{x}) = \alpha \mathbf{x} + (\mathbf{x} \otimes \mathbf{x}) : \beta^{\text{SGE}}, \quad (3.72)$$

where

$$\begin{aligned} \beta_{111}^{\text{SGE}} &= \beta_{111}, & \beta_{221}^{\text{SGE}} &= \beta_{221}, & \beta_{112}^{\text{SGE}} &= \beta_{112}, & \beta_{222}^{\text{SGE}} &= \beta_{222} \\ \beta_{211}^{\text{SGE}} &= \beta_{111} \mathcal{D}_1 + \beta_{221} \mathcal{D}_2 + \beta_{112} \mathcal{D}_3 + \beta_{222} \mathcal{D}_4, \\ \beta_{122}^{\text{SGE}} &= \beta_{111} \mathcal{D}_5 + \beta_{221} \mathcal{D}_6 + \beta_{112} \mathcal{D}_7 + \beta_{222} \mathcal{D}_8, \end{aligned} \quad (3.73)$$

in which

$$\begin{aligned}\mathcal{D}_1 &= \frac{2C_{13}^2 - C_{11}(C_{12} + C_{33})}{(C_{12} + C_{33})^2 - 4C_{13}C_{23}}, & \mathcal{D}_2 &= \frac{2C_{13}C_{23} - C_{33}(C_{12} + C_{33})}{(C_{12} + C_{33})^2 - 4C_{13}C_{23}}, & \mathcal{D}_3 &= \frac{C_{13}(C_{33} - C_{12})}{(C_{12} + C_{33})^2 - 4C_{13}C_{23}}, \\ \mathcal{D}_4 &= \frac{2C_{13}C_{22} - C_{23}(C_{12} + C_{33})}{(C_{12} + C_{33})^2 - 4C_{13}C_{23}}, & \mathcal{D}_5 &= \frac{2C_{11}C_{23} - C_{13}(C_{12} + C_{33})}{(C_{12} + C_{33})^2 - 4C_{13}C_{23}}, & \mathcal{D}_6 &= \frac{C_{23}(C_{12} - C_{33})}{4C_{13}C_{23} - (C_{12} + C_{33})^2}, \\ \mathcal{D}_7 &= \frac{C_{33}(C_{12} + C_{33}) - 2C_{13}C_{23}}{4C_{13}C_{23} - (C_{12} + C_{33})^2}, & \mathcal{D}_8 &= \frac{2C_{23}^2 - C_{22}(C_{12} + C_{33})}{(C_{12} + C_{33})^2 - 4C_{13}C_{23}}.\end{aligned}\quad (3.74)$$

From now on the constrained tensor β , due to Eqs.(3.73), will be denoted by β^{SGE} .

It follows that the strain \mathbf{p} and curvature \mathbf{q} vectors can be rewritten as

$$\mathbf{p}(\epsilon) = \mathbf{p}(\mathbf{a}, \mathbf{b}^{\text{SGE}}), \quad \mathbf{q}(\chi) = \mathbf{q}(\mathbf{b}^{\text{SGE}}), \quad (3.75)$$

where

$$\mathbf{b}^{\text{SGE}} = \mathbf{T}^{\text{SGE}} \mathbf{b}^*, \quad \text{with} \quad \mathbf{T}^{\text{SGE}} = \begin{pmatrix} 1 & 0 & 0 & 0 \\ 0 & 1 & 0 & 0 \\ 0 & 0 & 1 & 0 \\ 0 & 0 & 0 & 1 \\ 2\mathcal{D}_5 & 2\mathcal{D}_6 & 2\mathcal{D}_7 & 2\mathcal{D}_8 \\ 2\mathcal{D}_1 & 2\mathcal{D}_2 & 2\mathcal{D}_3 & 2\mathcal{D}_4 \end{pmatrix}, \quad (3.76)$$

so that the two above vectors reduce to

$$\begin{cases} \mathbf{p}^{\text{SGE}}(\mathbf{a}, \mathbf{b}^*) = \mathbf{a} + 2 \left(\mathbf{P}^{[1]} x_1^{(m,n)} + \mathbf{P}^{[2]} x_2^{(m,n)} \right) \mathbf{b}^* \\ \mathbf{q}^{\text{SGE}}(\mathbf{b}^*) = 2\mathbf{T}^{\text{SGE}} \mathbf{b}^*, \end{cases} \quad (3.77)$$

with

$$\mathbf{P}^{[1]} = \begin{pmatrix} 1 & 0 & 0 & 0 \\ \mathcal{D}_1 & \mathcal{D}_2 & \mathcal{D}_3 & \mathcal{D}_4 \\ \mathcal{D}_5 & \mathcal{D}_6 & \mathcal{D}_7 + 1 & \mathcal{D}_8 \end{pmatrix}, \quad \mathbf{P}^{[2]} = \begin{pmatrix} \mathcal{D}_5 & \mathcal{D}_6 & \mathcal{D}_7 & \mathcal{D}_8 \\ 0 & 0 & 0 & 1 \\ \mathcal{D}_1 & \mathcal{D}_2 + 1 & \mathcal{D}_3 & \mathcal{D}_4 \end{pmatrix}. \quad (3.78)$$

From Eqs.(3.73) and introducing $\mathbf{q}^* = 2\mathbf{b}^*$, the energy densities, Eqs.(3.68), can be rewritten as follow

$$\begin{cases} \mathcal{U}_{\mathbf{C}}(\mathbf{p}^{\text{SGE}}) = \frac{1}{2} C_{ij} p_i^{\text{SGE}} p_j^{\text{SGE}}, \\ \mathcal{U}_{\mathbf{M}}(\mathbf{p}^{\text{SGE}}, \mathbf{q}^*) = M_{jk}^* p_j^{\text{SGE}} q_k^*, & i, j = 1, 2, 3 \quad k, l = 1, \dots, 4 \\ \mathcal{U}_{\mathbf{A}}(\mathbf{q}^*) = \frac{1}{2} A_{kl}^* q_k^* q_l^*, \end{cases} \quad (3.79)$$

which implies that

$$\mathcal{U}_{\text{SGE}}(\mathbf{p}^{\text{SGE}}(\mathbf{a}, \mathbf{b}^*), \mathbf{q}^{\text{SGE}}(\mathbf{b}^*)) = \mathcal{U}_{\text{SGE}}(\mathbf{a}, \mathbf{b}^*). \quad (3.80)$$

In the energy expression Eq. (3.68) a *condensed representation* for the matrixes \mathbf{M} and \mathbf{A} has been introduced through matrixes \mathbf{A}_{kl}^* and \mathbf{M}_{jk}^* , which have reduced dimensions (the former is a rectangular 3×4 matrix and the latter is a symmetric

square matrices of order 4)

$$\mathbf{M}_{ij}^* = \begin{pmatrix} M_{11}^* & M_{12}^* & M_{13}^* & M_{14}^* \\ M_{21}^* & M_{22}^* & M_{23}^* & M_{24}^* \\ M_{31}^* & M_{32}^* & M_{33}^* & M_{34}^* \end{pmatrix}, \quad \mathbf{A}_{ij}^* = \begin{pmatrix} A_{11}^* & A_{12}^* & A_{13}^* & A_{14}^* \\ A_{12}^* & A_{22}^* & A_{23}^* & A_{24}^* \\ A_{13}^* & A_{23}^* & A_{33}^* & A_{34}^* \\ A_{14}^* & A_{24}^* & A_{34}^* & A_{44}^* \end{pmatrix}, \quad (3.81)$$

and are related to each other through

$$\mathbf{M}^* = \mathbf{M} \mathbf{T}^{\text{SGE}}, \quad \mathbf{A}^* = \left(\mathbf{T}^{\text{SGE}} \right)^T \mathbf{A} \mathbf{T}^{\text{SGE}}. \quad (3.82)$$

The elastic energy stored in an hexagonal element made up of second-gradient elastic continuum (with the same shape and location of the unit cell $\{m, n\}$ of the lattice) is obtained through integration of the strain energy density

$$\begin{aligned} U_{\text{SGE}}^{(m,n)}(\mathbf{a}, \mathbf{b}^*) &= \int_{\Omega(m,n)} u_{\text{SGE}}^{(m,n)}(\mathbf{a}, \mathbf{b}^*) d\Omega = \\ &= h\ell^2 \left\{ \mathbf{a} \cdot \mathbf{G}^{[1]}(C_{ij}) \mathbf{a} + 2\ell \mathbf{a} \cdot \left[m\mathbf{G}^{[2]}(C_{ij}) + n\mathbf{G}^{[3]}(C_{ij}) + \mathbf{G}^{[4]}(M_{ij}^*) \right] \mathbf{b}^* \right. \\ &\quad + \ell^2 \mathbf{b}^* \cdot \left[m^2 \mathbf{G}^{[5]}(C_{ij}) + n^2 \mathbf{G}^{[6]}(C_{ij}) + m n \mathbf{G}^{[7]}(C_{ij}) + m \mathbf{G}^{[8]}(M_{ij}^*) + \right. \\ &\quad \left. \left. + n \mathbf{G}^{[9]}(M_{ij}^*) + \mathbf{G}^{[10]}(C_{ij}, A_{ij}^*) \right] \mathbf{b}^* \right\}, \end{aligned} \quad (3.83)$$

where the coefficients of the matrixes $\mathbf{G}^{[r]}$ ($r = 1, \dots, 10$) are reported in Appendix A.

3.7 The equivalent second-gradient material

An energy matching can now be imposed between the lattice, Eq. (3.60), and an effective second-gradient material, Eq. (3.83), for every unit cell $\{m, n\}$ and every vectors \mathbf{a} and \mathbf{b}^*

$$U_{\text{lat}}^{(m,n)}(\mathbf{a}, \mathbf{b}^*) = U_{\text{SGE}}^{(m,n)}(\mathbf{a}, \mathbf{b}^*), \quad \forall m, n, \mathbf{a}, \mathbf{b}^*, \quad (3.84)$$

so that, using the representations (3.60) and (3.83), the following homogenization result is obtained

$$\mathbf{G}^{[r]} = \mathbf{H}^{[r]} \quad \forall r \in [1, 10]. \quad (3.85)$$

It is highlighted that the energy equivalence, Eq.(3.84), implies at first-order

$$\mathbf{G}^{[1]} = \mathbf{H}^{[1]}, \quad (3.86)$$

which directly defines all the coefficients of the matrix C_{ij} as

$$\begin{aligned} C_{11} = C_{22} &= \frac{2I_{[1]}I_{[2]} + 9I_{[3]}}{4\sqrt{3}I_{[2]}}, \quad C_{12} = \frac{2I_{[1]}I_{[2]} - 9I_{[3]}}{4\sqrt{3}I_{[2]}}, \\ C_{13} = C_{23} &= 0, \quad C_{33} = \frac{C_{11} - C_{12}}{2} = \frac{9I_{[3]}}{4\sqrt{3}I_{[2]}}, \end{aligned} \quad (3.87)$$

which values (coincide with those obtained in [20, 40] through a different identification technique) show that the two transformation matrices are the same for both the

lattice and the equivalent material,

$$\mathbf{T}^{\text{lat}} = \mathbf{T}^{\text{SGE}} \quad (3.88)$$

so that $\mathbf{b}^{\text{lat}} = \mathbf{b}^{\text{SGE}}$ and therefore $\boldsymbol{\beta}^{\text{lat}}(\mathbf{b}^*) = \boldsymbol{\beta}^{\text{SGE}}(\mathbf{b}^*)$ (see Sec. (3.8) for more details).

Finally, from Eq. (3.85) the ten components of the matrix A_{ij}^* are identified as

$$\begin{aligned} A_{13}^* &= 0, \quad A_{14}^* = 0, \quad A_{23}^* = 0, \quad A_{24}^* = 0, \\ A_{11}^* &= \frac{\sqrt{3}I_{[3]}\ell^2}{64I_{[1]}^2I_{[2]}^4} \left[-50\bar{k}^5(\hat{k} + \tilde{k})^3 - \bar{k}^4(\hat{k} + \tilde{k})^2 \left(100\hat{k}^2 + 359\hat{k}\tilde{k} + 100\tilde{k}^2 \right) + \right. \\ &\quad - \bar{k}^3(\hat{k} + \tilde{k}) \left(50\hat{k}^4 + 419\hat{k}^3\tilde{k} + 339\hat{k}^2\tilde{k}^2 + 419\hat{k}\tilde{k}^3 + 50\tilde{k}^4 \right) + \\ &\quad + 2\bar{k}^2\tilde{k}\tilde{k} \left(24\hat{k}^4 + 459\hat{k}^3\tilde{k} + 1853\hat{k}^2\tilde{k}^2 + 459\hat{k}\tilde{k}^3 + 24\tilde{k}^4 \right) + \\ &\quad \left. + \bar{k}\hat{k}^2\tilde{k}^2(\hat{k} + \tilde{k}) \left(219\hat{k}^2 + 1283\hat{k}\tilde{k} + 219\tilde{k}^2 \right) + 121\hat{k}^3\tilde{k}^3(\hat{k} + \tilde{k})^2 \right], \\ A_{12}^* &= \frac{\sqrt{3}I_{[3]}\ell^2}{64I_{[1]}^2I_{[2]}^4} \left[10\bar{k}^5(\hat{k} + \tilde{k})^3 + 5\bar{k}^4(\hat{k} + \tilde{k})^2 \left(4\hat{k}^2 + 5\hat{k}\tilde{k} + 4\tilde{k}^2 \right) + \right. \\ &\quad + \bar{k}^3(\hat{k} + \tilde{k}) \left(10\hat{k}^4 - 71\hat{k}^3\tilde{k} - 303\hat{k}^2\tilde{k}^2 - 71\hat{k}\tilde{k}^3 + 10\tilde{k}^4 \right) + \\ &\quad + 2\bar{k}^2\tilde{k}\tilde{k} \left(6\hat{k}^4 - 9\hat{k}^3\tilde{k} + 641\hat{k}^2\tilde{k}^2 - 9\hat{k}\tilde{k}^3 + 6\tilde{k}^4 \right) + \\ &\quad \left. - \bar{k}\hat{k}^2\tilde{k}^2(\hat{k} + \tilde{k}) \left(33\hat{k}^2 + \hat{k}\tilde{k} + 33\tilde{k}^2 \right) - 35\hat{k}^3\tilde{k}^3(\hat{k} + \tilde{k})^2 \right], \\ A_{22}^* &= \frac{\sqrt{3}I_{[3]}\ell^2}{64I_{[1]}^2I_{[2]}^4} \left[-10\bar{k}^5(\hat{k} + \tilde{k})^3 - \bar{k}^4(\hat{k} + \tilde{k})^2 \left(20\hat{k}^2 - 137\hat{k}\tilde{k} + 20\tilde{k}^2 \right) + \right. \\ &\quad - \bar{k}^3(\hat{k} + \tilde{k}) \left(10\hat{k}^4 - 53\hat{k}^3\tilde{k} + 219\hat{k}^2\tilde{k}^2 - 53\hat{k}\tilde{k}^3 + 10\tilde{k}^4 \right) + \\ &\quad + 2\bar{k}^2\tilde{k}\tilde{k} \left(12\hat{k}^4 - 45\hat{k}^3\tilde{k} + 349\hat{k}^2\tilde{k}^2 - 45\hat{k}\tilde{k}^3 + 12\tilde{k}^4 \right) + \\ &\quad \left. + \bar{k}\hat{k}^2\tilde{k}^2(\hat{k} + \tilde{k}) \left(51\hat{k}^2 - 197\hat{k}\tilde{k} + 51\tilde{k}^2 \right) + 17\hat{k}^3\tilde{k}^3(\hat{k} + \tilde{k})^2 \right], \\ A_{33}^* &= \frac{\sqrt{3}\ell^2}{192I_{[1]}^2I_{[2]}^4} \left[2\bar{k}^6(\hat{k} + \tilde{k})^3 \left(4\hat{k}^2 - 7\hat{k}\tilde{k} + 4\tilde{k}^2 \right) + \right. \\ &\quad + \bar{k}^5(\hat{k} + \tilde{k})^2 \left(16\hat{k}^4 - 132\hat{k}^3\tilde{k} + 181\hat{k}^2\tilde{k}^2 - 132\hat{k}\tilde{k}^3 + 16\tilde{k}^4 \right) + \\ &\quad + \bar{k}^4(\hat{k} + \tilde{k}) \left(8\hat{k}^6 - 110\hat{k}^5\tilde{k} + 301\hat{k}^4\tilde{k}^2 + 667\hat{k}^3\tilde{k}^3 + 301\hat{k}^2\tilde{k}^4 - 110\hat{k}\tilde{k}^5 + 8\tilde{k}^6 \right) + \\ &\quad + 2\bar{k}^3\tilde{k}\tilde{k} \left(4\hat{k}^6 + 27\hat{k}^5\tilde{k} - 101\hat{k}^4\tilde{k}^2 - 587\hat{k}^3\tilde{k}^3 - 101\hat{k}^2\tilde{k}^4 + 27\hat{k}\tilde{k}^5 + 4\tilde{k}^6 \right) + \\ &\quad - \bar{k}^2\hat{k}^2\tilde{k}^2(\hat{k} + \tilde{k}) \left(6\hat{k}^4 - 121\hat{k}^3\tilde{k} - 349\hat{k}^2\tilde{k}^2 - 121\hat{k}\tilde{k}^3 + 6\tilde{k}^4 \right) + \\ &\quad \left. - \bar{k}\hat{k}^3\tilde{k}^3(\hat{k} + \tilde{k})^2 \left(4\hat{k}^2 + 43\hat{k}\tilde{k} + 4\tilde{k}^2 \right) + 2\hat{k}^4\tilde{k}^4(\hat{k} + \tilde{k})^3 \right] \end{aligned} \quad (3.89)$$

$$\begin{aligned}
A_{34}^* &= \frac{\sqrt{3}\ell^2}{64I_{[1]}^2 I_{[2]}^4} \left[-2\bar{k}^6 (\hat{k} + \tilde{k})^3 (4\hat{k}^2 + 3\tilde{k}\hat{k} + 4\tilde{k}^2) + \right. \\
&\quad -\bar{k}^5 (\hat{k} + \tilde{k})^2 (16\hat{k}^4 + 4\hat{k}^3\tilde{k} - 63\hat{k}^2\tilde{k}^2 + 4\tilde{k}\hat{k}^3 + 16\tilde{k}^4) + \\
&\quad -\bar{k}^4 (\hat{k} + \tilde{k}) (8\hat{k}^6 + 6\hat{k}^5\tilde{k} - 267\hat{k}^4\tilde{k}^2 - 173\hat{k}^3\tilde{k}^3 - 267\hat{k}^2\tilde{k}^4 + 6\tilde{k}\hat{k}^5 + 8\tilde{k}^6) + \\
&\quad -2\bar{k}^3\tilde{k}\hat{k} (4\hat{k}^6 - 15\hat{k}^5\tilde{k} + 115\hat{k}^4\tilde{k}^2 + 461\hat{k}^3\tilde{k}^3 + 115\hat{k}^2\tilde{k}^4 - 15\tilde{k}\hat{k}^5 + 4\tilde{k}^6) + \\
&\quad +\bar{k}^2\tilde{k}^2\hat{k}^2 (\hat{k} + \tilde{k}) (6\hat{k}^4 + 71\hat{k}^3\tilde{k} + 43\hat{k}^2\tilde{k}^2 + 71\tilde{k}\hat{k}^3 + 6\tilde{k}^4) + \\
&\quad \left. +\bar{k}\hat{k}^3\tilde{k}^3 (\hat{k} + \tilde{k})^2 (4\hat{k}^2 + 35\tilde{k}\hat{k} + 4\tilde{k}^2) - 2\hat{k}^4\tilde{k}^4 (\hat{k} + \tilde{k})^3 \right], \\
A_{44}^* &= \frac{\sqrt{3}\ell^2}{64I_{[1]}^2 I_{[2]}^4} \left[2\bar{k}^6 (\hat{k} + \tilde{k})^3 (12\hat{k}^2 - \tilde{k}\hat{k} + 12\tilde{k}^2) + \right. \\
&\quad +\bar{k}^5 (\hat{k} + \tilde{k})^2 (48\hat{k}^4 + 260\hat{k}^3\tilde{k} + 103\hat{k}^2\tilde{k}^2 + 260\tilde{k}\hat{k}^3 + 48\tilde{k}^4) + \\
&\quad +\bar{k}^4 (\hat{k} + \tilde{k}) (24\hat{k}^6 + 286\hat{k}^5\tilde{k} + 583\hat{k}^4\tilde{k}^2 - 255\hat{k}^3\tilde{k}^3 + 583\hat{k}^2\tilde{k}^4 + 286\tilde{k}\hat{k}^5 + 24\tilde{k}^6) + \\
&\quad +2\bar{k}^3\tilde{k}\hat{k} (12\hat{k}^6 - 3\hat{k}^5\tilde{k} - 735\hat{k}^4\tilde{k}^2 - 1753\hat{k}^3\tilde{k}^3 - 735\hat{k}^2\tilde{k}^4 - 3\tilde{k}\hat{k}^5 + 12\tilde{k}^6) + \\
&\quad -\bar{k}^2\tilde{k}^2\hat{k}^2 (\hat{k} + \tilde{k}) (18\hat{k}^4 + 309\hat{k}^3\tilde{k} + 937\hat{k}^2\tilde{k}^2 + 309\tilde{k}\hat{k}^3 + 18\tilde{k}^4) + \\
&\quad \left. -\bar{k}\hat{k}^3\tilde{k}^3 (\hat{k} + \tilde{k})^2 (12\hat{k}^2 + 17\tilde{k}\hat{k} + 12\tilde{k}^2) + 6\hat{k}^4\tilde{k}^4 (\hat{k} + \tilde{k})^3 \right].
\end{aligned}$$

while the twelve components of the matrix M_{ij}^* as

$$\begin{aligned}
M_{11}^* &= M_{12}^* = M_{21}^* = M_{22}^* = M_{31}^* = M_{32}^* = M_{33}^* = M_{34}^* = 0, \\
M_{13}^* &= M_{23}^* = \frac{(\hat{k} - \tilde{k})(I_{[1]}I_{[2]} - 9I_{[3]})(\tilde{k}\hat{k} - 2\bar{k}(\hat{k} + \tilde{k}))}{8\sqrt{3}I_{[1]}I_{[2]}^2}\ell, \\
M_{14}^* &= M_{24}^* = -\frac{3(\hat{k} - \tilde{k})(I_{[1]}I_{[2]} + 3I_{[3]})(\tilde{k}\hat{k} - 2\bar{k}(\hat{k} + \tilde{k}))}{8\sqrt{3}I_{[1]}I_{[2]}^2}\ell.
\end{aligned} \tag{3.90}$$

The result provided by Eqs. (3.87)–(3.90) shows that

the mechanical response of an hexagonal lattice made of three different orders of linear elastic bars exhibits (i.) non-locality, (ii.) non-centrosymmetry, and (iii.) anisotropy. The effective response approaches that of a Cauchy elastic material in the limit of vanishing length of the lattice's bars, $\ell \rightarrow 0$, a condition for which $M_{ij} = A_{ij} = 0$.

Furthermore, the elastic coefficient matrices are invariant with respect the following permutation of $\{\bar{k}, \hat{k}, \tilde{k}\}$:

$$\begin{aligned}
\mathbf{C}(\kappa_1, \kappa_2, \kappa_3) &= \mathbf{C}(\kappa_1, \kappa_3, \kappa_2) = \mathbf{C}(\kappa_2, \kappa_1, \kappa_3) = \mathbf{C}(\kappa_2, \kappa_3, \kappa_1) = \mathbf{C}(\kappa_3, \kappa_1, \kappa_2) = \mathbf{C}(\kappa_3, \kappa_2, \kappa_1) \\
\mathbf{A}^*(\kappa_1, \kappa_2, \kappa_3) &= \mathbf{A}^*(\kappa_1, \kappa_3, \kappa_2), \quad \mathbf{M}^*(\kappa_1, \kappa_2, \kappa_3) = -\mathbf{M}^*(\kappa_1, \kappa_3, \kappa_2)
\end{aligned} \tag{3.91}$$

From Eqs. (3.87)–(3.90) it is evident that the stiffness ratio between the bars may have a dramatic effect on the equivalent solid response, that will be further discussed in the following chapters of this thesis.

3.8 A note on the quadratic displacement condition.

It is remarked that, although $\beta^{\text{SGE}} = \beta^{\text{lat}}$, the displacement fields imposed to the lattice differs from that imposed to the equivalent solid due to the presence of the

additional field $\Delta \mathbf{u}^{(m,n|i)}$ in the former.

From the practical point of view, the amplitude of such an additional field does not play an important role when compared to the amplitude of the quadratic part, so that the deformed configuration of the solid very well represents that of the lattice, even if in the latter the additional field is present.

To analyze the influence of the additional field on the kinematics of the lattice and of the equivalent solid, a rectangular domain (having sides $25\sqrt{3}\ell \times 37\ell$) is considered, occupied in one case by the lattice, which is shown on the left of Fig. 3.4, (625 hexagonal unit cells, namely, 25 along each axis of the rectangle) and in the other case by the equivalent continuum (not reported in Fig. 3.4). The solid is subject to a displacement field characterized by tensors α and β^{SGE} , while the lattice is subject to the same α and to β^{lat} , plus the additional field $\Delta \mathbf{u}^{(m,n|i)}$. In particular, the following values have been selected to produce the figure $\alpha_{11} = 0.018$, $\alpha_{22} = 0.02$, $\alpha_{12} = 0.02$ and $\beta_{111}^{\text{SGE}} = \beta_{111}^{\text{lat}} = 0.0029$, $\beta_{221}^{\text{SGE}} = \beta_{221}^{\text{lat}} = 0.00286$, $\beta_{112}^{\text{SGE}} = \beta_{112}^{\text{lat}} = 0.003$, $\beta_{222}^{\text{SGE}} = \beta_{222}^{\text{lat}} = 0.004$. Moreover, having selected the following bars' stiffness ratios $\hat{k}/\bar{k} = 2$ and $\tilde{k}/\bar{k} = 3$, the remaining components $\beta_{211}^{\text{SGE}} = \beta_{211}^{\text{lat}} = -0.007$, $\beta_{122}^{\text{SGE}} = \beta_{122}^{\text{lat}} = -0.0052$ have been calculated from Eq. (3.46) and (3.73). The additional field $\Delta \mathbf{u}^{(m,n|i)}$ applied to the lattice has been calculated with the given values of α and β^{lat} through Eq. (3.44), (3.45), and (3.51).

The deformed domains for the equivalent solid and the lattice are sketched on the right of Fig. 3.4, where the displacements of the lattice's nodes are reported as dots and the displacements of the equivalent solid as lines. The fact that the dots lie on the lines demonstrates that the additional field affects only marginally the displacement field of the lattice, in which the linear and quadratic displacement fields prevail.

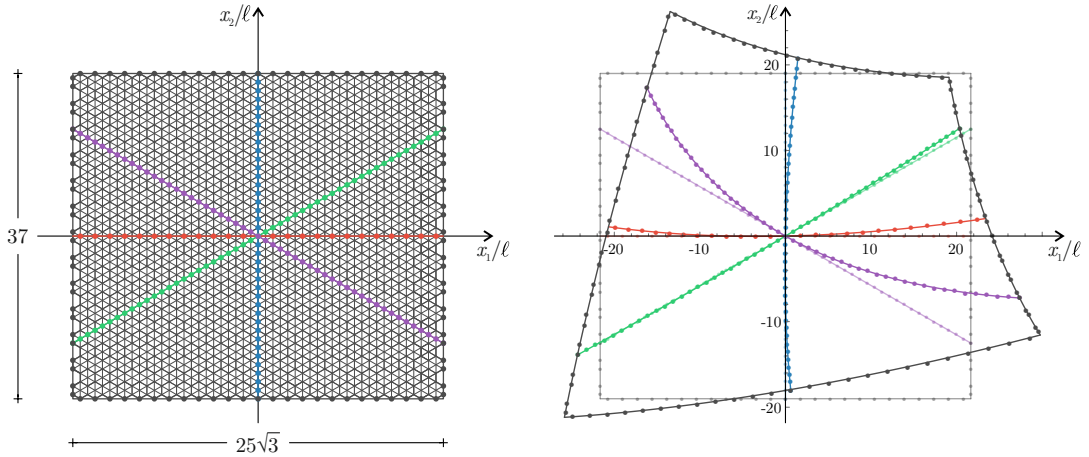


FIGURE 3.4: Nonlocal constitutive parameters M_{13}^* (left) and M_{14}^* (right) as functions of the bar stiffness ratios \hat{k}/\bar{k} and \tilde{k}/\bar{k} . The red lines represent the stiffness ratios pairs for which a centrosymmetric response is attained, while in all the other cases the solid equivalent to the hexagonal bars' lattice displays a non-centrosymmetric mechanical behaviour.

As an example, the higher-order constitutive parameters M_{13}^* and M_{14}^* ruling the non-centrosymmetric behaviour (and made dimensionless through division by $\bar{k}\ell$) are portrayed in Fig. 3.5 when two stiffness ratios \hat{k}/\bar{k} and \tilde{k}/\bar{k} are varied. The red lines highlight the condition for which both parameters are annihilated, so that, correspondingly, centrosymmetric response is retrieved.

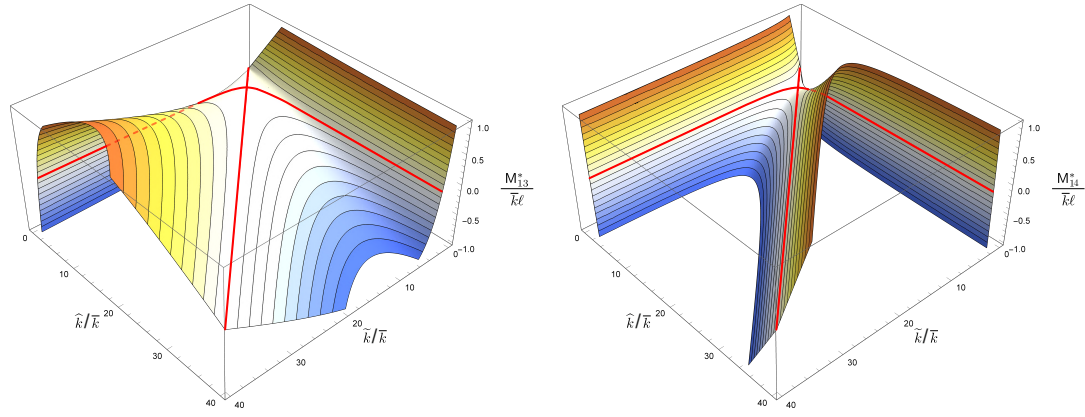


FIGURE 3.5: Nonlocal constitutive parameters M_{13}^* (left) and M_{14}^* (right) as functions of the bar stiffness ratios \hat{k}/\bar{k} and \tilde{k}/\bar{k} . The red lines represent the stiffness ratios pairs for which a centrosymmetric response is attained, while in all the other cases the solid equivalent to the hexagonal bars' lattice displays a non-centrosymmetric mechanical behaviour.

Chapter 4

Derivation of the constitutive law for the equivalent SGE

4.1 The equivalent second-gradient elastic material

The three constitutive matrices, which will be derived in the following *Chapter* from the ‘condensed’ constitutive material identified in *Chapter 3* of this thesis, $\mathbf{C}(\bar{k}, \hat{k}, \tilde{k})$, $\mathbf{M}(\bar{k}, \hat{k}, \tilde{k})$, and $\mathbf{A}(\bar{k}, \hat{k}, \tilde{k})$ are here presented

$$\begin{aligned} \mathbf{C}(\bar{k}, \hat{k}, \tilde{k}) &= \begin{pmatrix} \lambda' + 2\mu & \lambda' & 0 \\ \lambda' & \lambda' + 2\mu & 0 \\ 0 & 0 & \mu \end{pmatrix}, \\ \mathbf{M}(\bar{k}, \hat{k}, \tilde{k}) &= m_{13}\ell \begin{pmatrix} 0 & 0 & 1 & -1 & 1 & 0 \\ 0 & 0 & 1 & -1 & 1 & 0 \\ 0 & 0 & 0 & 0 & 0 & 0 \end{pmatrix}, \\ \mathbf{A}(\bar{k}, \hat{k}, \tilde{k}) &= \ell^2 \begin{pmatrix} a_{11} & a_{12} & 0 & 0 & 0 & a_{16} \\ a_{12} & a_{22} & 0 & 0 & 0 & a_{26} \\ 0 & 0 & a_{33} & a_{34} & a_{35} & 0 \\ 0 & 0 & a_{34} & a_{44} & a_{45} & 0 \\ 0 & 0 & a_{35} & a_{45} & a_{55} & 0 \\ a_{16} & a_{26} & 0 & 0 & 0 & a_{66} \end{pmatrix}, \end{aligned} \quad (4.1)$$

where $a_{22} = a_{11} - 2(a_{16} + a_{26})$, $a_{33} = a_{11} + a_{12} - 2(a_{16} + a_{26}) - a_{34}$, $a_{35} = a_{12} + a_{26} - a_{34}$, $a_{44} = a_{11} + a_{12} - a_{34}$, $a_{45} = -a_{12} + a_{16} + a_{34}$, $a_{55} = (a_{11} + a_{12} - a_{16} - a_{26} - 2a_{34})/2$, and $a_{66} = (a_{11} - a_{12} - a_{16} - a_{26})/2$.

The constitutive matrices $\mathbf{C}(\bar{k}, \hat{k}, \tilde{k})$, $\mathbf{M}(\bar{k}, \hat{k}, \tilde{k})$, and $\mathbf{A}(\bar{k}, \hat{k}, \tilde{k})$ are seen to belong, respectively, to the following symmetry classes $O(2)$ (Isotropy), Z_3 ($2/3\pi$ without reflection symmetry) and D_6 ($\pi/3$ with reflection symmetry). The constants of the equivalent material are given by

$$\lambda' = \frac{2I_{[1]}I_{[2]} - 9I_{[3]}}{4\sqrt{3}I_{[2]}}, \quad \mu = \frac{9I_{[3]}}{4\sqrt{3}I_{[2]}}, \quad (4.2)$$

for the Cauchy part of the equivalent elastic material, which are now expressed using the Lamé constants,

$$m_{13} = \frac{(\hat{k} - \tilde{k})(\tilde{k}\tilde{k} - 2\bar{k}(\hat{k} + \tilde{k}))}{8\sqrt{3}I_{[2]}}, \quad (4.3)$$

for the only one non-centrosymmetric part of the equivalent elastic material

$$\begin{aligned} a_{11} &= \frac{\sqrt{3}}{576I_{[2]}^3} \left[48\bar{k}^5(\hat{k} + \tilde{k})^2 + 4\bar{k}^4(\hat{k} + \tilde{k})(31\hat{k}^2 + 194\tilde{k}\tilde{k} + 31\tilde{k}^2) \right. \\ &\quad + \bar{k}^3(28\hat{k}^4 + 814\hat{k}^3\tilde{k} + 3024\hat{k}^2\tilde{k}^2 + 814\tilde{k}\tilde{k}^3 + 28\tilde{k}^4) \\ &\quad + 6I_{[3]}\bar{k}(\hat{k} + \tilde{k})(14\hat{k}^2 + 263\tilde{k}\tilde{k} + 14\tilde{k}^2) \\ &\quad \left. + I_{[3]}\tilde{k}\tilde{k}(84\hat{k}^2 + 757\tilde{k}\tilde{k} + 84\tilde{k}^2) + 28\tilde{k}^3\tilde{k}^3(\hat{k} + \tilde{k}) \right], \\ a_{12} &= \frac{3\sqrt{3}I_{[3]}}{64I_{[2]}^3} \left[8\bar{k}^3(\hat{k} + \tilde{k}) + \bar{k}^2(8\hat{k}^2 + 60\tilde{k}\tilde{k} + 8\tilde{k}^2) + 20I_{[3]}(\hat{k} + \tilde{k}) + 3\hat{k}^2\tilde{k}^2 \right], \\ a_{16} &= \frac{\sqrt{3}}{576I_{[2]}^2} \left[24\bar{k}^4(\hat{k} + \tilde{k}) + \bar{k}^3(62\hat{k}^2 + 256\tilde{k}\tilde{k} + 62\tilde{k}^2) \right. \\ &\quad + \bar{k}^2(\hat{k} + \tilde{k})(14\hat{k}^2 + 299\tilde{k}\tilde{k} + 14\tilde{k}^2) \\ &\quad \left. + 4I_{[3]}(7\hat{k}^2 + 19\tilde{k}\tilde{k} + 7\tilde{k}^2) + 14\hat{k}^2\tilde{k}^2(\hat{k} + \tilde{k}) \right], \\ a_{26} &= \frac{\sqrt{3}I_{[3]}}{64I_{[2]}^2} \left[12\bar{k}^2 + 7\bar{k}(\hat{k} + \tilde{k}) + 22\tilde{k}\tilde{k} \right], \\ a_{34} &= \frac{\sqrt{3}}{192I_{[2]}^3} \left[72I_{[3]}\bar{k}^3(\hat{k} + \tilde{k}) + \bar{k}^3(-8\hat{k}^4 + 40\hat{k}^3\tilde{k} + 492\hat{k}^2\tilde{k}^2 + 40\tilde{k}\tilde{k}^3 - 8\tilde{k}^4) \right. \\ &\quad \left. + 234I_{[3]}^2(\hat{k} + \tilde{k}) + 3I_{[3]}\tilde{k}\tilde{k}(2\hat{k}^2 + 31\tilde{k}\tilde{k} + 2\tilde{k}^2) - 2\hat{k}^3\tilde{k}^3(\hat{k} + \tilde{k}) \right] \end{aligned} \quad (4.4)$$

for the curvature part of the equivalent elastic material, and where h is the thickness of the lattice, $I_{[1]} = \bar{k} + \hat{k} + \tilde{k}$, $I_{[2]} = \bar{k}\tilde{k} + \tilde{k}\tilde{k} + \tilde{k}\tilde{k}$, $I_{[3]} = \bar{k}\tilde{k}\tilde{k}$, and λ' is λ for a *plane strain problem* while $\frac{2\lambda\mu}{\lambda + 2\mu}$ for a *plane stress problem*.

4.2 From the solid in the ‘condensed form’ to the full **SGE**: symmetries and positive definiteness

Based on a generic quadratic displacement field, the hexagonal lattice (only subject to axial forces) shown in Fig. 4.1 (left, characterized by three values of axial stiffness $\{\bar{k}, \hat{k}, \tilde{k}\}$) was found (in Chapter 3) to be energetically equivalent to a homogeneous solid modelled as a second-gradient elastic material (**SGE**),

$$u_{\text{SGE}}(\mathbf{p}, \mathbf{q}^*) = \underbrace{\frac{1}{2}\mathbf{p}^{\text{SGE}T} \mathbf{C}(\bar{k}, \tilde{k}, \hat{k}) \mathbf{p}^{\text{SGE}}}_{u_{\mathbf{C}}(\mathbf{p}^{\text{SGE}})} + \underbrace{\mathbf{p}^{\text{SGE}T} \mathbf{M}^*(\bar{k}, \tilde{k}, \hat{k}) \mathbf{q}^*}_{u_{\mathbf{M}^*}(\mathbf{p}^{\text{SGE}}, \mathbf{q}^*)} + \underbrace{\frac{1}{2}\mathbf{q}^{*T} \mathbf{A}^*(\bar{k}, \tilde{k}, \hat{k}) \mathbf{q}^*}_{u_{\mathbf{A}^*}(\mathbf{q}^*)}, \quad (4.5)$$

where vectors \mathbf{p}^{SGE} and \mathbf{q}^* respectively collect the ‘condensed’ components of the deformation ϵ and curvature χ tensors as $\mathbf{p}^{\text{SGE}} = [\epsilon_{11}, \epsilon_{22}, 2\epsilon_{12}]^T$ and $\mathbf{q}^* = [\chi_{111}, \chi_{221},$

$\chi_{112}, \chi_{222}]^T$ and the three matrices $\mathbf{C}(\bar{k}, \hat{k}, \tilde{k})$, $\mathbf{M}^*(\bar{k}, \hat{k}, \tilde{k})$, and $\mathbf{A}^*(\bar{k}, \hat{k}, \tilde{k})$ assume the following expressions

$$\mathbf{C} = \begin{pmatrix} C_{12} + 2C_{33} & C_{12} & 0 \\ C_{12} & C_{12} + 2C_{33} & 0 \\ 0 & 0 & C_{33} \end{pmatrix}, \quad \mathbf{M}^* = \frac{(\hat{k} - \tilde{k})(\tilde{k}\tilde{k} - 2\bar{k}(\hat{k} + \tilde{k}))\ell}{8\sqrt{3}I_{[1]}I_{[2]}^2} \begin{pmatrix} 0 & 0 & m_{13}^* & m_{14}^* \\ 0 & 0 & m_{13}^* & m_{14}^* \\ 0 & 0 & 0 & 0 \end{pmatrix},$$

$$\mathbf{A}^* = \frac{\sqrt{3}I_{[3]}\ell^2}{64I_{[1]}^2I_{[2]}^4} \begin{pmatrix} a_{11}^* & a_{12}^* & 0 & 0 \\ a_{12}^* & a_{22}^* & 0 & 0 \\ 0 & 0 & a_{33}^* & a_{34}^* \\ 0 & 0 & a_{34}^* & a_{44}^* \end{pmatrix}. \quad (4.6)$$

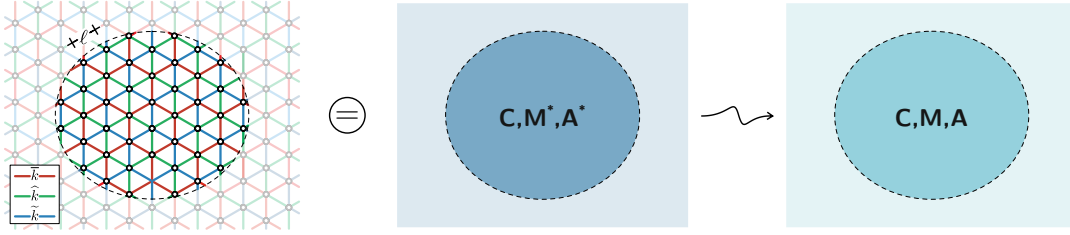


FIGURE 4.1: The second-gradient elastic material in the ‘condensed form’ (center) characterized by the matrices \mathbf{C} , \mathbf{M}^* , and \mathbf{A}^* (identified in Part I of this study) as the solid energetically equivalent to the hexagonal lattice microstructure (left) with elastic bars characterized by the three values of axial stiffness \bar{k} , \hat{k} and \tilde{k} (distinguished through different colours). The second-gradient elastic material (right) characterized by matrices \mathbf{C} , \mathbf{M} , and \mathbf{A} obtained from a relaxation of the solid in the ‘condensed form’.

The coefficients involved in the matrix \mathbf{C} were found (in Part I of this study) to be

$$C_{12} = \frac{2I_{[1]}I_{[2]} - 9I_{[3]}}{4\sqrt{3}I_{[2]}}, \quad C_{33} = \frac{9I_{[3]}}{4\sqrt{3}I_{[2]}}, \quad (4.7)$$

while matrix \mathbf{M}^* is characterized by

$$m_{13}^* = I_{[1]}I_{[2]} - 9I_{[3]}, \quad m_{14}^* = -3(I_{[1]}I_{[2]} + 3I_{[3]}), \quad (4.8)$$

while matrix \mathbf{A}^* is (in an alternative, but equivalent expression, to that given in Chapter 3)

$$\begin{aligned} a_{12}^* = & \left[10\bar{k}^5 (\hat{k} + \tilde{k})^3 + 5\bar{k}^4 (\hat{k} + \tilde{k})^2 (4\hat{k}^2 + 5\tilde{k}\hat{k} + 4\tilde{k}^2) \right. \\ & + \bar{k}^3 (\hat{k} + \tilde{k}) (10\hat{k}^4 - 71\hat{k}^3\tilde{k} - 303\hat{k}^2\tilde{k}^2 - 71\hat{k}\tilde{k}^3 + 10\tilde{k}^4) \\ & + 2\bar{k}^2\tilde{k}\hat{k} (6\hat{k}^4 - 9\hat{k}^3\tilde{k} + 641\hat{k}^2\tilde{k}^2 - 9\hat{k}\tilde{k}^3 + 6\tilde{k}^4) \\ & \left. - \bar{k}\hat{k}^2\tilde{k}^2 (\hat{k} + \tilde{k}) (33\hat{k}^2 + \tilde{k}\hat{k} + 33\tilde{k}^2) - 35\hat{k}^3\tilde{k}^3 (\hat{k} + \tilde{k})^2 \right], \end{aligned}$$

$$\begin{aligned}
a_{12}^* - a_{11}^* &= 12I_{[1]}I_{[2]} \left[\left(5\bar{k} (\hat{k} + \tilde{k}) - 13\tilde{k}\tilde{k} \right) (\bar{k}^2 (\hat{k} + \tilde{k}) \right. \\
&\quad \left. + \bar{k} (\hat{k}^2 + 6\tilde{k}\tilde{k} + \tilde{k}^2) + \tilde{k}\tilde{k} (\hat{k} + \tilde{k}) \right) \Big], \\
a_{11}^* - a_{22}^* &= 8I_{[1]}I_{[2]} \left[\left(13\tilde{k}\tilde{k} - 5\bar{k} (\hat{k} + \tilde{k}) \right) (\bar{k}^2 (\hat{k} + \tilde{k}) \right. \\
&\quad \left. + \bar{k} (\hat{k}^2 + 12\tilde{k}\tilde{k} + \tilde{k}^2) + \tilde{k}\tilde{k} (\hat{k} + \tilde{k}) \right) \Big], \\
a_{33}^* - a_{22}^* &= \frac{2}{3I_{[3]}} \left[\left(\bar{k}^2 (\hat{k} + \tilde{k}) + \bar{k} (\hat{k}^2 - 6\tilde{k}\tilde{k} + \tilde{k}^2) + \tilde{k}\tilde{k} (\hat{k} + \tilde{k}) \right)^2 \left(4\bar{k}^2 (\hat{k} + \tilde{k})^3 \right. \right. \\
&\quad \left. \left. - I_{[3]} \left(4\hat{k}^2 + 35\tilde{k}\tilde{k} + 4\tilde{k}^2 \right) + \hat{k}^2\tilde{k}^2 (\hat{k} + \tilde{k}) \right) \right], \\
a_{33}^* - a_{34}^* &= \frac{4I_{[1]}I_{[2]}}{3I_{[3]}} \left[\left(\bar{k}^2 (\hat{k} + \tilde{k}) + \bar{k} (\hat{k}^2 - 6\tilde{k}\tilde{k} + \tilde{k}^2) \right. \right. \\
&\quad \left. \left. + \tilde{k}\tilde{k} (\hat{k} + \tilde{k}) \right) (\bar{k}^2 (\hat{k} + \tilde{k}) (8\hat{k}^2 + \tilde{k}\tilde{k} + 8\tilde{k}^2) \right. \\
&\quad \left. \left. - I_{[3]} \left(8\hat{k}^2 + 31\tilde{k}\tilde{k} + 8\tilde{k}^2 \right) + 2\hat{k}^2\tilde{k}^2 (\hat{k} + \tilde{k}) \right) \right], \\
a_{44}^* - a_{33}^* &= \frac{8I_{[1]}I_{[2]}}{3I_{[3]}} \left[\left(\bar{k}^2 (\hat{k} + \tilde{k}) + \bar{k} (\hat{k}^2 + 12\tilde{k}\tilde{k} + \tilde{k}^2) \right. \right. \\
&\quad \left. \left. + \tilde{k}\tilde{k} (\hat{k} + \tilde{k}) \right) (\bar{k}^2 (\hat{k} + \tilde{k}) (8\hat{k}^2 + \tilde{k}\tilde{k} + 8\tilde{k}^2) \right. \\
&\quad \left. \left. - I_{[3]} \left(8\hat{k}^2 + 31\tilde{k}\tilde{k} + 8\tilde{k}^2 \right) + 2\hat{k}^2\tilde{k}^2 (\hat{k} + \tilde{k}) \right) \right],
\end{aligned} \tag{4.9}$$

The expression of the elastic energy for a ‘standard SGE’ material is the following one

$$\mathcal{U}_{\text{SGE}}(\mathbf{p}, \mathbf{q}) = \frac{1}{2} \mathbf{p}^T \mathbf{C} \mathbf{p} + \mathbf{p}^T \mathbf{M} \mathbf{q} + \frac{1}{2} \mathbf{q}^T \mathbf{A} \mathbf{q}. \tag{4.10}$$

When the ‘standard SGE’ is subjected to a quadratic and self-equilibrated displacement field Eqs. (3.71), the elastic energy that it stores Eq. (4.10) must be equal to the energy Eq. (4.5), i.e.

$$\mathcal{U}_{\text{SGE}}(\mathbf{p}^{\text{SGE}}, \mathbf{q}^{\text{SGE}}) = \mathcal{U}_{\text{SGE}}(\mathbf{p}, \mathbf{q}^*), \tag{4.11}$$

where

$$\mathcal{U}_{\text{SGE}}(\mathbf{p}^{\text{SGE}}, \mathbf{q}^{\text{SGE}}) = \frac{1}{2} \mathbf{p}^{\text{SGE}T} \mathbf{C} \mathbf{p}^{\text{SGE}} + \mathbf{p}^{\text{SGE}T} \mathbf{M} \mathbf{q}^{\text{SGE}} + \frac{1}{2} \mathbf{q}^{\text{SGE}T} \mathbf{A} \mathbf{q}^{\text{SGE}}. \tag{4.12}$$

The matrices \mathbf{M} and \mathbf{A} , and the curvature vector $\mathbf{q}^{\text{SGE}} = [\chi_{111}, \chi_{221}, \chi_{112}, \chi_{222}, \chi_{211}^{\text{SGE}}, \chi_{122}^{\text{SGE}}]^T$ are connected to matrices \mathbf{M}^* and \mathbf{A}^* of the condensed model, and the curvature vector \mathbf{q}^* through the following relations

$$\mathbf{M}^* = \mathbf{M} \mathbf{T}^{\text{SGE}}, \quad \mathbf{A}^* = \mathbf{T}^{\text{SGE}T} \mathbf{A} \mathbf{T}^{\text{SGE}}, \quad \mathbf{q}^{\text{SGE}} = \mathbf{T}^{\text{SGE}} \mathbf{q}^*, \tag{4.13}$$

where

$$\mathbf{T}^{\text{SGE}} = \begin{pmatrix} 1 & 0 & 0 & 0 \\ 0 & 1 & 0 & 0 \\ 0 & 0 & 1 & 0 \\ 0 & 0 & 0 & 1 \\ 0 & 0 & -\frac{2C_{33}}{C_{12} + C_{33}} & \frac{2C_{12}}{C_{12} + C_{33}} - 4 \\ \frac{2C_{12}}{C_{12} + C_{33}} - 4 & -\frac{2C_{33}}{C_{12} + C_{33}} & 0 & 0 \end{pmatrix}. \quad (4.14)$$

According to Eqs. (4.13), the matrices \mathbf{M} and \mathbf{A} can be obtained from the identified matrices \mathbf{M}^* and \mathbf{A}^* , and the vector \mathbf{q}^* can be related to the vector \mathbf{q}^{SGE} through the following linear relations

$$\mathbf{M} = \mathbf{M}^* \mathbf{Q} + \Delta \mathbf{M}, \quad \mathbf{A} = \mathbf{Q}^T \mathbf{A}^* \mathbf{Q} + \Delta \mathbf{A} \quad \text{and} \quad \mathbf{q}^* = \mathbf{Q} \mathbf{q}^{\text{SGE}}, \quad (4.15)$$

where $\Delta \mathbf{M}$ and $\Delta \mathbf{A}$ are additional constitutive matrices (the latter symmetric) yet to be identified, while \mathbf{Q} is a rectangular 4×6 transformation matrix, with the properties

$$\mathbf{Q} \mathbf{T}^{\text{SGE}} = \mathbf{I}, \quad \Delta \mathbf{M} \mathbf{T}^{\text{SGE}} = \mathbf{0}, \quad \Delta \mathbf{A} \mathbf{T}^{\text{SGE}} = \mathbf{0}, \quad (4.16)$$

(being \mathbf{I} the identity 4×4 matrix) so that the energy matching imposed for the condensed material implies that for the not condensed one, Eq. (4.11). It is noted that the constraint provided by Eqs. (4.16) does not completely define the matrices \mathbf{Q} , $\Delta \mathbf{M}$ and $\Delta \mathbf{A}$. Indeed, eight over the twenty-four coefficients of the transformation matrix \mathbf{Q} , six over the eighteen coefficients of $\Delta \mathbf{M}$ and three over the twenty-one independent coefficient of $\Delta \mathbf{A}$ remain still undetermined after imposing Eqs. (4.16).

The matrix \mathbf{Q} , $\Delta \mathbf{M}$, and $\Delta \mathbf{A}$ are

$$\begin{aligned} \mathbf{Q} &= -Z \begin{pmatrix} Q_{16} & 0 & 0 & Q_{15} & 0 & 0 \\ Q_{26} & 0 & 0 & Q_{25} & 0 & 0 \\ Q_{36} & 0 & 0 & Q_{35} & 0 & 0 \\ Q_{46} & 0 & 0 & Q_{45} & 0 & 0 \end{pmatrix} - Y \begin{pmatrix} 0 & Q_{16} & Q_{15} & 0 & 0 & 0 \\ 0 & Q_{26} & Q_{25} & 0 & 0 & 0 \\ 0 & Q_{36} & Q_{35} & 0 & 0 & 0 \\ 0 & Q_{46} & Q_{45} & 0 & 0 & 0 \end{pmatrix} + \begin{pmatrix} 1 & 0 & 0 & 0 & Q_{15} & Q_{16} \\ 0 & 1 & 0 & 0 & Q_{25} & Q_{26} \\ 0 & 0 & 1 & 0 & Q_{35} & Q_{36} \\ 0 & 0 & 0 & 1 & Q_{45} & Q_{46} \end{pmatrix}, \\ \Delta \mathbf{M} &= \begin{pmatrix} -\Delta M_{16}Z & -\Delta M_{16}Y & -\Delta M_{15}Y & -\Delta M_{15}Z & \Delta M_{15} & \Delta M_{16} \\ -\Delta M_{26}Z & -\Delta M_{26}Y & -\Delta M_{25}Y & -\Delta M_{25}Z & \Delta M_{25} & \Delta M_{26} \\ -\Delta M_{36}Z & -\Delta M_{36}Y & -\Delta M_{35}Y & -\Delta M_{35}Z & \Delta M_{35} & \Delta M_{36} \end{pmatrix}, \\ \Delta \mathbf{A} &= \begin{pmatrix} \Delta A_{11} & \frac{\Delta A_{11}Y}{Z} & -\Delta A_{15}Y & -\Delta A_{15}Z & \Delta A_{15} & -\frac{\Delta A_{11}}{Z} \\ \frac{\Delta A_{11}Y}{Z} & \frac{\Delta A_{11}Y^2}{Z^2} & -\frac{\Delta A_{15}Y^2}{Z} & -\Delta A_{15}Y & \frac{\Delta A_{15}Y}{Z} & -\frac{\Delta A_{11}Y}{Z^2} \\ -\Delta A_{15}Y & -\frac{\Delta A_{15}Y^2}{Z} & -\Delta A_{35}Y & -\Delta A_{35}Z & \Delta A_{35} & \frac{\Delta A_{15}Y}{Z} \\ -\Delta A_{15}Z & -\Delta A_{15}Y & -\Delta A_{35}Z & -\frac{\Delta A_{35}Z^2}{Y} & \frac{\Delta A_{35}Z}{Y} & \Delta A_{15} \\ \Delta A_{15} & \frac{\Delta A_{15}Y}{Z} & \Delta A_{35} & \frac{\Delta A_{35}Z}{Y} & -\frac{\Delta A_{35}}{Y} & -\frac{\Delta A_{15}}{Z} \\ -\frac{\Delta A_{11}}{Z} & -\frac{\Delta A_{11}Y}{Z^2} & \frac{\Delta A_{15}Y}{Z} & \Delta A_{15} & -\frac{\Delta A_{15}}{Z} & \frac{\Delta A_{11}}{Z^2} \end{pmatrix}. \end{aligned} \quad (4.17)$$

where $Y = -\frac{2C_{33}}{C_{12} + C_{33}}$ and $Z = -\frac{2(C_{12} + 2C_{33})}{C_{12} + C_{33}}$.

In this *Chapter* it is first shown that the three identified matrices $\mathbf{C}(\bar{k}, \hat{k}, \tilde{k})$, $\mathbf{M}^*(\bar{k}, \hat{k}, \tilde{k})$, and $\mathbf{A}^*(\bar{k}, \hat{k}, \tilde{k})$ respectively belong to the following symmetry classes: $O(2)$ (isotropy), Z_3 ($2/3\pi$ without reflection symmetry) and D_6 ($\pi/3$ with reflection symmetry), then the symmetry properties are going to be used to further constraint the undetermined coefficients of the matrices \mathbf{Q} , $\Delta\mathbf{M}$, and $\Delta\mathbf{A}$. The domain of positive definiteness of the equivalent (condensed and un-condensed) material is then investigated, and required to be the same, at varying of the two independent stiffness ratios of the lattice. Finally, a way is proposed to define the remaining undetermined parameters in the constitutive equations.

4.3 Anisotropy characterization

Recalling the transformation matrices $\mathbf{S}_{[p]}$, $\mathbf{R}_{[p]}(\theta)$, $\mathbf{S}_{[q]}$ and, $\mathbf{R}_{[q]}(\theta)$ seen in *Chapter 2* to introduce a rotation or reflection of a reference system, it is possible to investigate the anisotropy of the elastic coefficients matrix C_{ij} .

4.3.1 Isotropy of the first-order equivalent material \mathbf{C}

The material is said to be symmetric with respect to the rotation θ when

$$\mathbf{R}_{[p]}^T(\theta)\mathbf{C}\mathbf{R}_{[p]}(\theta) = \mathbf{C}, \quad (4.18)$$

and mirror symmetric with respect to the reflection $\mathbf{S}_{[p]}$ when

$$\mathbf{S}_{[p]}^T\mathbf{C}\mathbf{S}_{[p]} = \mathbf{C}. \quad (4.19)$$

When condition (4.18) holds true for all $\theta \in [0, 2\pi]$ and condition (4.19) is also verified, the material is isotropic and centrosymmetric, as is the case of the effective first-order material \mathbf{C} , Eq. (4.6)₁.

4.3.2 The condensed transformation matrix and the characterization of \mathbf{M}^* and \mathbf{A}^*

In a reference system denoted with symbol $\#$ the following relations hold

$$\mathbf{q}^{\text{SGE}\#} = \mathbf{T}^{\text{SGE}\#}\mathbf{q}^{*\#}, \quad \mathbf{q}^{*\#} = \mathbf{Q}^{\#}\mathbf{q}^{\text{SGE}\#}, \quad (4.20)$$

so that the analogous of Eq. (4.16) can now be written as

$$\mathbf{Q}^{\#}\mathbf{T}^{\text{SGE}\#} = \mathbf{I}, \quad (4.21)$$

while the non condensed vector \mathbf{q}^{SGE} transforms as

$$\mathbf{q}^{\text{SGE}\#} = \mathbf{D}_{[q]}\mathbf{q}^{\text{SGE}}, \quad (4.22)$$

and the condensed vector \mathbf{q}^* transforms with the rule

$$\mathbf{q}^{*\#} = \mathbf{D}_{[q^*]}^*\mathbf{q}^*, \quad (4.23)$$

where $\mathbf{D}_{[q^*]}^*$ is the condensed version of $\mathbf{D}_{[q]}$ and can be found as follows.

It is important to underline that the above equations simplify because the first order material is isotropic, so that

$$\mathbf{T}^{\text{SGE}\#} = \mathbf{T}^{\text{SGE}}, \quad \mathbf{Q} = \mathbf{Q}^\#.$$
 (4.24)

Substituting Eq. (4.13)₃ into Eq. (4.22)₁ and pre-multiplying the results by the transformation matrix \mathbf{Q} it follows

$$\mathbf{Q}\mathbf{q}^{\text{SGE}\#} = \mathbf{Q}\mathbf{D}_{[\mathbf{q}]} \mathbf{T}^{\text{SGE}} \mathbf{q}^*,$$
 (4.25)

so that the left side of Eq. (4.25) is the transformed contracted curvature vector $\mathbf{q}^{*\#}$, Eq. (4.20)₂, which compared with Eq. (4.23), yields

$$\mathbf{D}_{[\mathbf{q}^*]}^* = \mathbf{Q}\mathbf{D}_{[\mathbf{q}]} \mathbf{T}^{\text{SGE}},$$
 (4.26)

providing the relation between $\mathbf{D}_{[\mathbf{q}^*]}^*$ and $\mathbf{D}_{[\mathbf{q}]}$.

A replacement of $\mathbf{D}_{[\mathbf{q}]}$ by the rotation $\mathbf{R}_{[\mathbf{q}]}$ or by the reflection $\mathbf{S}_{[\mathbf{q}]}$ in the law (4.26) provides the condensed rotation $\mathbf{R}_{[\mathbf{q}^*]}^*$ and reflection $\mathbf{S}_{[\mathbf{q}^*]}^*$ as

$$\mathbf{R}_{[\mathbf{q}^*]}^*(\theta) = \begin{pmatrix} \mathbf{R}_1 & \mathbf{R}_2 \\ \mathbf{R}_3 & \mathbf{R}_4 \end{pmatrix}, \quad \mathbf{S}_{[\mathbf{q}^*]}^* = \begin{pmatrix} 1 & 0 & 0 & 0 \\ 0 & 1 & 0 & 0 \\ 0 & 0 & -1 & 0 \\ 0 & 0 & 0 & -1 \end{pmatrix}. \quad (4.27)$$

where

$$\mathbf{R}_1 = \begin{pmatrix} \frac{c(\theta)((3C_{12} + 5C_{33})c(2\theta) - C_{12} - 3C_{33})}{2(C_{12} + C_{33})} & \frac{(C_{12} - C_{33})s^2(\theta)c(\theta)}{C_{12} + C_{33}} \\ \frac{(3C_{12} + 5C_{33})s^2(\theta)c(\theta)}{C_{12} + C_{33}} & \frac{c(\theta)((C_{12} - C_{33})c(2\theta) + C_{12} + 3C_{33})}{2(C_{12} + C_{33})} \end{pmatrix} \quad (4.28a)$$

$$\mathbf{R}_2 = \begin{pmatrix} \frac{(C_{33} - C_{12})s(\theta)c^2(\theta)}{C_{12} + C_{33}} & \frac{s(\theta)((3C_{12} + 5C_{33})c(2\theta) + C_{12} + 3C_{33})}{2(C_{12} + C_{33})} \\ \frac{s(\theta)((C_{12} - C_{33})c(2\theta) - C_{12} - 3C_{33})}{2(C_{12} + C_{33})} & -\frac{(3C_{12} + 5C_{33})s(\theta)c^2(\theta)}{C_{12} + C_{33}} \end{pmatrix} \quad (4.28b)$$

$$\mathbf{R}_3 = \begin{pmatrix} \frac{(3C_{12} + 5C_{33})s(\theta)c^2(\theta)}{C_{12} + C_{33}} & \frac{s(\theta)((C_{33} - C_{12})c(2\theta) + C_{12} + 3C_{33})}{2(C_{12} + C_{33})} \\ -\frac{s(\theta)((3C_{12} + 5C_{33})c(2\theta) + C_{12} + 3C_{33})}{2(C_{12} + C_{33})} & \frac{(C_{12} - C_{33})s(\theta)c^2(\theta)}{C_{12} + C_{33}} \end{pmatrix} \quad (4.28c)$$

$$\mathbf{R}_4 = \begin{pmatrix} \frac{c(\theta)((C_{12} - C_{33})c(2\theta) + C_{12} + 3C_{33})}{2(C_{12} + C_{33})} & \frac{(3C_{12} + 5C_{33})s^2(\theta)c(\theta)}{C_{12} + C_{33}} \\ \frac{(C_{12} - C_{33})s^2(\theta)c(\theta)}{C_{12} + C_{33}} & \frac{c(\theta)((3C_{12} + 5C_{33})c(2\theta) - C_{12} - 3C_{33})}{2(C_{12} + C_{33})} \end{pmatrix} \quad (4.28d)$$

Note that both $\mathbf{R}_{[\mathbf{q}^*]}^*(\theta)$ and $\mathbf{S}_{[\mathbf{q}^*]}^*$ do not depend on the coefficients of \mathbf{Q} , a property which follows from the isotropy of the first-order effective material \mathbf{C} .

4.3.3 Anisotropy characterization of \mathbf{M}^*

The material is said to be symmetric with respect to the rotation θ when

$$\mathbf{R}_{[\mathbf{p}]}^T(\theta) \mathbf{M}^* \mathbf{R}_{[\mathbf{q}^*]}^*(\theta) = \mathbf{M}^*, \quad (4.29)$$

and mirror symmetric with respect to the reflection $\mathbf{S}_{[\mathbf{p}]}$ when

$$\mathbf{S}_{[\mathbf{p}]}^T \mathbf{M}^* \mathbf{S}_{[\mathbf{q}^*]}^* = \mathbf{M}^*. \quad (4.30)$$

For the elastic equivalent material defined by matrix \mathbf{M}^* the condition (4.29) is verified when $\theta = 2/3\pi$, so that the material belongs to Z_3 class of symmetry. Moreover, condition (4.30) is never verified, so that the material is never centrosymmetric.

There is only an exception to the above rules, which occurs when $\mathbf{M}^* = 0$, which is achieved when

$$\frac{(\widehat{k} - \widetilde{k})(\widetilde{k}\widetilde{k} - 2\bar{k}(\widehat{k} + \widetilde{k}))\ell}{8\sqrt{3}I_{[1]}I_{[2]}^2} = 0. \quad (4.31)$$

in which case the material is centrosymmetric and matrix $\mathbf{M}^* = 0$ does not impose restrictions on the anisotropy. Note that Eq. (4.31) leads to the following constraints on the stiffnesses \bar{k} , \widehat{k} , and \widetilde{k}

$$\widehat{k} = \widetilde{k} \quad \text{or} \quad \bar{k} = \frac{\widetilde{k}\widetilde{k}}{2(\widehat{k} + \widetilde{k})}. \quad (4.32)$$

4.3.4 Anisotropy characterization of \mathbf{A}^*

The material is said to be symmetric with respect to the rotation θ when

$$\mathbf{R}_{[\mathbf{q}^*]}^{*T}(\theta)\mathbf{A}^*\mathbf{R}_{[\mathbf{q}^*]}^*(\theta) = \mathbf{A}^*, \quad (4.33)$$

and mirror symmetric with respect to the reflection $\mathbf{S}_{[\mathbf{p}]}$ when

$$\mathbf{S}_{[\mathbf{q}^*]}^{*T}\mathbf{A}^*\mathbf{S}_{[\mathbf{q}^*]}^* = \mathbf{A}^*. \quad (4.34)$$

For the elastic equivalent material defined by matrix \mathbf{A}^* the condition (4.33) is verified when $\theta = \pi/3$ and the condition (4.34) it always is, so that the material belongs to D_6 class of symmetry. To annihilate the anisotropic component of the matrix \mathbf{A}^* and reduce it to an isotropic one, it is necessary to have the following constrain on \bar{k} , \widehat{k} , and \widetilde{k}

$$\bar{k} = \frac{\widetilde{k}\widetilde{k}(4\widehat{k}^2 + 35\widetilde{k}\widetilde{k} + 4\widetilde{k}^2) \pm 3\sqrt{3}\sqrt{\widehat{k}^3\widetilde{k}^3(8\widehat{k}^2 + 43\widetilde{k}\widetilde{k} + 8\widetilde{k}^2)}}{8(\widehat{k} + \widetilde{k})^3}. \quad (4.35)$$

4.3.5 Isotropic and centrosymmetric second-gradient equivalent material

The only possibility of obtaining a second-gradient elastic material characterized by an isotropic (which implies centrosymmetry) response occurs when both Eqs. (4.31) and (4.35) are satisfied, which leads to the following constraint on \bar{k} , \widehat{k} , and \widetilde{k}

$$\widehat{k} = \widetilde{k} \quad \text{and} \quad \bar{k} = \frac{43 \pm 3\sqrt{177}}{64}\widetilde{k}. \quad (4.36)$$

Now that the symmetries of the ‘condensed’ material have been characterized, it is desirable that these symmetries also characterize the ‘relaxed’ material. This can be achieved by constraining all the free parameters, except Q_{35} , ΔM_{15} , ΔM_{16} , and ΔA_{11} , in the matrices \mathbf{Q} , $\Delta\mathbf{M}$, and $\Delta\mathbf{A}$, Eq. (4.17).

4.4 The directional properties of the elastic energy for the SGE material

Inspired by [29], a further insight on the anisotropy of the effective SGE material is provided by analyzing the effect on the stored energy density \mathcal{U}_{SGE} related to a rotation of a fixed kinematic input. Restricting for the moment the attention only to the curvature part $\mathcal{U}_{\mathbf{A}^*}$ of the energy density \mathcal{U}_{SGE} , Eq. (4.5), generated by a curvature input \mathbf{q}^* transformed by the rotation matrix $\mathbf{R}_{[\mathbf{q}^*]}^T(\theta)$,

$$\mathcal{U}_{\mathbf{A}^*}(\mathbf{q}^*, \theta) = \frac{1}{2} \mathbf{q}^{*T} \mathbf{R}_{[\mathbf{q}^*]}^{*T}(\theta) \mathbf{A}^* \mathbf{R}_{[\mathbf{q}^*]}^*(\theta) \mathbf{q}^*, \quad (4.37)$$

the energy density $\mathcal{U}_{\mathbf{A}^*}$ related to a ‘condensed’ SGE material, equivalent to a lattice with stiffness bar ratios $\widehat{k}/\bar{k} = 10$, $\widetilde{k}/\bar{k} = 100$, is reported as polar diagrams in Fig. 4.2 for four different curvature inputs,

$$\mathbf{q}^{*[1]} = \begin{bmatrix} 0 \\ 0 \\ -0.278 \\ 0.961 \end{bmatrix}, \mathbf{q}^{*[2]} = \begin{bmatrix} 0.967 \\ -0.254 \\ 0 \\ 0 \end{bmatrix}, \mathbf{q}^{*[3]} = \begin{bmatrix} 0 \\ 0 \\ 0.961 \\ 0.278 \end{bmatrix}, \mathbf{q}^{*[4]} = \begin{bmatrix} 0.254 \\ 0.967 \\ 0 \\ 0 \end{bmatrix}, \quad (4.38)$$

corresponding to the four eigenvectors of the ‘condensed’ matrix \mathbf{A}^* , normalized to have a unit modulus. The polar diagrams, normalized through division by the maximum value of the energy attained with a specific rotation of the kinematic input, highlight the direction sensitivity of the energy and symmetry in the response with rotations given by a rotation of $\theta = n\pi/3$ with $n \in \mathbb{Z}$.

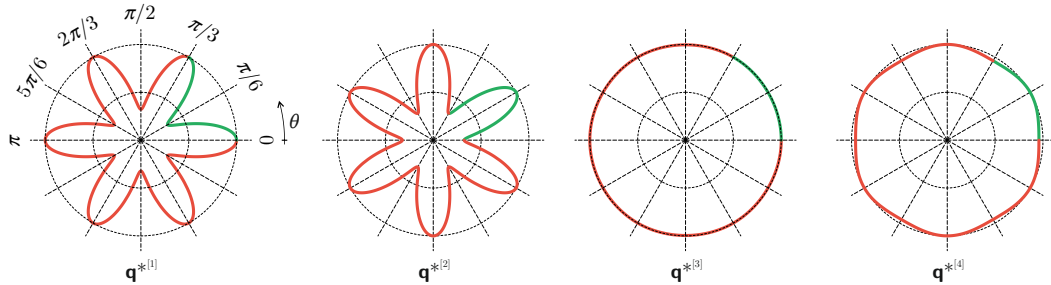


FIGURE 4.2: Polar diagrams of the curvature energy density $\mathcal{U}_{\mathbf{A}^*}$ stored within a ‘condensed’ SGE material, equivalent to a lattice with stiffness bar ratios $\widehat{k}/\bar{k} = 10$, $\widetilde{k}/\bar{k} = 100$, when subject to a specific curvature input $\mathbf{q}^{*[j]}$ ($j = 1, \dots, 4$), Eq. (4.38). The diagrams show the $\pi/3$ symmetry (green coloured curve part) in the constitutive response related to curvature through the matrix \mathbf{A}^* . The energy density with varying the rotation angle θ of the related kinematic input $\mathbf{q}^{*[j]}$ ($j = 1, \dots, 4$) is reported along the radial coordinate normalized through division by its maximum value.

The total elastic energy density \mathcal{U}_{SGE} , Eq. (4.5), given by the sum of the Cauchy, $\mathcal{U}_{\mathbf{C}}$, curvature, $\mathcal{U}_{\mathbf{A}^*}$, and mutual $\mathcal{U}_{\mathbf{M}^*}$ terms, can be rewritten as

$$\mathcal{U}_{\text{SGE}} = \frac{1}{2} \mathbf{t}^{*T} \mathbf{L}^* \left(\bar{k}, \widehat{k}, \widetilde{k} \right) \mathbf{t}^*, \quad (4.39)$$

where the vector \mathbf{t}^* collects the strain and curvature vectors and the matrix $\mathbf{L}^* (\bar{k}, \hat{k}, \tilde{k})$ collects the matrices $(\mathbf{C}, \mathbf{M}^*, \mathbf{A}^*)$ characterizing the ‘condensed’ equivalent SGE,

$$\mathbf{t}^* = \begin{bmatrix} \mathbf{p}^{\text{SGE}^T} \\ \mathbf{q}^{*T} \end{bmatrix}, \quad \mathbf{L}^* = \begin{bmatrix} \mathbf{C} & \mathbf{M}^* \\ \mathbf{M}^{*T} & \mathbf{A}^* \end{bmatrix} \quad (4.40)$$

With the purpose of analyzing the directional property of the total energy, the following Lagrangian function is introduced

$$\mathcal{L}^* = \mathbf{t}^{*T} \mathbf{L}^* \mathbf{t}^* - \psi (\mathbf{t}^* \cdot \mathbf{t}^* - 1), \quad (4.41)$$

where ψ is a Lagrangian multiplier. Imposing the stationarity of the Lagrangian function, Eqn. (4.41), is equivalent to the following system of equations

$$\begin{cases} \frac{\partial \mathcal{L}}{\partial \mathbf{t}^*} = 2(\mathbf{L}^* - \psi \mathbf{I}) \mathbf{t}^* = \mathbf{0}, \\ \frac{\partial \mathcal{L}}{\partial \psi} = \mathbf{t}^* \cdot \mathbf{t}^* - 1 = 0, \end{cases} \quad (4.42)$$

with Eq. (4.42)₁ defining the eigenvectors of the matrix \mathbf{L}^* , corresponding to the seven principal deformations, and Eq. (4.42)₂ constraining the norm of such eigenvectors to the unitary hypersphere. With reference to the considered ‘condensed’ SGE, equivalent to the lattice with stiffness ratios $\hat{k}/\bar{k} = 10, \tilde{k}/\bar{k} = 100$, the following seven eigenvectors of unit modulus are obtained

$$\begin{aligned} \mathbf{t}^{*[1]} = \begin{bmatrix} 0.671 \\ 0.671 \\ 0 \\ 0 \\ 0 \\ -0.091 \\ 0.303 \end{bmatrix}, \mathbf{t}^{*[2]} = \begin{bmatrix} -0.223 \\ -0.223 \\ 0 \\ 0 \\ 0 \\ -0.225 \\ 0.922 \end{bmatrix}, \mathbf{t}^{*[3]} = \begin{bmatrix} -0.011 \\ -0.011 \\ 0 \\ 0 \\ 0 \\ -0.970 \\ -0.242 \end{bmatrix}, \mathbf{t}^{*[4]} = \begin{bmatrix} 0 \\ 0 \\ 0 \\ 0.967 \\ -0.254 \\ 0 \\ 0 \end{bmatrix}, \\ \mathbf{t}^{*[5]} = \begin{bmatrix} 0 \\ 0 \\ 0 \\ 0.254 \\ 0.967 \\ 0 \\ 0 \end{bmatrix}, \mathbf{t}^{*[6]} = \begin{bmatrix} 0.707 \\ -0.707 \\ 0 \\ 0 \\ 0 \\ 0 \\ 0 \end{bmatrix}, \mathbf{t}^{*[7]} = \begin{bmatrix} 0 \\ 0 \\ 1 \\ 0 \\ 0 \\ 0 \\ 0 \end{bmatrix}, \end{aligned} \quad (4.43)$$

showing that only the first three eigenvectors have non-null components related to both deformation and curvature, while $\mathbf{t}^{*[4]}$ and $\mathbf{t}^{*[5]}$ have non-null components only related to curvature, and $\mathbf{t}^{*[6]}$ and $\mathbf{t}^{*[7]}$ only related to deformation. These seven eigenvectors are used as kinematic input rotated by an angle θ to analyze the energy and, similarly to Fig. 4.2, the corresponding polar diagrams are reported in Fig. 4.3 (for a material equivalent to the same pair of stiffness ratios, $\hat{k}/\bar{k} = 10, \tilde{k}/\bar{k} = 100$).

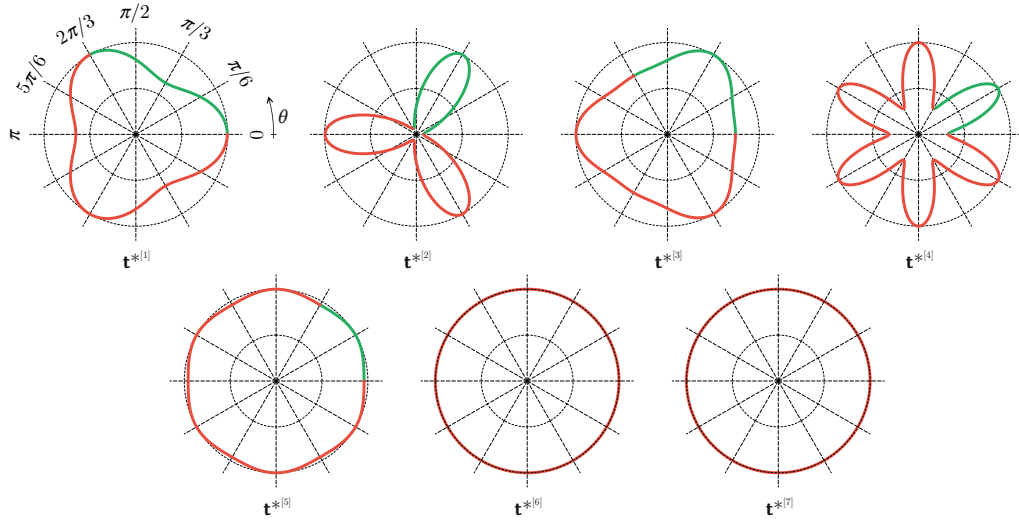


FIGURE 4.3: As for Fig. 4.2, but for the total energy density $\mathcal{U}_{\text{SGE}^*}$ considering the specific kinematic input $\mathbf{t}^{*[j]}$ ($j = 1, \dots, 7$), Eq. (4.43). The diagrams show different periodicity in the response: the $2\pi/3$ symmetry in the mutual constitutive response for $\mathbf{t}^{*[1]}$, $\mathbf{t}^{*[2]}$, and $\mathbf{t}^{*[3]}$, the $\pi/3$ symmetry in the curvature only constitutive response, as evident for $\mathbf{t}^{*[4]}$, $\mathbf{t}^{*[5]}$ as counterpart of kinematic input $\mathbf{q}^{*[2]}$, $\mathbf{q}^{*[4]}$, and the *isotropic* behaviour, provided by the symmetry in Cauchy constitutive response, for null curvature inputs $\mathbf{t}^{*[6]}$ and $\mathbf{t}^{*[7]}$.

4.5 Positive definiteness

Stability of the response for higher-order material equivalent to the lattice is related to the positive definiteness of the obtained effective constitutive tensors. It is known however that positive definiteness of equivalent higher-order equivalent solids is not always verified at varying the microstructure properties [5, 6, 15, 45].

With reference to the energy density \mathcal{U}_{SGE} , Eq. (4.39), the positive definiteness of the ‘condensed’ SGE corresponds to the positive definiteness of the matrix \mathbf{L}^* collecting the matrices $(\mathbf{C}, \mathbf{M}^*, \mathbf{A}^*)$, Eq. (4.40)₂, and defining the ‘condensed’ equivalent SGE. Considering positive bar stiffnesses (for which the equivalent Cauchy material, Eq. (4.1), is positive definite), the sets of bar stiffnesses (made dimensionless through division by \bar{k}) for which the equivalent material is positive definite and indefinite are displayed in Fig. 4.4 as green and red regions, respectively.

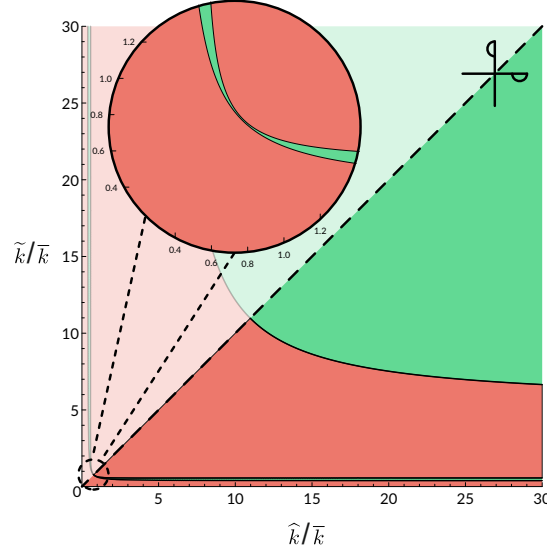


FIGURE 4.4: The values of bar stiffnesses corresponding to a positive definite equivalent second-gradient elastic material correspond to the green zone; in the red zone the equivalent material is indefinite.

The two cases of isotropy, given by Eq. (4.36), are remarkable. In fact, for both of them the equivalent material is positive definite, while in the case of three equal bar stiffnesses, the equivalent material is not positive definite. Note that the positive definiteness of the equivalent material is not affected by a permutation of \hat{k} with \tilde{k} . The non positive definiteness issue is discussed further by analyzing the elastic energy stored within a circular domain at increasing its size.

4.5.1 Variation of the elastic energy with the characteristic length.

Even in the case of non positive definite equivalent constitutive response, the elastic energy stored within a disk of equivalent material of radius ρ centred at the origin of the reference system and generated by a quadratic self-equilibrated displacement field is always positive whenever the ratio between the disk radius ρ and the hexagonal lattice side ℓ exceeds a finite value. Restricting attention to a purely quadratic self-equilibrated displacement conditions ($\alpha = \mathbf{0}$)¹, the integration of the energy density, Eq. (4.5), over the aforementioned disk yields

$$U_{\text{SGE}} = \underbrace{\rho^4 c \left(\mathbf{C}(\bar{k}, \hat{k}, \tilde{k}), \beta \right)}_{U_{\text{C}}} + \underbrace{\rho^2 \ell^2 \mathcal{A} \left(\mathbf{A}^*(\bar{k}, \hat{k}, \tilde{k}), \beta \right)}_{U_{\mathbf{A}^*}}, \quad (4.44)$$

where $c \left(\mathbf{C}(\bar{k}, \hat{k}, \tilde{k}), \beta \right)$ is always positive while $\mathcal{A} \left(\mathbf{A}^*(\bar{k}, \hat{k}, \tilde{k}), \beta \right)$ has no restriction on its sign, and showing that the Cauchy U_{C} and the higher-order $U_{\mathbf{A}^*}$ energy parts are ruled by different powers in the disk radius ρ (while the mutual energy $U_{\mathbf{M}^*}$ is null because of the integration of an odd function over a symmetric domain).

Introducing the parameter \mathcal{R} as ratio between the higher-order $U_{\mathbf{A}^*}$ and Cauchy U_{C} parts of the elastic energy, as

$$\mathcal{R} = \frac{U_{\mathbf{A}^*}}{U_{\text{C}}}, \quad (4.45)$$

¹The condition of purely quadratic self-equilibrated displacement ($\alpha = \mathbf{0}$) is the most restrictive for storing a positive energy within a domain, being the Cauchy part U_{C} of the elastic energy always positive due to the positive definiteness of the matrix \mathbf{C} .

the elastic energy U_{SGE} (4.5) can be rewritten as

$$U_{\text{SGE}} = (1 + \mathcal{R})U_{\text{C}}. \quad (4.46)$$

Considering expression (4.44), the parameter \mathcal{R} (4.45) reduces to

$$\mathcal{R} = \frac{\mathcal{A}(\mathbf{A}^*(\bar{k}, \hat{k}, \tilde{k}), \boldsymbol{\beta})}{c(\mathbf{C}(\bar{k}, \hat{k}, \tilde{k}), \boldsymbol{\beta})} \left(\frac{\ell}{\rho}\right)^2, \quad (4.47)$$

and the following two considerations can be made:

- a positive value for the stored energy U_{SGE} , Eq. (4.44), is achieved when following constraint on \mathcal{R} holds

$$\frac{\mathcal{A}(\mathbf{A}^*(\bar{k}, \hat{k}, \tilde{k}), \boldsymbol{\beta})}{c(\mathbf{C}(\bar{k}, \hat{k}, \tilde{k}), \boldsymbol{\beta})} \left(\frac{\ell}{\rho}\right)^2 > -1. \quad (4.48)$$

which is always satisfied if $\mathcal{A}(\mathbf{A}^*(\bar{k}, \hat{k}, \tilde{k}), \boldsymbol{\beta})$ is greater than zero, since $c(\mathbf{C}(\bar{k}, \hat{k}, \tilde{k}), \boldsymbol{\beta})$ always is;

- the larger is the higher-order part $U_{\mathbf{A}^*}$ energy than the Cauchy U_{C} energy, the larger becomes the parameter \mathcal{R} , which can be both achieved either by increasing the ratio ℓ/ρ or the ratio $\mathcal{A}(\mathbf{A}^*(\bar{k}, \hat{k}, \tilde{k}), \boldsymbol{\beta}) / c(\mathbf{C}(\bar{k}, \hat{k}, \tilde{k}), \boldsymbol{\beta})$.

The behaviour of the parameter \mathcal{R} with varying the ratio ℓ/ρ is displayed in Fig. 4.5 for the pairs of stiffness bars ratio $\{\hat{k}/\bar{k}, \tilde{k}/\bar{k}\}$ and the non-null components of the tensor $\boldsymbol{\beta}$ given by $\beta_{222} = -\beta_{112} = -\beta_{211} = 1$, showing that for sufficiently large disks the stored energy is positive.

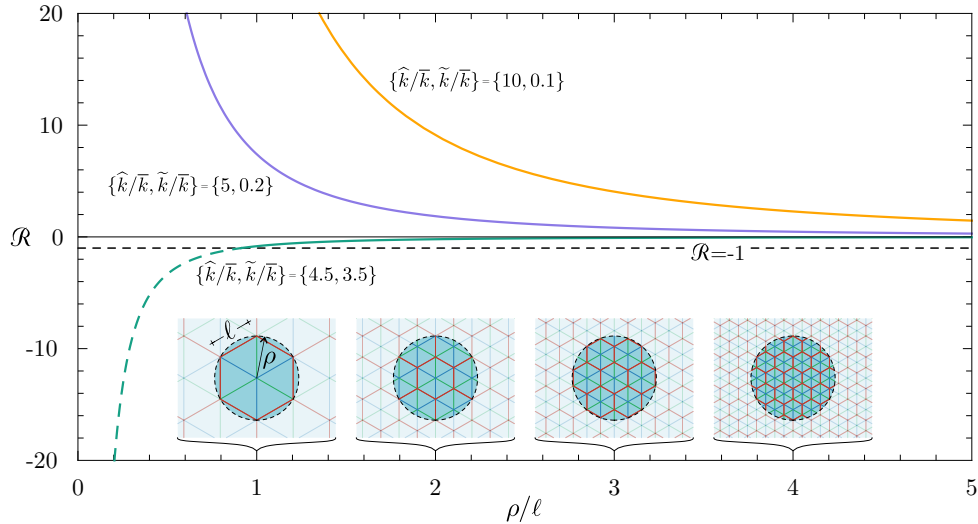


FIGURE 4.5: Parameter \mathcal{R} , Eq. (4.45) versus the ratio ρ/ℓ for non-null components of the tensor $\boldsymbol{\beta}$ given by $\beta_{222} = -\beta_{112} = -\beta_{211} = 1$. Curves are reported for different pairs of stiffness bars ratio $\{\hat{k}/\bar{k}, \tilde{k}/\bar{k}\}$, given by $\{4.5, 3.5\}$ (green), $\{5, 0.2\}$ (purple) and $\{10, 0.1\}$ (orange).

As a further remark, it is also observed that the higher-order energy contribution $U_{\mathbf{A}^*}$ becomes negligible with respect to the Cauchy part $U_{\mathbf{C}}$ for a threshold of the ratio ρ/ℓ depending on the considered stiffness bars ratio $\{\hat{k}/\bar{k}, \tilde{k}/\bar{k}\}$.

4.6 Derivation of the constitutive law for the equivalent second-gradient elastic material

The identification procedure introduced in *Chapter 3* of this thesis and so far exploited only defines an equivalent material in a ‘condensed form’, so that there are ∞^4 second-gradient materials all providing a correct energy balance with the discrete lattice. At this stage a ‘relaxation of the constraints’ has to be introduced to yield an equivalent second-gradient elastic material in a standard form. This relaxation can be introduced in several ways and an optimization scheme could be introduced, however, the simplest approach is pursued in the following, which corresponds to imposing from the beginning the equivalence between the elastic energies neglecting the equilibrium constraint on the coefficients β_{ijk} [Eqs. (3.46) and (3.73) of *Chapter 3*]. The constraint limiting the variability of the possible coefficients β_{ijk} is the reason why a ‘condensed relation’ was derived.

Removing the constraint on the coefficients β_{ijk} yields the following expressions for the four coefficients Q_{35} , A_{11} , ΔM_{15} , and ΔM_{16} , completely defining the second-gradient elastic material

$$\begin{aligned} Q_{35} &= \frac{I_{[1]}}{4C} \left[26\bar{k}^3(\hat{k} + \tilde{k})^2 - 2\bar{k}^2(\hat{k} + \tilde{k}) \left(5\hat{k}^2 - 16\hat{k}\tilde{k} + 5\tilde{k}^2 \right) + \right. \\ &\quad \left. I_{[3]} \left(-47\hat{k}^2 + 40\hat{k}\tilde{k} - 47\tilde{k}^2 \right) - 10\hat{k}^2\tilde{k}^2(\hat{k} + \tilde{k}) \right], \\ \Delta A_{11} &= - \frac{\left(2\bar{k}^2(\hat{k} + \tilde{k}) + \bar{k} \left(2\hat{k}^2 + 15\hat{k}\tilde{k} + 2\tilde{k}^2 \right) + 2\hat{k}\tilde{k}(\hat{k} + \tilde{k}) \right)^2 \ell^2}{192\sqrt{3}I_{[2]}^2 C} \left[-60\bar{k}^4(\hat{k} + \tilde{k}) \right. \\ &\quad \left. + \bar{k}^3 \left(-155\hat{k}^2 + 818\hat{k}\tilde{k} - 155\tilde{k}^2 \right) - \bar{k}^2(\hat{k} + \tilde{k}) \left(35\hat{k}^2 - 211\hat{k}\tilde{k} + 35\tilde{k}^2 \right) \right. \\ &\quad \left. + I_{[3]} \left(182\hat{k}^2 - 253\hat{k}\tilde{k} + 182\tilde{k}^2 \right) + 28\hat{k}^2\tilde{k}^2(\hat{k} + \tilde{k}) \right], \\ \Delta M_{15} &= \Delta M_{16} = 0, \end{aligned} \tag{4.49}$$

where C is

$$\begin{aligned} C &= 5\bar{k}^4(\hat{k} + \tilde{k})^2 + \bar{k}^3(\hat{k} + \tilde{k}) \left(10\hat{k}^2 - 69\hat{k}\tilde{k} + 10\tilde{k}^2 \right) + \bar{k}^2 \left(5\hat{k}^4 + 13\hat{k}^3\tilde{k} - 78\hat{k}^2\tilde{k}^2 + 13\hat{k}\tilde{k}^3 + 5\tilde{k}^4 \right) \\ &\quad - 13I_{[3]}(\hat{k} + \tilde{k}) \left(2\hat{k}^2 - 3\hat{k}\tilde{k} + 2\tilde{k}^2 \right) - 4\hat{k}^2\tilde{k}^2(\hat{k} + \tilde{k})^2. \end{aligned} \tag{4.50}$$

The above coefficients have to be substitute in Eqs. (4.17), which are also constrained by the material symmetry of the ‘condensed solid’ remarked in Sec. 4.3, which yield to the three constitutive tensors $\mathbf{C}(\bar{k}, \hat{k}, \tilde{k})$, $\mathbf{M}(\bar{k}, \hat{k}, \tilde{k})$, and $\mathbf{A}(\bar{k}, \hat{k}, \tilde{k})$ Eqs. (4.1). It is highlighted that with this choice of coefficients Eqs. (4.49), the domain of positive definiteness remains the same as the ‘condensed material’.

Chapter 5

Capability of the SGE solid to be equivalent to the hexagonal lattice

The capability of the identified strain-gradient elastic solid equivalent to the hexagonal lattice is assessed through comparisons in their mechanical response. These behaviours are analyzed for two basic boundary value problems, simple shear and uniaxial strain for two different directions (Fig. 5.1), for which the response of the homogeneous material is provided in closed-form expressions.

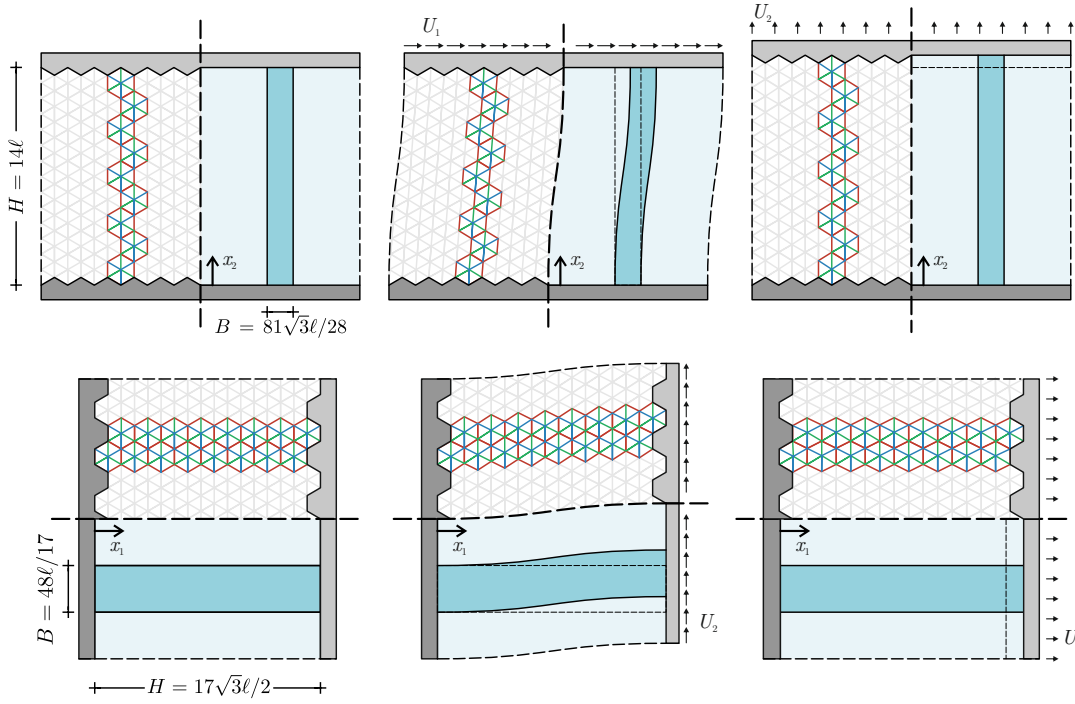


FIGURE 5.1: Upper row from left to right: Undeformed lattice and equivalent SGE material; simple shear parallel to the horizontal direction; uniaxial strain in the vertical direction. Lower row from left to right: Undeformed lattice and equivalent SGE material; simple shear parallel to the vertical direction; uniaxial strain in the horizontal direction. The deformed configurations for the lattice are displayed for the three bars having the same stiffness, $\hat{k}/\bar{k} = \tilde{k}/\bar{k} = 1$.

In the absence of body forces, the stress σ_{ij} and the double-stress τ_{kij} fields within a homogeneous SGE material are governed by the equilibrium equations

$$\sigma_{ij,j} - \tau_{kji,kj} = 0, \quad (5.1)$$

moreover, the components of the resultant traction vector $\mathbf{P}(\mathbf{n})$ associated with the surface defined by the normal unit vector \mathbf{n} are given by

$$P_k(\mathbf{n}) = \sigma_{jk} n_j - n_i n_j D(\tau_{ijk}) - 2n_j D_i(\tau_{ijk}) + (n_i n_j D_l(n_l) - D_j(n_i)) \tau_{ijk}, \quad (5.2)$$

where the operators $D_j(\cdot)$ and $D(\cdot)$ are defined as

$$D_j(\cdot) = (\delta_{jl} - n_j n_l)(\cdot)_{,l}, \quad D(\cdot) = n_l(\cdot)_{,l}. \quad (5.3)$$

The mechanical response of the lattice and of the related equivalent homogeneous solid is compared for different stiffness ratios pairs \hat{k}/\bar{k} and \tilde{k}/\bar{k} and corresponding identified constitutive parameters μ , λ , m_{13} , a_{11} , a_{22} , a_{33} , and a_{44} of the equivalent SGE defined as the six Example cases (Ex1, Ex2, Ex3, Ex4, Ex5, and Ex6) reported in Table 5.1. The comparison is performed by analysing displacement and strain energy density fields. As far as regards the geometry:

- for simple shear and uniaxial strain respectively aligned parallel to the x_1 -axis and to the x_2 -axis, the lattice structure is considered to be realized as the periodic repetition along the x_1 -axis of one line of 9 unit cells, so that the strip of equivalent homogeneous solid has sides $H = 14\ell$ and (by imposing the equivalence of area) $B = 81\sqrt{3}\ell/28$, Fig. 5.1 (top);
- for simple shear and uniaxial strain respectively aligned parallel to the x_2 -axis and to the x_1 -axis, the periodic repetition along the x_2 axis of two lines of 8 unit cells realizes the lattice structure, so that the equivalent homogeneous strip has sides $H = 17\sqrt{3}\ell/2$ and (by imposing the equivalence of area) $B = 48\ell/17$, Fig. 5.1 (bottom).

TABLE 5.1: The six stiffness ratios pairs \hat{k}/\bar{k} and \tilde{k}/\bar{k} and the corresponding equivalent constitutive parameters μ , λ , m_{13} , a_{11} , a_{22} , a_{33} , and a_{44} (made dimensionless through division by the bar stiffness \bar{k}) used for the comparisons reported in Figs. 5.2-5.5.

	\hat{k}/\bar{k}	\tilde{k}/\bar{k}	μ/\bar{k}	λ/\bar{k}	m/\bar{k}	a_{11}/\bar{k}	a_{22}/\bar{k}	a_{33}/\bar{k}	a_{44}/\bar{k}
Ex1	1	1	0.433	0.433	0	1.27	0.153	0.135	1.25
Ex2	25	25	1.20	13.52	0	5.902	0.426	0.554	6.03
Ex3	1500	10	1.18	435	78	129	0.413	14.4	143
Ex4	0.75	0.75	0.354	0.367	0	1.19	0.125	0.127	1.188
Ex5	0.05	0.5	0.056	0.39	0.06	0.823	$5.45 \cdot 10^{-4}$	0.034	0.857
Ex6	0.5	0.05	0.056	0.39	-0.06	0.823	$5.45 \cdot 10^{-4}$	0.034	0.857

5.1 Simple shear problem

The kinematical boundary conditions for a SGE material subject to a simple shear aligned parallel to the I -axis ($I = 1, 2$) are

$$\begin{aligned} u_I(x_J = 0) = 0, \quad u_I(x_J = H) = U_I, \quad u_{I,J}(x_J = 0) = 0, \quad u_{I,J}(x_J = H) = 0, \\ u_J(x_J = 0) = 0, \quad u_J(x_J = H) = 0, \quad u_{J,I}(x_J = 0) = 0, \quad u_{J,I}(x_J = H) = 0, \end{aligned} \quad \text{for } \begin{cases} I = 1, 2, \\ J = 1, 2, \\ J \neq I, \end{cases} \quad (5.4)$$

where U_I is the imposed displacement aligned parallel the I -direction at the coordinate $x_J = H$ (reported on the left part in Fig. 5.1 for $I = 1$ and $J = 2$, top and bottom part, respectively). Because the boundary conditions are independent of x_I and the SGE material is homogeneous, the displacement fields are only dependent on x_J ,

$$u_I = u_I(x_J), \quad u_J = u_J(x_J), \quad (5.5)$$

so that the equilibrium equations (5.1) in the case of simple shear aligned parallel the x_1 -axis ($I = 1, J = 2$) reduce to

$$\begin{cases} u_{1,22}(x_2) - \ell^2 \frac{a_{22}}{\mu} u_{1,2222}(x_2) = 0, \\ u_{2,22}(x_2) - \ell^2 \frac{a_{44}}{(\lambda + 2\mu)} u_{2,2222}(x_2) = 0, \end{cases} \quad (5.6)$$

and the resultant traction components Eq. (5.2) which arise on a surface parallel to the x_1 -axis (and therefore $\mathbf{n} = \mathbf{e}_2$) result

$$\begin{cases} P_1(\mathbf{e}_2) = \sigma_{12} - \tau_{221,2}, \\ P_2(\mathbf{e}_2) = \sigma_{22} - \tau_{222,2}. \end{cases} \quad (5.7)$$

Differently, for simple shear aligned parallel the x_2 -axis ($I = 2, J = 1$), the equilibrium equations (5.1) reduce to

$$\begin{cases} u_{1,11}(x_1) + \ell \left(\frac{m}{\lambda + 2\mu} u_{2,111}(x_1) - \ell \frac{a_{11}}{\lambda + 2\mu} u_{1,1111}(x_1) \right) = 0, \\ u_{2,11}(x_1) - \ell \left(\frac{m}{\mu} u_{1,111}(x_1) + \ell \frac{a_{33}}{\mu} u_{2,1111}(x_1) \right) = 0, \end{cases} \quad (5.8)$$

and the resultant traction components Eq. (5.2) which arise on a surface parallel to the x_2 -axis result

$$\begin{cases} P_1(\mathbf{e}_1) = \sigma_{11} - \tau_{111,1}, \\ P_2(\mathbf{e}_1) = \sigma_{12} - \tau_{112,1}, \end{cases} \quad (5.9)$$

where $a_{22} = a_{11} - 2(a_{16} + a_{26})$, $a_{33} = a_{11} + a_{12} - 2(a_{16} + a_{26}) - a_{34}$, and $a_{44} = a_{11} + a_{12} - a_{34}$ as given by Eq. (4.1)₃.

It can be noted that the differential equations governing the displacement components are uncoupled when the simple shear is aligned parallel to the x_1 -axis, while these become coupled when the simple shear is aligned parallel to the x_2 -axis, because of the equivalent non-centrosymmetric behaviour.

The dimensionless differences in the total energy¹ is reported in Table 5.2 for the two directions of simple shear. The difference in the energy is computed between that stored in the lattice U_{lat} , within one line of 9 unit cells and two lines of 8 unit cells, respectively, and that stored within the strip of equivalent solid, with sides $B = 81\sqrt{3}\ell/28$ and $H = 14\ell$, and $B = 48\ell/17$ and $H = 17\sqrt{3}\ell/2$, respectively. More specifically, the energy difference is evaluated with respect to the energy stored

¹For energy principle, the dimensionless difference in the total energy also coincides with the dimensionless difference in the resultant shear stress component, computed as $(R_{IJ} - B\sigma_{IJ}^{\text{Cau}})/R_{IJ}$ for the equivalent Cauchy and as $(R_{IJ} - BP_I(\mathbf{e}_J))/R_{IJ}$ for the equivalent SGE. In these expressions, σ_{IJ}^{Cau} is the stress component realized within the equivalent Cauchy solid and R_{IJ} is the component along the x_J axis of the resultant force in equilibrium with the lattice cut with a plane with normal \mathbf{e}_I (being I the direction of the simple shear, and $J \neq I$, with $\{I, J\} = \{1, 2\}$).

within an equivalent Cauchy solid, U_{Cau} , and that stored within the identified equivalent SGE solid, U_{SGE} . The reported values show how the difference between the lattice and the model is reduced when the equivalent SGE solid is used for modelling the lattice.

TABLE 5.2: Errors in the energy matching and in the resultant shear force between the lattice and the equivalent Cauchy solid and the equivalent strain-gradient solid for the simple shear problem parallel to x_1 and x_2 axis considering stiffness ratios Ex1, Ex2, and Ex3 as defined by Table 5.1.

	Simple shear parallel to x_1 -axis		Simple shear parallel to x_2 -axis	
	$\frac{U_{\text{lat}} - U_{\text{Cau}}}{U_{\text{lat}}}$	$\frac{U_{\text{lat}} - U_{\text{SGE}}}{U_{\text{lat}}}$	$\frac{U_{\text{lat}} - U_{\text{Cau}}}{U_{\text{lat}}}$	$\frac{U_{\text{lat}} - U_{\text{SGE}}}{U_{\text{lat}}}$
Ex1	10.46%	2.14%	16.26%	9.38%
Ex2	16.58%	8.83%	26.74%	19.3%
Ex3	16.4%	8.69%	25.63%	1.14%

The two cases of simple shear aligned parallel the x_1 -axis and parallel to the x_2 -axis are now analyzed in detail.

5.1.1 Simple shear parallel to the x_1 -axis

Solving the equilibrium equations (5.6) subject to the boundary conditions (5.4) leads to the following displacement fields within the SGE solid

$$u_1(x_2) = \frac{\cosh(\mathcal{Z}_s) x_2 + \left[\sinh\left(\mathcal{Z}_s \left(1 - \frac{2x_2}{H}\right)\right) - \sinh(\mathcal{Z}_s) \right] \frac{H}{2\mathcal{Z}_s} \frac{U_2}{H}}{\cosh \mathcal{Z}_s - \frac{1}{\mathcal{Z}_s} \sinh \mathcal{Z}_s}, \quad u_2(x_2) = 0, \quad (5.10)$$

and to the corresponding stress and double stress fields

$$\begin{aligned} \sigma_{12}(x_2) &= \mu \frac{2 \sinh\left(\frac{x_2}{H} \mathcal{Z}_s\right) \sinh\left(\mathcal{Z}_s \left(1 - \frac{x_2}{H}\right)\right)}{\cosh \mathcal{Z}_s - \frac{1}{\mathcal{Z}_s} \sinh \mathcal{Z}_s} \frac{U_2}{H}, \quad \tau_{221}(x_2) = \frac{a_{22}}{a_{12}} \tau_{111}(x_2), \\ \tau_{111}(x_2) &= \ell \frac{\frac{2\ell}{H} \mathcal{Z}_s \sinh\left(\mathcal{Z}_s \left(1 - \frac{2x_2}{H}\right)\right)}{\cosh \mathcal{Z}_s - \frac{1}{\mathcal{Z}_s} \sinh \mathcal{Z}_s} \frac{U_2}{H}, \quad \tau_{122}(x_2) = \frac{a_{26}}{a_{12}} \tau_{111}(x_2), \end{aligned} \quad (5.11)$$

showing a centrosymmetric response because of the loading symmetry imposed to the non-centrosymmetric SGE. From these fields, the components of the resultant

traction vector associated with the normal $\mathbf{n} = \mathbf{e}_2$ are found to be given as the following constants

$$P_1(\mathbf{e}_2) = \frac{\mu}{1 - \frac{1}{\mathcal{Z}_s} \tanh \mathcal{Z}_s} \frac{U_2}{H}, \quad P_2(\mathbf{e}_2) = 0, \quad (5.12)$$

and the three contributions $\mathcal{U}_{\mathbf{C}}$, $\mathcal{U}_{\mathbf{M}}$, and $\mathcal{U}_{\mathbf{A}}$ to the strain energy density are given by

$$\begin{aligned} \mathcal{U}_{\mathbf{C}}(x_2) &= \mu \frac{2 \sinh^2 \left(\mathcal{Z}_s \left(1 - \frac{x_2}{H} \right) \right) \sinh^2 \left(\frac{x_2}{H} \mathcal{Z}_s \right) \frac{U_2^2}{H^2}}{\left(\cosh \mathcal{Z}_s - \frac{1}{\mathcal{Z}_s} \sinh \mathcal{Z}_s \right)^2}, \quad \mathcal{U}_{\mathbf{M}}(x_2) = 0, \\ \mathcal{U}_{\mathbf{A}}(x_2) &= \mu \frac{\sinh^2 \left(\mathcal{Z}_s \left(1 - \frac{2x_2}{H} \right) \right) \frac{U_2^2}{H^2}}{2 \left(\cosh \mathcal{Z}_s - \frac{1}{\mathcal{Z}_s} \sinh \mathcal{Z}_s \right)^2} \end{aligned} \quad (5.13)$$

where

$$\mathcal{Z}_s = \frac{H}{2\ell} \sqrt{\frac{\mu}{a_{22}}}. \quad (5.14)$$

A comparison in the mechanical response between the lattice, the equivalent Cauchy solid and the equivalent SGE solid is reported in Fig. 5.2 for the stiffness pairs Ex1 (upper part), Ex2 (central part), and Ex3 (lower part) defined in Table 5.1. In particular, the deformed configuration, the displacement $u_1(x_2)$, and the strain energy density $\mathcal{U}(x_2)$ are reported from left to right. Averages over each unit cell are reported as yellow dots, while the fields evaluated within the equivalent Cauchy and the SGE solids are reported as dashed and purple lines, respectively. The improvement in modeling the lattice with the identified SGE instead of the equivalent Cauchy material may be noted analyzing the comparisons in the mechanical fields for the different cases.

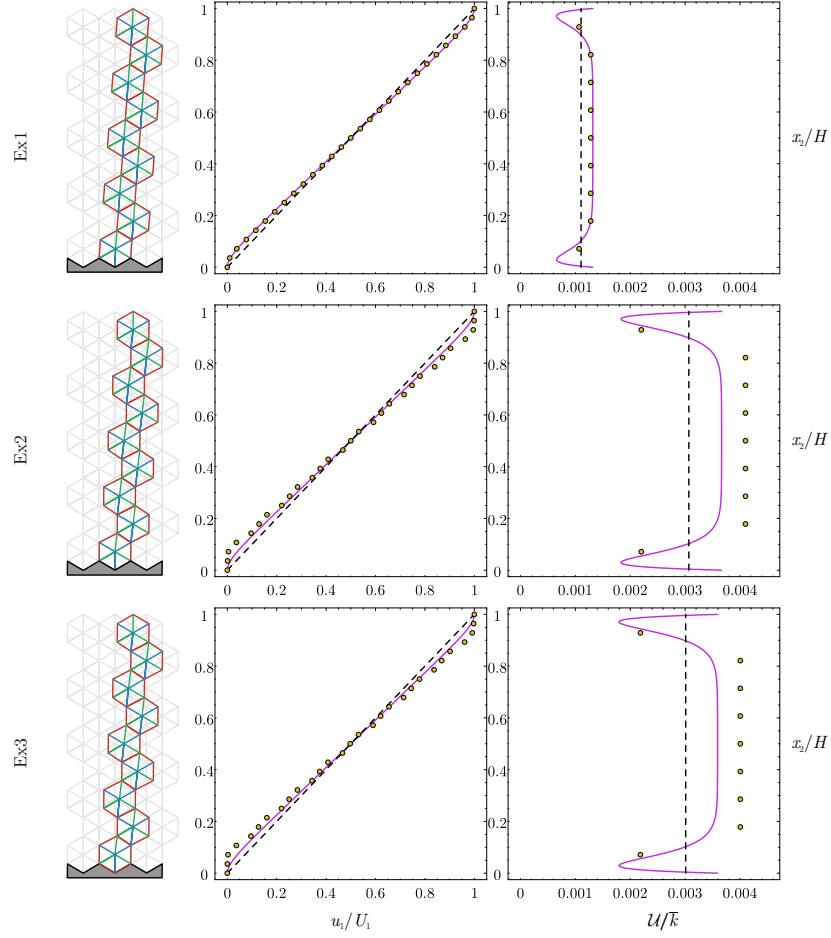


FIGURE 5.2: Simple shear aligned parallel the x_1 -axis. From left to right: Deformed configuration, displacement field $u_1(x_2)$, and strain energy density $\mathcal{U}(x_2)$ for the three cases Ex1 (upper part), Ex2 (central part), and Ex3 (lower part) as defined in Table 5.1. Mechanical fields within the equivalent Cauchy and SGE solids are reported as dashed and purple lines, respectively, while the values averaged within the lattice (at the same coordinate x_2) are reported as yellow dots.

5.1.2 Simple shear parallel the x_2 -axis

In this case the governing equilibrium equations (5.8) are coupled. When subject to the boundary conditions (5.4), their solution can be obtained in a closed-form but very convoluted, because of the non-centrosymmetric terms, so that is not reported here. As for the previous case, the mechanical responses for the stiffness ratios corresponding to Ex1, Ex2, and Ex3 (defined in Table 5.1) are reported in Fig. 5.3 (from left to right) with reference to the deformed configuration, the displacement field $u_2(x_1)$, and the strain energy density $\mathcal{U}(x_1)$ (from the upper part to the lower part).

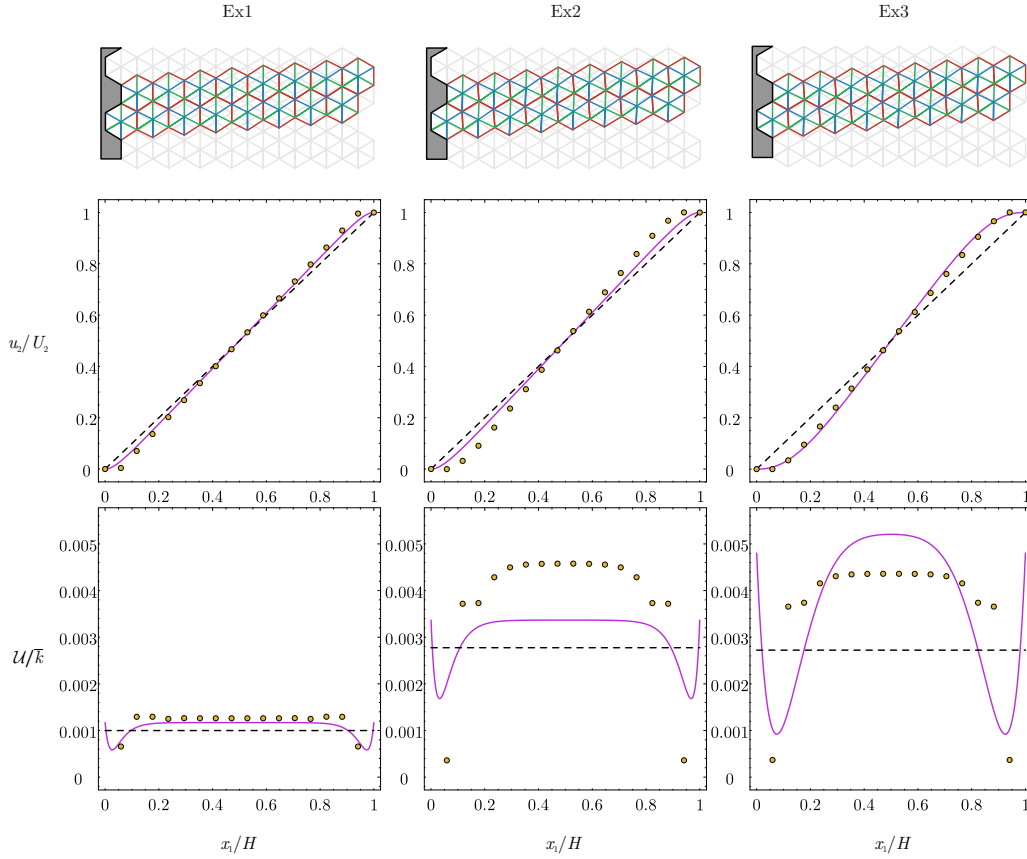


FIGURE 5.3: From top to bottom: deformed configuration, displacement field $u_2(x_1)$, and strain energy density $\mathcal{U}(x_1)$ for the stiffness ratios Ex1, Ex2, and Ex3 as defined by Table 5.1 from left to right. In purple it is portrayed the solution for the SGE material, in black-dashed the solution for a classic Cauchy material, and the yellow dots the quantities related to the lattice.

5.2 Uniaxial strain problem

The kinematical boundary conditions for a SGE material subject to a uniaxial strain parallel to the I -axis ($I = 1, 2$) are

$$\begin{aligned} u_I(x_I = 0) = 0, \quad u_I(x_I = H) = U_I, \quad u_{I,J}(x_I = 0) = 0, \quad u_{I,J}(x_I = H) = 0, \\ u_J(x_I = 0) = 0, \quad u_J(x_I = H) = 0, \quad u_{J,J}(x_I = 0) = 0, \quad u_{J,J}(x_I = H) = 0, \end{aligned} \quad \text{for } \begin{cases} I = 1, 2, \\ J = 1, 2, \\ J \neq I, \end{cases} \quad (5.15)$$

where U_I is the imposed displacement aligned parallel the I -direction at the coordinate $x_I = H$ (reported on the right of Fig. 5.1 for the cases $I = 1$ and $J = 2$, respectively top and bottom). Because the boundary conditions are independent of x_J and the SGE material is homogeneous, the displacement fields are only dependent on x_I ,

$$u_I = u_I(x_I), \quad u_J = u_J(x_I), \quad (5.16)$$

so that the equilibrium (5.1) and the traction (5.2) equations, in the case of uniaxial strain aligned parallel the x_1 -axis ($I = 1, J = 2$) reduce to Eqs. (5.8) and Eqs. (5.9), respectively, while for uniaxial strain aligned parallel the x_2 -axis ($I = 2, J = 1$) reduce to Eqs. (5.6) and Eqs. (5.7), respectively.

As for the simple shear case, the governing equations are uncoupled when the uniaxial strain is imposed aligned parallel the x_2 -axis, while are coupled when the uniaxial strain is aligned parallel the x_1 -axis because of the effective non-centrosymmetric response. Similarly to the Table 5.2 for the simple shear analysis, the energy equivalence differences for the uniaxial strain examples are presented in Table 5.3 for Ex1, Ex4, and Ex5 as defined by Table 5.1.²

TABLE 5.3: Errors in the energy matching and in the resultant normal force between the lattice and the equivalent Cauchy solid and the equivalent strain-gradient solid for the uniaxial problem parallel to x_1 and x_2 axis considering stiffness ratios Ex1, Ex4, and Ex5 as defined by Table 5.1.

	Uniaxial strain parallel to x_1 -axis		Uniaxial strain parallel to x_2 -axis	
	$\frac{U_{\text{lat}} - U_{\text{Cau}}}{U_{\text{lat}}}$	$\frac{U_{\text{lat}} - U_{\text{SGE}}}{U_{\text{lat}}}$	$\frac{U_{\text{lat}} - U_{\text{Cau}}}{U_{\text{lat}}}$	$\frac{U_{\text{lat}} - U_{\text{SGE}}}{U_{\text{lat}}}$
Ex1	8.16%	-6.83%	14.52%	-1.24%
Ex4	8.67%	-7.47%	14.75%	0.57%
Ex5	11.93%	-8.23%	16.5%	-0.72%

5.2.1 Uniaxial strain parallel to the x_2 -axis

Considering the boundary conditions (5.15) for the governing equations (5.6) leads to the following displacement field within the SGE solid

$$u_1(x_2) = 0, \quad u_2(x_2) = \frac{x_2 \cosh(\mathcal{Z}_u) + \frac{H}{2\mathcal{Z}_u} \left[\sinh\left(\mathcal{Z}_u \left(1 - \frac{2x_2}{H}\right)\right) - \sinh(\mathcal{Z}_u) \right]}{\cosh(\mathcal{Z}_u) - \frac{1}{\mathcal{Z}_u} \sinh(\mathcal{Z}_u)} \frac{U_2}{H}, \quad (5.17)$$

to which correspond the stress fields

$$\begin{aligned} \sigma_{11}(x_2) &= \frac{\lambda \left[\cosh(\mathcal{Z}_u) - \cosh\left(\mathcal{Z}_u \left(1 - \frac{2x_2}{H}\right)\right) \right] - \frac{2\ell}{H} m \mathcal{Z}_u \sinh\left(\mathcal{Z}_u \left(1 - \frac{2x_2}{H}\right)\right)}{\cosh(\mathcal{Z}_u) - \frac{1}{\mathcal{Z}_u} \sinh(\mathcal{Z}_u)} \frac{U_2}{H}, \\ \sigma_{22}(x_2) &= \frac{(\lambda + 2\mu) \left[\cosh(\mathcal{Z}_u) - \cosh\left(\mathcal{Z}_u \left(1 - \frac{2x_2}{H}\right)\right) \right] - \frac{2\ell}{H} m \mathcal{Z}_u \sinh\left(\mathcal{Z}_u \left(1 - \frac{2x_2}{H}\right)\right)}{\cosh(\mathcal{Z}_u) - \frac{1}{\mathcal{Z}_u} \sinh(\mathcal{Z}_u)} \frac{U_2}{H}, \end{aligned} \quad (5.18)$$

²As in the simple shear case, the dimensionless energy difference reported in Table 5.3 also expresses the dimensionless difference in the resultant normal stress evaluated as $(R_{II} - B\sigma_{II})/R_{II}$ for the equivalent Cauchy and as $(R_{II} - BP_I(\mathbf{e}_I))/R_{II}$ for the equivalent SGE, where R_{II} is the component along the x_I axis of the resultant force in equilibrium with the lattice cut with a plane with normal \mathbf{e}_I (being I the direction of the uniaxial strain, $I = \{1, 2\}$).

and double stress fields

$$\begin{aligned}
 \tau_{112}(x_2) &= \ell \frac{m \left[\cosh(\mathcal{Z}_u) - \cosh \left(\mathcal{Z}_u \left(1 - \frac{2x_2}{H} \right) \right) \right] + \frac{2\ell}{H} a_{34} \mathcal{Z}_u \sinh \left(\mathcal{Z}_u \left(1 - \frac{2x_2}{H} \right) \right)}{\cosh(\mathcal{Z}_u) - \frac{1}{\mathcal{Z}_u} \sinh(\mathcal{Z}_u)} \frac{U_2}{H}, \\
 \tau_{222}(x_2) &= \ell \frac{-m \left[\cosh(\mathcal{Z}_u) - \cosh \left(\mathcal{Z}_u \left(1 - \frac{2x_2}{H} \right) \right) \right] + \frac{2\ell}{H} a_{44} \mathcal{Z}_u \sinh \left(\mathcal{Z}_u \left(1 - \frac{2x_2}{H} \right) \right)}{\cosh(\mathcal{Z}_u) - \frac{1}{\mathcal{Z}_u} \sinh(\mathcal{Z}_u)} \frac{U_2}{H}, \\
 \tau_{211}(x_2) &= \ell \frac{m \left[\cosh(\mathcal{Z}_u) - \cosh \left(\mathcal{Z}_u \left(1 - \frac{2x_2}{H} \right) \right) \right] + \frac{2\ell}{H} a_{45} \mathcal{Z}_u \sinh \left(\mathcal{Z}_u \left(1 - \frac{2x_2}{H} \right) \right)}{\cosh(\mathcal{Z}_u) - \frac{1}{\mathcal{Z}_u} \sinh(\mathcal{Z}_u)} \frac{U_2}{H},
 \end{aligned} \tag{5.19}$$

showing that, although the governing equations (5.8) are decoupled, the mechanical fields are affected by possible non-centrosymmetry terms. The components of resultant traction vector associated with the normal $\mathbf{n} = \mathbf{e}_2$ can be obtained as the following constants

$$P_1(\mathbf{e}_2) = 0, \quad P_2(\mathbf{e}_2) = \frac{\lambda + 2\mu}{1 - \frac{1}{\mathcal{Z}_u} \tanh \mathcal{Z}_u} \frac{U_2}{H}, \tag{5.20}$$

and the three contributions $\mathcal{U}_{\mathbf{C}}$, $\mathcal{U}_{\mathbf{M}}$, and $\mathcal{U}_{\mathbf{A}}$ of the strain energy density can be evaluated as

$$\begin{aligned}
 \mathcal{U}_{\mathbf{C}}(x_2) &= \frac{(\lambda + 2\mu) \left[\cosh(\mathcal{Z}_u) - \cosh \left(\mathcal{Z}_u \left(1 - \frac{2x_2}{H} \right) \right) \right]^2}{2 \left(\cosh(\mathcal{Z}_u) - \frac{1}{\mathcal{Z}_u} \sinh(\mathcal{Z}_u) \right)^2}, \\
 \mathcal{U}_{\mathbf{M}}(x_2) &= \frac{2\ell}{H} \frac{m \mathcal{Z}_u \sinh \left(\mathcal{Z}_u \left(1 - \frac{2x_2}{H} \right) \right) \left[\cosh \left(\mathcal{Z}_u \left(1 - \frac{2x_2}{H} \right) \right) - \cosh(\mathcal{Z}_u) \right]}{\left(\cosh(\mathcal{Z}_u) - \frac{\sinh(\mathcal{Z}_u)}{\mathcal{Z}_u} \right)^2} \frac{U_2^2}{H^2}, \\
 \mathcal{U}_{\mathbf{A}}(x_2) &= \frac{(\lambda + 2\mu) \sinh^2 \left(\mathcal{Z}_u \left(1 - \frac{2x_2}{H} \right) \right)}{2 \left(\cosh(\mathcal{Z}_u) - \frac{1}{\mathcal{Z}_u} \sinh(\mathcal{Z}_u) \right)^2},
 \end{aligned} \tag{5.21}$$

where

$$\mathcal{Z}_u = \frac{H}{2\ell} \sqrt{\frac{\lambda + 2\mu}{a_{44}}}. \tag{5.22}$$

It is worth to note that the mutual energy, given as the integral of $\mathcal{U}_{\mathbf{M}}(x_2)$ over the set $x_2 \in [0, H]$, is always null.

To better appreciate the improvement in the modelling by considering the identified SGE solid instead of a Cauchy solid, their mechanical responses are compared with that of the lattice in Fig. 5.4 for the stiffness ratios corresponding to Ex1, Ex4,

and Ex5 as defined in Table 5.1 from upper to lower part. In particular, the deformed configuration, the displacement $u_2(x_2)$, and the strain energy density $\mathcal{U}(x_2)$ are reported from left to right. Similarly to Figs. 5.2 and 5.3, the averages over each unit cell are reported as yellow dots, while the fields evaluated within the equivalent Cauchy and the SGE solids are reported as black-dashed and purple lines, respectively. It is worth to mention that for Ex5, due to its non-centrosymmetric response, the strain energy density is not symmetric across the height H , namely $\mathcal{U}(x_2) \neq \mathcal{U}(H - x_2)$.

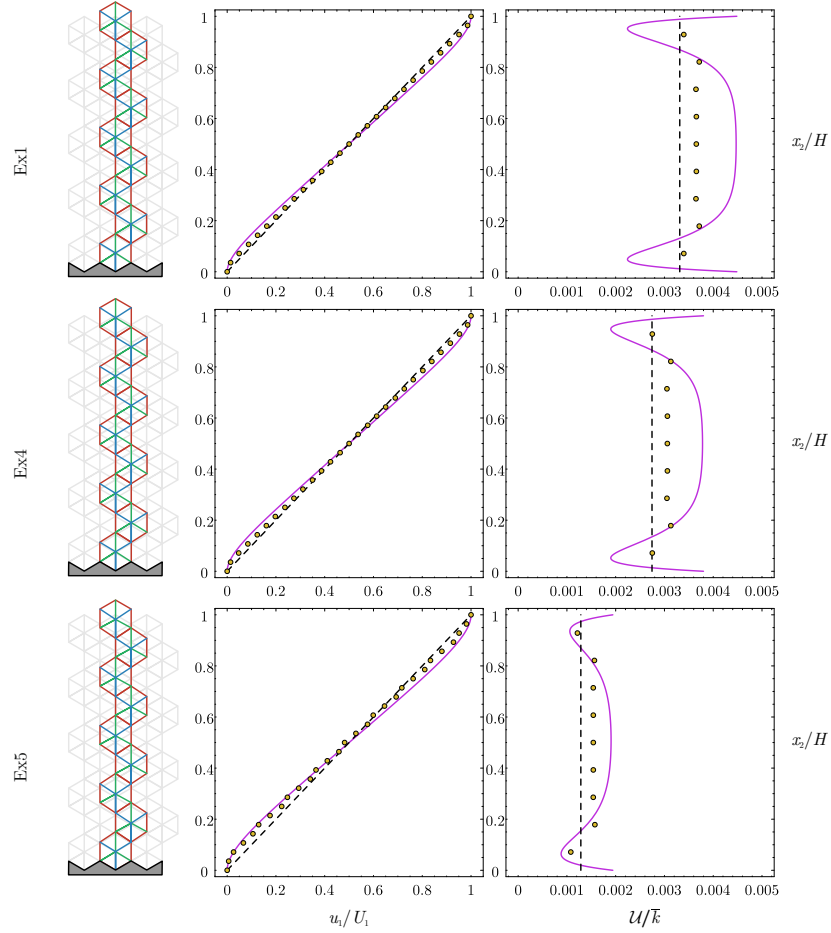


FIGURE 5.4: Uniaxial strain aligned parallel to the x_2 -axis. From left to right: Deformed configuration, displacement field $u_2(x_2)$, and strain energy density $\mathcal{U}(x_2)$ for the three stiffness ratios Ex1, Ex4, and Ex5 defined in Table 5.1 from top to bottom. In purple it is portrayed the solution for the SGE material, in black-dashed the solution for a classic Cauchy material, and the yellow dots the quantities related to the lattice.

5.2.2 Uniaxial strain parallel to the x_1 -axis

Similarly to the case of the simple shear problem aligned parallel the x_2 axis, the solution of the equilibrium equations (5.8) subject to the boundary conditions of uniaxial strain aligned parallel the x_1 -axis (5.15) is provided by tangled expressions, due to presence of non-centrosymmetric terms, and therefore not reported for conciseness. The mechanical responses for the three stiffness ratios Ex1, Ex4, and Ex5

(defined in Table 5.1) are reported in Fig. 5.5 (left to right), with reference to the deformed configuration, the displacement field $u_1(x_1)$, and the strain energy density $\mathcal{U}(x_1)$ (from the upper part to the lower part).

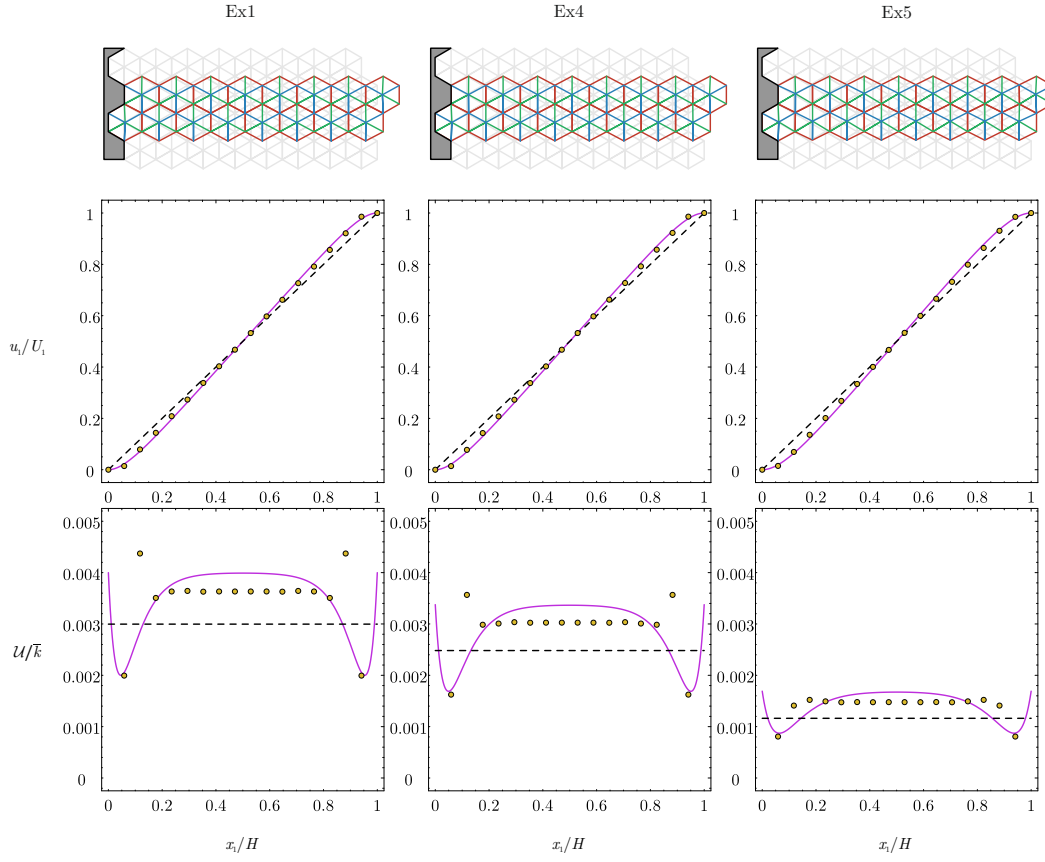


FIGURE 5.5: Uniaxial strain aligned parallel to the x_1 -axis. From top to bottom: Deformed configuration, displacement field $u_1(x_1)$, and strain energy density \mathcal{U} for the three stiffness ratios corresponding to Ex1, Ex4, and Ex5 defined in Table 5.1 (from left to right). In purple it is portrayed the solution for the SGE material, in black-dashed the solution for a classic Cauchy material, and the yellow dots the quantities related to the lattice.

5.2.3 An example of extreme reticular structures far from a Cauchy solid

In this short section is presented an example for which, due to the use of extreme high values for the ratio between the stiffnesses, the effective Cauchy material is no longer capable of produce an acceptable representation for the lattice structure, while the second gradient material performs very well.

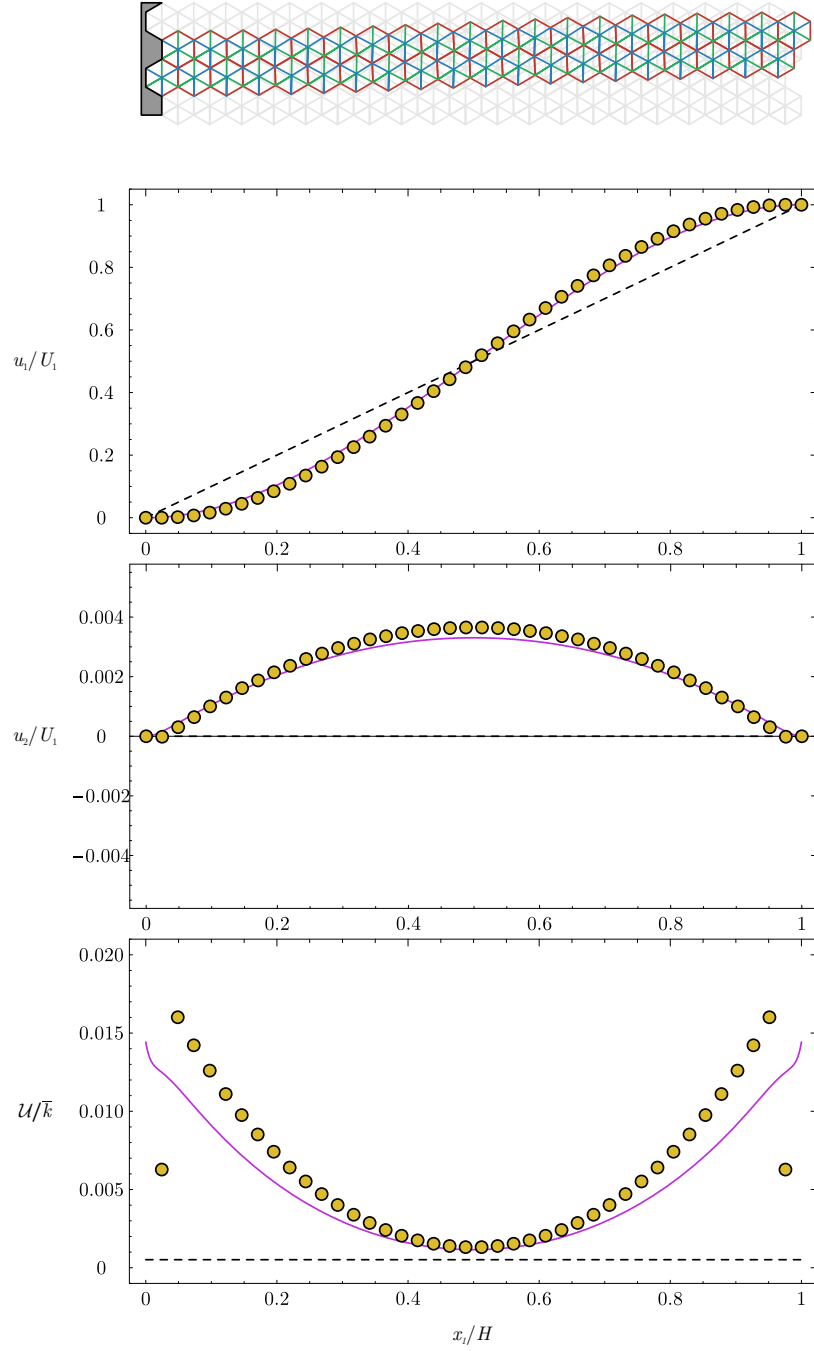


FIGURE 5.6: From top to bottom: deformed configuration, displacement field $u_1(x_1)$, displacement field $u_2(x_1)$, and strain energy density $\mathcal{U}(x_1)$ for the following stiffness bars ratios $\tilde{k}/\bar{k} = \{1, 2.5 \cdot 10^4, 5 \cdot 10^4\}$. In purple it is portrayed the solution for the SGE material, in black-dashed the solution for a classic Cauchy material, and the yellow dots the quantities related to the lattice.

TABLE 5.4: Evaluation of the discrepancy between the dimensionless energy of both the equivalent Cauchy (U_{Cau}) and the equivalent second-gradient elastic (U_{SGE}) solids and the dimensionless energy of the lattice (U_{lat}) for the two uniaxial problems.

		Shear strain x_2 -axis	
\hat{k}/\bar{k}	\tilde{k}/\bar{k}	$\frac{U_{\text{lat}} - U_{\text{Cau}}}{U_{\text{lat}}}$	$\frac{U_{\text{lat}} - U_{\text{SGE}}}{U_{\text{lat}}}$
$2.5 \cdot 10^4$	$5 \cdot 10^4$	91.63%	15.52%

5.2.4 A remark on non-centro-symmetric behaviour

A last remark is made on the possible non-centrosymmetric behaviour predicted for identified SGE solid equivalent to the lattice structure. As highlighted in the anisotropy analysis, such a non-centrosymmetric response arises whenever the three stiffnesses \bar{k} , \hat{k} , and \tilde{k} do not satisfy Eq. (4.32). On the other hand, the following relations for the equivalent matrices $\mathbf{C}(\bar{k}, \hat{k}, \tilde{k})$, $\mathbf{M}(\bar{k}, \hat{k}, \tilde{k})$, and $\mathbf{A}(\bar{k}, \hat{k}, \tilde{k})$, Eq. (4.1), hold with the permutation of the non-perimeter springs

$$\begin{aligned} \mathbf{C}(\kappa_1, \kappa_2, \kappa_3) &= \mathbf{C}(\kappa_1, \kappa_3, \kappa_2), \quad \mathbf{M}(\kappa_1, \kappa_2, \kappa_3) = -\mathbf{M}(\kappa_1, \kappa_3, \kappa_2), \\ \mathbf{A}(\kappa_1, \kappa_2, \kappa_3) &= \mathbf{A}(\kappa_1, \kappa_3, \kappa_2), \end{aligned} \quad (5.23)$$

where three stiffnesses κ_1 , κ_2 , and κ_3 defining the lattice structure.

With the purpose to provide evidence of non-centrosymmetric response for the lattice and the appropriate modelling of the identified equivalent SGE material, overcoming the inherent limits of the equivalent Cauchy material, the deformed configurations and the transversal displacement field $u_2(x_1)$ are displayed in Fig. 5.7 for uniaxial strain condition. More in particular, the behaviour is reported for lattices, and corresponding equivalent SGE solids, characterized by stiffness ratios Ex5 and Ex6 as defined in Table 5.1 subject to compressive ($U_1 < 0$) and tensile ($U_1 > 0$) uniaxial strain for a geometry defined by $H = \{4\sqrt{3} + 1/2, 8\sqrt{3} + 1/2, 16\sqrt{3} + 1/2\}\ell$. Being Ex5 obtained as the permutation of the perimeter springs of Ex6 (and viceversa), the respective equivalent constitutive parameters \mathbf{m} have same absolute value but different sign, so that a permutation of the non-perimeter springs is expected to introduce a change in sign in the transversal displacement field $u_2(x_1)$, as shown in Fig. 5.7. It is finally noted that the diagrams $u_2(x_1)/U_1$ are insensitive of the sign of the imposed displacement U_1 , and that an effective Cauchy solid would simply predict null transversal displacement $u_2(x_1) = 0$, and therefore would not capture such a feature of the lattice motion.

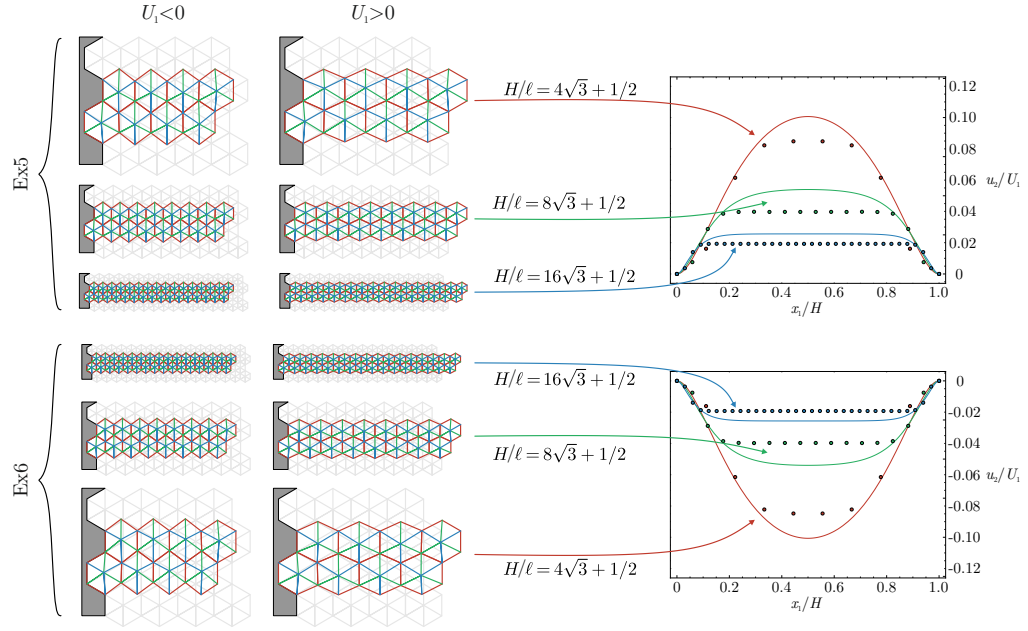


FIGURE 5.7: Deformed configurations and dimensionless transversal displacement $u_2(x_1)/U_1$ for lattice (and corresponding equivalent SGE solid) of properties Ex5 and Ex6 (one is the permutation in the non-perimeter springs of the other, Table 5.1) subject to compressive ($U_1 < 0$) and tensile ($U_1 > 0$) uniaxial strain aligned parallel to the x_1 -axis. Different geometries are reported, $H = \{4\sqrt{3} + 1/2, 8\sqrt{3} + 1/2, 16\sqrt{3} + 1/2\}\ell$.

Chapter 6

Conclusions

A class of homogeneous second-gradient elastic materials has been identified as energetically equivalent to an hexagonal lattice structure with three orders of different linear elastic bars hinged at the ends. The energy matching has been imposed by considering at infinity a quadratic displacement boundary condition, which has required the introduction of corrective fields to enforce equilibrium. The identified homogeneous material displays mechanical properties of: (i.) non-locality, (ii.) non-centrosymmetry, and (iii.) anisotropy (although the local behaviour is isotropic as consequent to the hexagonal geometry). The second-gradient elastic material has been analyzed in terms of symmetry classes and positive definiteness of the elastic energy, disclosing special sets of lattice properties for which centrosymmetry and isotropy are recovered. A comparison is provided between lattice structures (subject to overall conditions of simple shear and uniaxial strain), which can be analytically solved with Mathematica, and their equivalent material counterparts, for which analytical solutions have been derived, and the results provides a validation to our homogenization technique both qualitatively and quantitatively.

Appendix A

Components of the matrices $\mathbf{H}^{[r]}$ and $\mathbf{G}^{[r]}$

The coefficients of the $\mathbf{H}^{[r]}$ are

$$\begin{aligned} H_{11}^{[1]} &= \frac{3}{16} \left(2I_{[1]} + \frac{9I_{[3]}}{I_{[2]}} \right), \quad H_{12}^{[1]} = \frac{3}{16} \left(2I_{[1]} - \frac{9I_{[3]}}{I_{[2]}} \right), \quad H_{13}^{[1]} = 0, \\ H_{22}^{[1]} &= \frac{3}{16} \left(2I_{[1]} + \frac{9I_{[3]}}{I_{[2]}} \right), \quad H_{23}^{[1]} = 0, \quad H_{33}^{[1]} = \frac{27I_{[3]}}{16I_{[2]}} \end{aligned} \quad (\text{A.1})$$

$$\begin{aligned} H_{11}^{[2]} &= \frac{27\sqrt{3}I_{[3]}(2I_{[1]}I_{[2]} + 9I_{[3]})}{16I_{[1]}I_{[2]}^2}, \quad H_{12}^{[2]} = \frac{27\sqrt{3}I_{[3]}(9I_{[3]} - 2I_{[1]}I_{[2]})}{16I_{[1]}I_{[2]}^2}, \quad H_{13}^{[2]} = 0, \\ H_{14}^{[2]} &= 0, \quad H_{21}^{[2]} = -\frac{81\sqrt{3}I_{[3]}(2I_{[1]}I_{[2]} + 3I_{[3]})}{16I_{[1]}I_{[2]}^2}, \quad H_{22}^{[2]} = -\frac{27\sqrt{3}I_{[3]}(2I_{[1]}I_{[2]} + 9I_{[3]})}{16I_{[1]}I_{[2]}^2}, \\ H_{23}^{[2]} &= 0, \quad H_{24}^{[2]} = 0, \quad H_{31}^{[2]} = 0, \end{aligned}$$

$$H_{32}^{[2]} = 0, \quad H_{33}^{[2]} = \frac{27\sqrt{3}I_{[3]}(2I_{[1]}I_{[2]} - 9I_{[3]})}{16I_{[1]}I_{[2]}^2}, \quad H_{34}^{[2]} = -\frac{27\sqrt{3}I_{[3]}(2I_{[1]}I_{[2]} + 9I_{[3]})}{16I_{[1]}I_{[2]}^2} \quad (\text{A.2})$$

$$\begin{aligned} H_{11}^{[3]} &= \frac{27\sqrt{3}I_{[3]}(2I_{[1]}I_{[2]} + 9I_{[3]})}{32I_{[1]}I_{[2]}^2}, \quad H_{12}^{[3]} = \frac{27\sqrt{3}I_{[3]}(9I_{[3]} - 2I_{[1]}I_{[2]})}{32I_{[1]}I_{[2]}^2}, \\ H_{13}^{[3]} &= -\frac{81I_{[3]}(2I_{[1]}I_{[2]} + 9I_{[3]})}{32I_{[1]}I_{[2]}^2}, \quad H_{14}^{[3]} = -\frac{243I_{[3]}(2I_{[1]}I_{[2]} + 3I_{[3]})}{32I_{[1]}I_{[2]}^2}, \\ H_{21}^{[3]} &= -\frac{81\sqrt{3}I_{[3]}(2I_{[1]}I_{[2]} + 3I_{[3]})}{32I_{[1]}I_{[2]}^2}, \quad H_{22}^{[3]} = -\frac{27\sqrt{3}I_{[3]}(2I_{[1]}I_{[2]} + 9I_{[3]})}{32I_{[1]}I_{[2]}^2}, \\ H_{23}^{[3]} &= \frac{81I_{[3]}(9I_{[3]} - 2I_{[1]}I_{[2]})}{32I_{[1]}I_{[2]}^2}, \quad H_{24}^{[3]} = \frac{81I_{[3]}(2I_{[1]}I_{[2]} + 9I_{[3]})}{32I_{[1]}I_{[2]}^2}, \\ H_{31}^{[3]} &= -\frac{81I_{[3]}(2I_{[1]}I_{[2]} + 9I_{[3]})}{32I_{[1]}I_{[2]}^2}, \quad H_{32}^{[3]} = \frac{81I_{[3]}(2I_{[1]}I_{[2]} - 9I_{[3]})}{32I_{[1]}I_{[2]}^2}, \\ H_{33}^{[3]} &= \frac{27\sqrt{3}I_{[3]}(2I_{[1]}I_{[2]} - 9I_{[3]})}{32I_{[1]}I_{[2]}^2}, \quad H_{34}^{[3]} = -\frac{27\sqrt{3}I_{[3]}(2I_{[1]}I_{[2]} + 9I_{[3]})}{32I_{[1]}I_{[2]}^2} \end{aligned} \quad (\text{A.3})$$

$$\begin{aligned}
H_{11}^{[4]} &= 0, \quad H_{12}^{[4]} = 0, \quad H_{13}^{[4]} = \frac{3(\widehat{k} - \widetilde{k})(I_{[1]}I_{[2]} - 9I_{[3]})(\widehat{k}\widetilde{k} - 2k(\widehat{k} + \widetilde{k}))}{16I_{[1]}I_{[2]}^2}, \\
H_{14}^{[4]} &= -\frac{9(\widehat{k} - \widetilde{k})(I_{[1]}I_{[2]} + 3I_{[3]})(\widehat{k}\widetilde{k} - 2k(\widehat{k} + \widetilde{k}))}{16I_{[1]}I_{[2]}^2}, \quad H_{21}^{[4]} = 0, \quad H_{22}^{[4]} = 0, \\
H_{23}^{[4]} &= \frac{3(\widehat{k} - \widetilde{k})(I_{[1]}I_{[2]} - 9I_{[3]})(\widehat{k}\widetilde{k} - 2k(\widehat{k} + \widetilde{k}))}{16I_{[1]}I_{[2]}^2}, \\
H_{24}^{[4]} &= -\frac{9(\widehat{k} - \widetilde{k})(I_{[1]}I_{[2]} + 3I_{[3]})(\widehat{k}\widetilde{k} - 2k(\widehat{k} + \widetilde{k}))}{16I_{[1]}I_{[2]}^2}, \\
H_{31}^{[4]} &= 0, \quad H_{32}^{[4]} = 0, \quad H_{33}^{[4]} = 0, \quad H_{34}^{[4]} = 0
\end{aligned} \tag{A.4}$$

$$\begin{aligned}
H_{11}^{[5]} &= \frac{81I_{[3]}(2I_{[1]}I_{[2]} + 9I_{[3]})(8I_{[1]}I_{[2]} + 9I_{[3]})}{16I_{[1]}^2I_{[2]}^3}, \quad H_{12}^{[5]} = \frac{2187I_{[3]}^2(2I_{[1]}I_{[2]} + 3I_{[3]})}{16I_{[1]}^2I_{[2]}^3}, \\
H_{13}^{[5]} &= 0, \quad H_{14}^{[5]} = 0, \quad H_{22}^{[5]} = \frac{729I_{[3]}^2(2I_{[1]}I_{[2]} + 9I_{[3]})}{16I_{[1]}^2I_{[2]}^3}, \quad H_{23}^{[5]} = 0, \\
H_{24}^{[5]} &= 0, \quad H_{33}^{[5]} = \frac{81I_{[3]}(2I_{[1]}I_{[2]} - 9I_{[3]})^2}{16I_{[1]}^2I_{[2]}^3}, \quad H_{34}^{[5]} = \frac{81I_{[3]}\left(\frac{81I_{[3]}^2}{I_{[1]}^2} - 4I_{[2]}^2\right)}{16I_{[2]}^3}, \\
H_{44}^{[5]} &= \frac{81I_{[3]}(2I_{[1]}I_{[2]} + 9I_{[3]})^2}{16I_{[1]}^2I_{[2]}^3}
\end{aligned} \tag{A.5}$$

$$\begin{aligned}
H_{11}^{[6]} &= \frac{81I_{[3]}(2I_{[1]}I_{[2]} + 9I_{[3]})(7I_{[1]}I_{[2]} + 18I_{[3]})}{32I_{[1]}^2I_{[2]}^3}, \quad H_{12}^{[6]} = \frac{243I_{[3]}\left(-2I_{[1]}^2I_{[2]}^2 + 9I_{[1]}I_{[2]}I_{[3]} + 54I_{[3]}^2\right)}{32I_{[1]}^2I_{[2]}^3}, \\
H_{13}^{[6]} &= -\frac{81\sqrt{3}I_{[3]}(2I_{[1]}I_{[2]} + 9I_{[3]})}{32I_{[1]}I_{[2]}^2}, \quad H_{14}^{[6]} = -\frac{243\sqrt{3}I_{[3]}(2I_{[1]}I_{[2]} + 3I_{[3]})}{32I_{[1]}I_{[2]}^2}, \\
H_{22}^{[6]} &= \frac{243I_{[3]}\left(2I_{[1]}^2I_{[2]}^2 - 15I_{[1]}I_{[2]}I_{[3]} + 54I_{[3]}^2\right)}{32I_{[1]}^2I_{[2]}^3}, \quad H_{23}^{[6]} = \frac{81\sqrt{3}I_{[3]}(2I_{[1]}I_{[2]} - 9I_{[3]})}{32I_{[1]}I_{[2]}^2}, \\
H_{24}^{[6]} &= -\frac{81\sqrt{3}I_{[3]}(2I_{[1]}I_{[2]} + 9I_{[3]})}{32I_{[1]}I_{[2]}^2}, \quad H_{33}^{[6]} = \frac{81I_{[3]}\left(2I_{[1]}^2I_{[2]}^2 + 9I_{[1]}I_{[2]}I_{[3]} + 162I_{[3]}^2\right)}{32I_{[1]}^2I_{[2]}^3}, \\
H_{34}^{[6]} &= \frac{81I_{[3]}\left(-2I_{[1]}^2I_{[2]}^2 + 81I_{[1]}I_{[2]}I_{[3]} + 162I_{[3]}^2\right)}{32I_{[1]}^2I_{[2]}^3}, \quad H_{44}^{[6]} = \frac{81I_{[3]}(2I_{[1]}I_{[2]} + 9I_{[3]})(13I_{[1]}I_{[2]} + 18I_{[3]})}{32I_{[1]}^2I_{[2]}^3}
\end{aligned} \tag{A.6}$$

$$\begin{aligned}
H_{11}^{[7]} &= \frac{81I_{[3]}(2I_{[1]}I_{[2]} + 9I_{[3]})(8I_{[1]}I_{[2]} + 9I_{[3]})}{16I_{[1]}^2I_{[2]}^3}, & H_{12}^{[7]} &= \frac{2187I_{[3]}^2(2I_{[1]}I_{[2]} + 3I_{[3]})}{16I_{[1]}^2I_{[2]}^3}, \\
H_{13}^{[7]} &= -\frac{81\sqrt{3}I_{[3]}(2I_{[1]}I_{[2]} + 9I_{[3]})}{16I_{[1]}I_{[2]}^2}, & H_{14}^{[7]} &= -\frac{243\sqrt{3}I_{[3]}(2I_{[1]}I_{[2]} + 3I_{[3]})}{16I_{[1]}I_{[2]}^2}, \\
H_{22}^{[7]} &= \frac{729I_{[3]}^2(2I_{[1]}I_{[2]} + 9I_{[3]})}{16I_{[1]}^2I_{[2]}^3}, & H_{23}^{[7]} &= \frac{81\sqrt{3}I_{[3]}(2I_{[1]}I_{[2]} - 9I_{[3]})}{16I_{[1]}I_{[2]}^2}, \\
H_{24}^{[7]} &= -\frac{81\sqrt{3}I_{[3]}(2I_{[1]}I_{[2]} + 9I_{[3]})}{16I_{[1]}I_{[2]}^2}, & H_{33}^{[7]} &= \frac{81I_{[3]}(2I_{[1]}I_{[2]} - 9I_{[3]})^2}{16I_{[1]}^2I_{[2]}^3}, \\
H_{34}^{[7]} &= \frac{81I_{[3]}\left(\frac{81I_{[3]}^2}{I^2} - 4I_{[2]}^2\right)}{16I_{[2]}^3}, & H_{44}^{[7]} &= \frac{81I_{[3]}(2I_{[1]}I_{[2]} + 9I_{[3]})^2}{16I_{[1]}^2I_{[2]}^3}
\end{aligned} \tag{A.7}$$

$$H_{11}^{[8]} = 0, \quad H_{12}^{[8]} = 0,$$

$$\begin{aligned}
H_{13}^{[8]} &= -\frac{27\sqrt{3}I_{[3]}(\hat{k} - \tilde{k})(I_{[1]}I_{[2]} - 9I_{[3]})(\tilde{k}\tilde{k} - 2k(\hat{k} + \tilde{k}))}{16I_{[1]}^2I_{[2]}^3}, \\
H_{14}^{[8]} &= \frac{81\sqrt{3}I_{[3]}(\hat{k} - \tilde{k})(I_{[1]}I_{[2]} + 3I_{[3]})(\tilde{k}\tilde{k} - 2k(\hat{k} + \tilde{k}))}{16I_{[1]}^2I_{[2]}^3}, & H_{22}^{[8]} &= 0, \\
H_{23}^{[8]} &= -\frac{27\sqrt{3}I_{[3]}(\hat{k} - \tilde{k})(I_{[1]}I_{[2]} - 9I_{[3]})(\tilde{k}\tilde{k} - 2k(\hat{k} + \tilde{k}))}{16I_{[1]}^2I_{[2]}^3}, \\
H_{24}^{[8]} &= \frac{81\sqrt{3}I_{[3]}(\hat{k} - \tilde{k})(I_{[1]}I_{[2]} + 3I_{[3]})(\tilde{k}\tilde{k} - 2k(\hat{k} + \tilde{k}))}{16I_{[1]}^2I_{[2]}^3}, \\
H_{33}^{[8]} &= 0, \quad H_{34}^{[8]} = 0, \quad H_{44}^{[8]} = 0
\end{aligned} \tag{A.8}$$

$$\begin{aligned}
H_{11}^{[9]} &= 0, \quad H_{12}^{[9]} = 0, \\
H_{13}^{[9]} &= -\frac{27\sqrt{3}I_{[3]}(\widehat{k} - \widetilde{k})(I_{[1]}I_{[2]} - 9I_{[3]})(\widetilde{k}\widetilde{k} - 2k(\widehat{k} + \widetilde{k}))}{32I_{[1]}^2 I_{[2]}^3}, \\
H_{14}^{[9]} &= \frac{81\sqrt{3}I_{[3]}(\widehat{k} - \widetilde{k})(I_{[1]}I_{[2]} + 3I_{[3]})(\widetilde{k}\widetilde{k} - 2k(\widehat{k} + \widetilde{k}))}{32I_{[1]}^2 I_{[2]}^3}, \quad H_{22}^{[9]} = 0, \\
H_{23}^{[9]} &= -\frac{27\sqrt{3}I_{[3]}(\widehat{k} - \widetilde{k})(I_{[1]}I_{[2]} - 9I_{[3]})(\widetilde{k}\widetilde{k} - 2k(\widehat{k} + \widetilde{k}))}{32I_{[1]}^2 I_{[2]}^3}, \\
H_{24}^{[9]} &= \frac{81\sqrt{3}I_{[3]}(\widehat{k} - \widetilde{k})(I_{[1]}I_{[2]} + 3I_{[3]})(\widetilde{k}\widetilde{k} - 2k(\widehat{k} + \widetilde{k}))}{32I_{[1]}^2 I_{[2]}^3}, \\
H_{33}^{[9]} &= -\frac{81I_{[3]}(\widehat{k} - \widetilde{k})(I_{[1]}I_{[2]} - 9I_{[3]})(\widetilde{k}\widetilde{k} - 2k(\widehat{k} + \widetilde{k}))}{16I_{[1]}^2 I_{[2]}^3}, \\
H_{34}^{[9]} &= \frac{81I_{[3]}(\widehat{k} - \widetilde{k})(I_{[1]}I_{[2]} + 9I_{[3]})(\widetilde{k}\widetilde{k} - 2k(\widehat{k} + \widetilde{k}))}{16I_{[1]}^2 I_{[2]}^3}, \\
H_{44}^{[9]} &= \frac{243I_{[3]}(\widehat{k} - \widetilde{k})(I_{[1]}I_{[2]} + 3I_{[3]})(\widetilde{k}\widetilde{k} - 2k(\widehat{k} + \widetilde{k}))}{16I_{[1]}^2 I_{[2]}^3} \\
H_{13}^{[10]} &= H_{14}^{[10]} = H_{23}^{[10]} = H_{24}^{[10]} = 0
\end{aligned} \tag{A.9}$$

$$\begin{aligned}
H_{11}^{[10]} &= \frac{9I_{[3]}}{64I_{[1]}^2 I_{[2]}^4} \left[\left(-50(\widehat{k} + \widetilde{k})^3 \bar{k}^5 - (\widehat{k} + \widetilde{k})^2 \left(100\widehat{k}^2 + 359\widetilde{k}\widehat{k} + 100\widetilde{k}^2 \right) \bar{k}^4 + \right. \right. \\
&\quad \left. \left. - (\widehat{k} + \widetilde{k}) \left(50\widehat{k}^4 + 419\widetilde{k}\widehat{k}^3 + 339\widetilde{k}^2\widehat{k}^2 + 419\widetilde{k}^3\widehat{k} + 50\widetilde{k}^4 \right) \bar{k}^3 + \right. \right. \\
&\quad \left. \left. + 2\widetilde{k}\widehat{k} \left(24\widehat{k}^4 + 459\widetilde{k}\widehat{k}^3 + 1853\widetilde{k}^2\widehat{k}^2 + 459\widetilde{k}^3\widehat{k} + 24\widetilde{k}^4 \right) \bar{k}^2 + \right. \right. \\
&\quad \left. \left. + \widehat{k}^2\widetilde{k}^2(\widehat{k} + \widetilde{k}) \left(219\widehat{k}^2 + 1283\widetilde{k}\widehat{k} + 219\widetilde{k}^2 \right) \bar{k} + 121\widehat{k}^3\widetilde{k}^3(\widehat{k} + \widetilde{k})^2 \right) \ell^2 \right] + \\
&\quad + \left[45I_{[3]}(2I_{[1]}I_{[2]} + 9I_{[3]})(5I_{[1]}I_{[2]} + 9I_{[3]}) \right] / \left(64I_{[1]}^2 I_{[2]}^3 \right), \\
H_{12}^{[10]} &= \frac{9I_{[3]}}{64I_{[1]}^2 I_{[2]}^4} \left[\left(10(\widehat{k} + \widetilde{k})^3 \bar{k}^5 + 5(\widehat{k} + \widetilde{k})^2 \left(4\widehat{k}^2 + 5\widetilde{k}\widehat{k} + 4\widetilde{k}^2 \right) \bar{k}^4 + \right. \right. \\
&\quad \left. \left. + (\widehat{k} + \widetilde{k}) \left(10\widehat{k}^4 - 71\widetilde{k}\widehat{k}^3 - 303\widetilde{k}^2\widehat{k}^2 - 71\widetilde{k}^3\widehat{k} + 10\widetilde{k}^4 \right) \bar{k}^3 + \right. \right. \\
&\quad \left. \left. + 2\widetilde{k}\widehat{k} \left(6\widehat{k}^4 - 9\widetilde{k}\widehat{k}^3 + 641\widetilde{k}^2\widehat{k}^2 - 9\widetilde{k}^3\widehat{k} + 6\widetilde{k}^4 \right) \bar{k}^2 + \right. \right. \\
&\quad \left. \left. - \widehat{k}^2\widetilde{k}^2(\widehat{k} + \widetilde{k}) \left(33\widehat{k}^2 + \widetilde{k}\widehat{k} + 33\widetilde{k}^2 \right) \bar{k} - 35\widehat{k}^3\widetilde{k}^3(\widehat{k} + \widetilde{k})^2 \right) \ell^2 \right] + \\
&\quad + \left[(45I_{[3]} \left(-2I_{[1]}^2 I_{[2]}^2 + 27I_{[1]}I_{[2]}I_{[3]} + 81I_{[3]}^2 \right)) \right] / \left(64I_{[1]}^2 I_{[2]}^3 \right), \\
H_{22}^{[10]} &= \frac{9I_{[3]}}{64I_{[1]}^2 I_{[2]}^4} \left[\left(-10(\widehat{k} + \widetilde{k})^3 \bar{k}^5 - (\widehat{k} + \widetilde{k})^2 \left(20\widehat{k}^2 - 137\widetilde{k}\widehat{k} + 20\widetilde{k}^2 \right) \bar{k}^4 + \right. \right. \\
&\quad \left. \left. - (\widehat{k} + \widetilde{k}) \left(10\widehat{k}^4 - 53\widetilde{k}\widehat{k}^3 + 219\widetilde{k}^2\widehat{k}^2 - 53\widetilde{k}^3\widehat{k} + 10\widetilde{k}^4 \right) \bar{k}^3 + \right. \right. \\
&\quad \left. \left. + 2\widetilde{k}\widehat{k} \left(12\widehat{k}^4 - 45\widetilde{k}\widehat{k}^3 + 349\widetilde{k}^2\widehat{k}^2 - 45\widetilde{k}^3\widehat{k} + 12\widetilde{k}^4 \right) \bar{k}^2 + \right. \right. \\
&\quad \left. \left. + \widehat{k}^2\widetilde{k}^2(\widehat{k} + \widetilde{k}) \left(51\widehat{k}^2 - 197\widetilde{k}\widehat{k} + 51\widetilde{k}^2 \right) \bar{k} + 17\widehat{k}^3\widetilde{k}^3(\widehat{k} + \widetilde{k})^2 \right) \ell^2 \right] + \\
&\quad + \left[45I_{[3]} \left(2I_{[1]}^2 I_{[2]}^2 - 9I_{[1]}I_{[2]}I_{[3]} + 81I_{[3]}^2 \right) \right] / \left(64I_{[1]}^2 I_{[2]}^3 \right), \\
H_{33}^{[10]} &= \frac{3}{64I_{[1]}^2 I_{[2]}^4} \left[\left(2(\widehat{k} + \widetilde{k})^3 \left(4\widehat{k}^2 - 7\widetilde{k}\widehat{k} + 4\widetilde{k}^2 \right) \bar{k}^6 + \right. \right. \\
&\quad \left. \left. + (\widehat{k} + \widetilde{k})^2 \left(16\widehat{k}^4 - 132\widetilde{k}\widehat{k}^3 + 181\widetilde{k}^2\widehat{k}^2 - 132\widetilde{k}^3\widehat{k} + 16\widetilde{k}^4 \right) \bar{k}^5 + \right. \right. \\
&\quad \left. \left. + (\widehat{k} + \widetilde{k}) \left(8\widehat{k}^6 - 110\widetilde{k}\widehat{k}^5 + 301\widetilde{k}^2\widehat{k}^4 + 667\widetilde{k}^3\widehat{k}^3 + 301\widetilde{k}^4\widehat{k}^2 - 110\widetilde{k}^5\widehat{k} + 8\widetilde{k}^6 \right) \bar{k}^4 + \right. \right. \\
&\quad \left. \left. + 2\widetilde{k}\widehat{k} \left(4\widehat{k}^6 + 27\widetilde{k}\widehat{k}^5 - 101\widetilde{k}^2\widehat{k}^4 - 587\widetilde{k}^3\widehat{k}^3 - 101\widetilde{k}^4\widehat{k}^2 + 27\widetilde{k}^5\widehat{k} + 4\widetilde{k}^6 \right) \bar{k}^3 + \right. \right. \\
&\quad \left. \left. - \widehat{k}^2\widetilde{k}^2(\widehat{k} + \widetilde{k}) \left(6\widehat{k}^4 - 121\widetilde{k}\widehat{k}^3 - 349\widetilde{k}^2\widehat{k}^2 - 121\widetilde{k}^3\widehat{k} + 6\widetilde{k}^4 \right) \bar{k}^2 + \right. \right. \\
&\quad \left. \left. - \widehat{k}^3\widetilde{k}^3(\widehat{k} + \widetilde{k})^2 \left(4\widehat{k}^2 + 43\widetilde{k}\widehat{k} + 4\widetilde{k}^2 \right) \bar{k} + 2\widehat{k}^4\widetilde{k}^4(\widehat{k} + \widetilde{k})^3 \right) \ell^2 \right] + \\
&\quad + \left[45I_{[3]} \left(2I_{[1]}^2 I_{[2]}^2 - 9I_{[1]}I_{[2]}I_{[3]} + 81I_{[3]}^2 \right) \right] / \left(64I_{[1]}^2 I_{[2]}^3 \right),
\end{aligned} \tag{A.10}$$

$$\begin{aligned}
\mathbf{H}_{34}^{[10]} &= -\frac{9}{64I_{[1]}^2 I_{[2]}^4} \left[\left(2(\widehat{k} + \widetilde{k})^3 \left(4\widehat{k}^2 + 3\widetilde{k}\widehat{k} + 4\widetilde{k}^2 \right) \bar{k}^6 + \right. \right. \\
&\quad + (\widehat{k} + \widetilde{k})^2 \left(16\widehat{k}^4 + 4\widetilde{k}\widehat{k}^3 - 63\widetilde{k}^2\widehat{k}^2 + 4\widetilde{k}^3\widehat{k} + 16\widetilde{k}^4 \right) \bar{k}^5 + \\
&\quad + (\widehat{k} + \widetilde{k}) \left(8\widehat{k}^6 + 6\widetilde{k}\widehat{k}^5 - 267\widetilde{k}^2\widehat{k}^4 - 173\widetilde{k}^3\widehat{k}^3 - 267\widetilde{k}^4\widehat{k}^2 + 6\widetilde{k}^5\widehat{k} + 8\widetilde{k}^6 \right) \bar{k}^4 + \\
&\quad + 2\widetilde{k}\widehat{k} \left(4\widehat{k}^6 - 15\widetilde{k}\widehat{k}^5 + 115\widetilde{k}^2\widehat{k}^4 + 461\widetilde{k}^3\widehat{k}^3 + 115\widetilde{k}^4\widehat{k}^2 - 15\widetilde{k}^5\widehat{k} + 4\widetilde{k}^6 \right) \bar{k}^3 + \\
&\quad - \widetilde{k}^2\widehat{k}^2 (\widehat{k} + \widetilde{k}) \left(6\widehat{k}^4 + 71\widetilde{k}\widehat{k}^3 + 43\widetilde{k}^2\widehat{k}^2 + 71\widetilde{k}^3\widehat{k} + 6\widetilde{k}^4 \right) \bar{k}^2 + \\
&\quad \left. - \widetilde{k}^3\widehat{k}^3 (\widehat{k} + \widetilde{k})^2 \left(4\widehat{k}^2 + 35\widetilde{k}\widehat{k} + 4\widetilde{k}^2 \right) \bar{k} + 2\widehat{k}^4\widetilde{k}^4 (\widehat{k} + \widetilde{k})^3 \right) \ell^2 \Big] + \\
&\quad + \left[45I_{[3]} \left(-2I_{[1]}^2 I_{[2]}^2 + 27I_{[1]} I_{[2]} I_{[3]} + 81I_{[3]}^2 \right) \right] / \left(64I_{[1]}^2 I_{[2]}^3 \right), \\
\mathbf{H}_{44}^{[10]} &= \frac{9}{64I_{[1]}^2 I_{[2]}^4} \left[\left(2(\widehat{k} + \widetilde{k})^3 \left(12\widehat{k}^2 - \widetilde{k}\widehat{k} + 12\widetilde{k}^2 \right) \bar{k}^6 + \right. \right. \\
&\quad + (\widehat{k} + \widetilde{k})^2 \left(48\widehat{k}^4 + 260\widetilde{k}\widehat{k}^3 + 103\widetilde{k}^2\widehat{k}^2 + 260\widetilde{k}^3\widehat{k} + 48\widetilde{k}^4 \right) \bar{k}^5 + \\
&\quad + (\widehat{k} + \widetilde{k}) \left(24\widehat{k}^6 + 286\widetilde{k}\widehat{k}^5 + 583\widetilde{k}^2\widehat{k}^4 - 255\widetilde{k}^3\widehat{k}^3 + 583\widetilde{k}^4\widehat{k}^2 + 286\widetilde{k}^5\widehat{k} + 24\widetilde{k}^6 \right) \bar{k}^4 + \\
&\quad + 2\widetilde{k}\widehat{k} \left(12\widehat{k}^6 - 3\widetilde{k}\widehat{k}^5 - 735\widetilde{k}^2\widehat{k}^4 - 1753\widetilde{k}^3\widehat{k}^3 - 735\widetilde{k}^4\widehat{k}^2 - 3\widetilde{k}^5\widehat{k} + 12\widetilde{k}^6 \right) \bar{k}^3 + \\
&\quad - \widetilde{k}^2\widehat{k}^2 (\widehat{k} + \widetilde{k}) \left(18\widehat{k}^4 + 309\widetilde{k}\widehat{k}^3 + 937\widetilde{k}^2\widehat{k}^2 + 309\widetilde{k}^3\widehat{k} + 18\widetilde{k}^4 \right) \bar{k}^2 + \\
&\quad \left. - \widetilde{k}^3\widehat{k}^3 (\widehat{k} + \widetilde{k})^2 \left(12\widehat{k}^2 + 17\widetilde{k}\widehat{k} + 12\widetilde{k}^2 \right) \bar{k} + 6\widehat{k}^4\widetilde{k}^4 (\widehat{k} + \widetilde{k})^3 \right) \ell^2 \Big] + \\
&\quad + \left[45I_{[3]} (2I_{[1]} I_{[2]} + 9I_{[3]}) (5I_{[1]} I_{[2]} + 9I_{[3]}) \right] / \left(64I_{[1]}^2 I_{[2]}^3 \right)
\end{aligned}$$

and the coefficients of the $\mathbf{G}^{[r]}$ are

$$\mathbf{G}_{ij}^{[1]} = \frac{3}{4} \sqrt{3} \mathbf{C}_{ij} \quad (\text{A.11})$$

$$\begin{aligned}
\mathbf{G}_{11}^{[2]} &= \frac{9}{2} (\mathbf{C}_{11} + \mathbf{C}_{12}\mathcal{D}_1 + \mathbf{C}_{13}\mathcal{D}_5), & \mathbf{G}_{12}^{[2]} &= \frac{9}{2} (\mathbf{C}_{12}\mathcal{D}_2 + \mathbf{C}_{13}\mathcal{D}_6), \\
\mathbf{G}_{13}^{[2]} &= \frac{9}{2} (\mathbf{C}_{12}\mathcal{D}_3 + \mathbf{C}_{13}\mathcal{D}_7 + \mathbf{C}_{13}), & \mathbf{G}_{14}^{[2]} &= \frac{9}{2} (\mathbf{C}_{12}\mathcal{D}_4 + \mathbf{C}_{13}\mathcal{D}_8), \\
\mathbf{G}_{21}^{[2]} &= \frac{9}{2} (\mathbf{C}_{12} + \mathbf{C}_{22}\mathcal{D}_1 + \mathbf{C}_{23}\mathcal{D}_5), & \mathbf{G}_{22}^{[2]} &= \frac{9}{2} (\mathbf{C}_{22}\mathcal{D}_2 + \mathbf{C}_{23}\mathcal{D}_6), \\
\mathbf{G}_{23}^{[2]} &= \frac{9}{2} (\mathbf{C}_{22}\mathcal{D}_3 + \mathbf{C}_{23}\mathcal{D}_7 + \mathbf{C}_{23}), & \mathbf{G}_{24}^{[2]} &= \frac{9}{2} (\mathbf{C}_{22}\mathcal{D}_4 + \mathbf{C}_{23}\mathcal{D}_8), \\
\mathbf{G}_{31}^{[2]} &= \frac{9}{2} (\mathbf{C}_{13} + \mathbf{C}_{23}\mathcal{D}_1 + \mathbf{C}_{33}\mathcal{D}_5), & \mathbf{G}_{32}^{[2]} &= \frac{9}{2} (\mathbf{C}_{23}\mathcal{D}_2 + \mathbf{C}_{33}\mathcal{D}_6), \\
\mathbf{G}_{33}^{[2]} &= \frac{9}{2} (\mathbf{C}_{23}\mathcal{D}_3 + \mathbf{C}_{33}\mathcal{D}_7 + \mathbf{C}_{33}), & \mathbf{G}_{34}^{[2]} &= \frac{9}{2} (\mathbf{C}_{23}\mathcal{D}_4 + \mathbf{C}_{33}\mathcal{D}_8).
\end{aligned} \quad (\text{A.12})$$

$$\begin{aligned}
G_{11}^{[3]} &= \frac{9}{4} \left(\sqrt{3}C_{11}\mathcal{D}_5 + C_{11} + C_{12}\mathcal{D}_1 + C_{13} \left(\sqrt{3}\mathcal{D}_1 + \mathcal{D}_5 \right) \right), \\
G_{12}^{[3]} &= \frac{9}{4} \left(\sqrt{3}C_{11}\mathcal{D}_6 + C_{12}\mathcal{D}_2 + C_{13} \left(\sqrt{3}\mathcal{D}_2 + \mathcal{D}_6 + \sqrt{3} \right) \right), \\
G_{13}^{[3]} &= \frac{9}{4} \left(\sqrt{3}C_{11}\mathcal{D}_7 + C_{12}\mathcal{D}_3 + C_{13} \left(\sqrt{3}\mathcal{D}_3 + \mathcal{D}_7 + 1 \right) \right), \\
G_{14}^{[3]} &= \frac{9}{4} \left(\sqrt{3}C_{11}\mathcal{D}_8 + C_{12} \left(\mathcal{D}_4 + \sqrt{3} \right) + C_{13} \left(\sqrt{3}\mathcal{D}_4 + \mathcal{D}_8 \right) \right), \\
G_{21}^{[3]} &= \frac{9}{4} \left(\sqrt{3}C_{12}\mathcal{D}_5 + C_{12} + C_{22}\mathcal{D}_1 + C_{23} \left(\sqrt{3}\mathcal{D}_1 + \mathcal{D}_5 \right) \right), \\
G_{22}^{[3]} &= \frac{9}{4} \left(\sqrt{3}C_{12}\mathcal{D}_6 + C_{22}\mathcal{D}_2 + C_{23} \left(\sqrt{3}\mathcal{D}_2 + \mathcal{D}_6 + \sqrt{3} \right) \right), \\
G_{23}^{[3]} &= \frac{9}{4} \left(\sqrt{3}C_{12}\mathcal{D}_7 + C_{22}\mathcal{D}_3 + C_{23} \left(\sqrt{3}\mathcal{D}_3 + \mathcal{D}_7 + 1 \right) \right), \\
G_{24}^{[3]} &= \frac{9}{4} \left(\sqrt{3}C_{12}\mathcal{D}_8 + C_{22} \left(\mathcal{D}_4 + \sqrt{3} \right) + C_{23} \left(\sqrt{3}\mathcal{D}_4 + \mathcal{D}_8 \right) \right), \\
G_{31}^{[3]} &= \frac{9}{4} \left(\sqrt{3}C_{13}\mathcal{D}_5 + C_{13} + C_{23}\mathcal{D}_1 + C_{33} \left(\sqrt{3}\mathcal{D}_1 + \mathcal{D}_5 \right) \right), \\
G_{32}^{[3]} &= \frac{9}{4} \left(\sqrt{3}C_{13}\mathcal{D}_6 + C_{23}\mathcal{D}_2 + C_{33} \left(\sqrt{3}\mathcal{D}_2 + \mathcal{D}_6 + \sqrt{3} \right) \right), \\
G_{33}^{[3]} &= \frac{9}{4} \left(\sqrt{3}C_{13}\mathcal{D}_7 + C_{23}\mathcal{D}_3 + C_{33} \left(\sqrt{3}\mathcal{D}_3 + \mathcal{D}_7 + 1 \right) \right), \\
G_{34}^{[3]} &= \frac{9}{4} \left(\sqrt{3}C_{13}\mathcal{D}_8 + C_{23} \left(\mathcal{D}_4 + \sqrt{3} \right) + C_{33} \left(\sqrt{3}\mathcal{D}_4 + \mathcal{D}_8 \right) \right).
\end{aligned} \tag{A.13}$$

$$G_{ij}^{[4]} = \frac{3}{2\ell} \sqrt{3} M_{ij}^* \tag{A.14}$$

$$\begin{aligned}
G_{11}^{[5]} &= 9\sqrt{3} (C_{11} + 2C_{12}\mathcal{D}_1 + 2\mathcal{D}_5(C_{13} + C_{23}\mathcal{D}_1) + C_{22}\mathcal{D}_1^2 + C_{33}\mathcal{D}_5^2), \\
G_{12}^{[5]} &= 9\sqrt{3}(\mathcal{D}_2(C_{12} + C_{22}\mathcal{D}_1 + C_{23}\mathcal{D}_5) + \mathcal{D}_6(C_{13} + C_{23}\mathcal{D}_1 + C_{33}\mathcal{D}_5)), \\
G_{13}^{[5]} &= 9\sqrt{3}(\mathcal{D}_3(C_{12} + C_{22}\mathcal{D}_1) + C_{13}(\mathcal{D}_7 + 1) \\
&\quad + C_{23}(\mathcal{D}_1\mathcal{D}_7 + \mathcal{D}_1 + \mathcal{D}_3\mathcal{D}_5) + C_{33}\mathcal{D}_5(\mathcal{D}_7 + 1)), \\
G_{14}^{[5]} &= 9\sqrt{3}(\mathcal{D}_4(C_{12} + C_{22}\mathcal{D}_1 + C_{23}\mathcal{D}_5) + \mathcal{D}_8(C_{13} + C_{23}\mathcal{D}_1 + C_{33}\mathcal{D}_5)), \\
G_{22}^{[5]} &= 9\sqrt{3} (C_{22}\mathcal{D}_2^2 + \mathcal{D}_6(2C_{23}\mathcal{D}_2 + C_{33}\mathcal{D}_6)), \tag{A.15} \\
G_{23}^{[5]} &= 9\sqrt{3}(C_{22}\mathcal{D}_2\mathcal{D}_3 + C_{23}(\mathcal{D}_2\mathcal{D}_7 + \mathcal{D}_2 + \mathcal{D}_3\mathcal{D}_6) + C_{33}\mathcal{D}_6(\mathcal{D}_7 + 1)), \\
G_{24}^{[5]} &= 9\sqrt{3}(C_{22}\mathcal{D}_2\mathcal{D}_4 + C_{23}\mathcal{D}_2\mathcal{D}_8 + C_{23}\mathcal{D}_4\mathcal{D}_6 + C_{33}\mathcal{D}_6\mathcal{D}_8), \\
G_{33}^{[5]} &= 9\sqrt{3} (\mathcal{D}_3(C_{22}\mathcal{D}_3 + 2C_{23}(\mathcal{D}_7 + 1)) + C_{33}(\mathcal{D}_7 + 1)^2), \\
G_{34}^{[5]} &= 9\sqrt{3}(C_{22}\mathcal{D}_3\mathcal{D}_4 + C_{23}(\mathcal{D}_3\mathcal{D}_8 + \mathcal{D}_4\mathcal{D}_7 + \mathcal{D}_4) + C_{33}(\mathcal{D}_7 + 1)\mathcal{D}_8), \\
G_{44}^{[5]} &= 9\sqrt{3} (C_{22}\mathcal{D}_4^2 + \mathcal{D}_8(2C_{23}\mathcal{D}_4 + C_{33}\mathcal{D}_8)).
\end{aligned}$$

$$\begin{aligned}
G_{11}^{[6]} &= \frac{9}{4} \left(\left(3\sqrt{3}C_{11} + 6C_{13} + \sqrt{3}C_{33} \right) \mathcal{D}_5^2 \right. \\
&\quad + 2 \left(3C_{11} + \left(3C_{12} + \sqrt{3}C_{23} + 3C_{33} \right) \mathcal{D}_1 + \sqrt{3}C_{13}(3\mathcal{D}_1 + 1) \right) \mathcal{D}_5 + \\
&\quad \left. + \sqrt{3}C_{11} + \mathcal{D}_1 \left(2\sqrt{3}C_{12} + 6C_{13} + \left(\sqrt{3}C_{22} + 6C_{23} + 3\sqrt{3}C_{33} \right) \mathcal{D}_1 \right) \right), \\
G_{12}^{[6]} &= \frac{9}{4} \left(\sqrt{3}C_{12}\mathcal{D}_2 + 3C_{11}\mathcal{D}_6 + C_{13} \left(3\mathcal{D}_2 \left(\sqrt{3}\mathcal{D}_5 + 1 \right) + \right. \right. \\
&\quad \left. \left. \sqrt{3}(3\mathcal{D}_1 + 1)\mathcal{D}_6 + 3\mathcal{D}_5 \left(2\mathcal{D}_6 + \sqrt{3} \right) + 3 \right) + \right. \\
&\quad \left. + \mathcal{D}_1 \left(\sqrt{3}C_{22}\mathcal{D}_2 + 3C_{12}\mathcal{D}_6 + 3C_{33} \left(\sqrt{3}\mathcal{D}_2 + \mathcal{D}_6 + \sqrt{3} \right) \right. \right. \\
&\quad \left. \left. + C_{23} \left(6\mathcal{D}_2 + \sqrt{3}\mathcal{D}_6 + 3 \right) \right) + \right. \\
&\quad \left. + \mathcal{D}_5 \left(3C_{12}\mathcal{D}_2 + C_{33} \left(3\mathcal{D}_2 + \sqrt{3}\mathcal{D}_6 + 3 \right) + \sqrt{3}(C_{23}\mathcal{D}_2 + 3C_{11}\mathcal{D}_6) \right) \right), \\
G_{13}^{[6]} &= \frac{9}{4} \left(\sqrt{3}C_{12}\mathcal{D}_3 + 3C_{11}\mathcal{D}_7 + \mathcal{D}_5 \left(\left(3C_{12} + \sqrt{3}C_{23} + 3C_{33} \right) \mathcal{D}_3 \right. \right. \\
&\quad \left. \left. + \sqrt{3}(\mathcal{D}_7C_{33} + C_{33} + 3C_{11}\mathcal{D}_7) \right) + \right. \\
&\quad \left. + C_{13} \left(3\mathcal{D}_5 + \sqrt{3}(3\mathcal{D}_1\mathcal{D}_7 + \mathcal{D}_7 + 1) + 3 \left(\sqrt{3}\mathcal{D}_5\mathcal{D}_3 + \mathcal{D}_3 + 2\mathcal{D}_5\mathcal{D}_7 \right) \right) + \right. \\
&\quad \left. + \mathcal{D}_1 \left(\sqrt{3}C_{22}\mathcal{D}_3 + 3C_{12}\mathcal{D}_7 + 3C_{33} \left(\sqrt{3}\mathcal{D}_3 + \mathcal{D}_7 + 1 \right) \right. \right. \\
&\quad \left. \left. + C_{23} \left(6\mathcal{D}_3 + \sqrt{3}(\mathcal{D}_7 + 1) \right) \right) \right), \\
G_{14}^{[6]} &= \frac{9}{4} \left(C_{22}\mathcal{D}_1 \left(\sqrt{3}\mathcal{D}_4 + 3 \right) + C_{12} \left(3\mathcal{D}_5\mathcal{D}_4 + \sqrt{3}\mathcal{D}_4 + 3\sqrt{3}\mathcal{D}_5 + 3\mathcal{D}_1\mathcal{D}_8 + 3 \right) \right. \\
&\quad \left. + 3C_{11} \left(\sqrt{3}\mathcal{D}_5\mathcal{D}_8 + \mathcal{D}_8 \right) + \right. \\
&\quad \left. + C_{33} \left(3\mathcal{D}_4\mathcal{D}_5 + \sqrt{3}\mathcal{D}_8\mathcal{D}_5 + 3\mathcal{D}_1 \left(\sqrt{3}\mathcal{D}_4 + \mathcal{D}_8 \right) \right) \right. \\
&\quad \left. + C_{13} \left(\sqrt{3}(3\mathcal{D}_1 + 1)\mathcal{D}_8 + 3 \left(\sqrt{3}\mathcal{D}_5\mathcal{D}_4 + \mathcal{D}_4 + 2\mathcal{D}_5\mathcal{D}_8 \right) \right) + \right. \\
&\quad \left. + C_{23} \left(\left(\sqrt{3}\mathcal{D}_4 + 3 \right) \mathcal{D}_5 + \mathcal{D}_1 \left(6\mathcal{D}_4 + \sqrt{3}(\mathcal{D}_8 + 3) \right) \right) \right), \\
G_{22}^{[6]} &= \frac{9}{4} \left(\sqrt{3}C_{22}\mathcal{D}_2^2 + 2C_{23} \left(3\mathcal{D}_2 + \sqrt{3}\mathcal{D}_6 + 3 \right) \mathcal{D}_2 \right. \\
&\quad \left. + 3\mathcal{D}_6 \left(2C_{12}\mathcal{D}_2 + \sqrt{3}C_{11}\mathcal{D}_6 + 2C_{13} \left(\sqrt{3}\mathcal{D}_2 + \mathcal{D}_6 + \sqrt{3} \right) \right) + \right. \\
&\quad \left. + C_{33} \left(3\sqrt{3}\mathcal{D}_2^2 + 6 \left(\mathcal{D}_6 + \sqrt{3} \right) \mathcal{D}_2 + \mathcal{D}_6 \left(\sqrt{3}\mathcal{D}_6 + 6 \right) + 3\sqrt{3} \right) \right),
\end{aligned}$$

$$\begin{aligned}
G_{23}^{[6]} &= \frac{9}{4} \left(\sqrt{3}C_{22}\mathcal{D}_2\mathcal{D}_3 + 3 \left(C_{12}\mathcal{D}_2 + \sqrt{3}C_{13}(\mathcal{D}_2 + 1) \right) \mathcal{D}_7 \right. \\
&\quad + 3\mathcal{D}_6 \left(\sqrt{3}\mathcal{D}_3C_{13} + 2\mathcal{D}_7C_{13} + C_{13} + C_{12}\mathcal{D}_3 + \sqrt{3}C_{11}\mathcal{D}_7 \right) + \\
&\quad + C_{23} \left(\mathcal{D}_3 \left(6\mathcal{D}_2 + \sqrt{3}\mathcal{D}_6 + 3 \right) + \sqrt{3}\mathcal{D}_2(\mathcal{D}_7 + 1) \right) \\
&\quad \left. + C_{33} \left(3\mathcal{D}_3 \left(\sqrt{3}\mathcal{D}_2 + \mathcal{D}_6 + \sqrt{3} \right) + \left(3\mathcal{D}_2 + \sqrt{3}\mathcal{D}_6 + 3 \right) (\mathcal{D}_7 + 1) \right) \right), \\
G_{24}^{[6]} &= \frac{9}{4} \left(C_{22}\mathcal{D}_2 \left(\sqrt{3}\mathcal{D}_4 + 3 \right) + 3\sqrt{3}C_{12}\mathcal{D}_6 + 3 \left(C_{12}\mathcal{D}_2 + \sqrt{3}C_{13}(\mathcal{D}_2 + 1) \right) \mathcal{D}_8 + \right. \\
&\quad + 3\mathcal{D}_6 \left(C_{12}\mathcal{D}_4 + \sqrt{3}C_{13}\mathcal{D}_4 + \sqrt{3}C_{11}\mathcal{D}_8 + 2C_{13}\mathcal{D}_8 \right) \\
&\quad + C_{33} \left(3\mathcal{D}_4 \left(\sqrt{3}\mathcal{D}_2 + \mathcal{D}_6 + \sqrt{3} \right) + \left(3\mathcal{D}_2 + \sqrt{3}\mathcal{D}_6 + 3 \right) \mathcal{D}_8 \right) + \\
&\quad \left. + C_{23} \left(\sqrt{3}\mathcal{D}_4\mathcal{D}_6 + 3 \left(\mathcal{D}_4 + \mathcal{D}_6 + \sqrt{3} \right) + \mathcal{D}_2 \left(6\mathcal{D}_4 + \sqrt{3}(\mathcal{D}_8 + 3) \right) \right) \right), \\
G_{33}^{[6]} &= \frac{9}{4} \left(\sqrt{3}C_{22}\mathcal{D}_3^2 + 2C_{23} \left(3\mathcal{D}_3 + \sqrt{3}(\mathcal{D}_7 + 1) \right) \mathcal{D}_3 \right. \\
&\quad + C_{33} \left(3\sqrt{3}\mathcal{D}_3^2 + 6(\mathcal{D}_7 + 1)\mathcal{D}_3 + \sqrt{3}(\mathcal{D}_7 + 1)^2 \right) + \\
&\quad \left. + 3\mathcal{D}_7 \left(2C_{12}\mathcal{D}_3 + \sqrt{3}C_{11}\mathcal{D}_7 + 2C_{13} \left(\sqrt{3}\mathcal{D}_3 + \mathcal{D}_7 + 1 \right) \right) \right), \\
G_{34}^{[6]} &= \frac{9}{4} \left(C_{22}\mathcal{D}_3 \left(\sqrt{3}\mathcal{D}_4 + 3 \right) + 3\sqrt{3}C_{12}\mathcal{D}_7 \right. \\
&\quad + 3\mathcal{D}_4 \left(\left(C_{12} + \sqrt{3}C_{13} \right) \mathcal{D}_7 + C_{33} \left(\sqrt{3}\mathcal{D}_3 + \mathcal{D}_7 + 1 \right) \right) + \\
&\quad + \left(3(C_{12} + C_{33})\mathcal{D}_3 + 3C_{13} \left(\sqrt{3}\mathcal{D}_3 + 2\mathcal{D}_7 + 1 \right) \right. \\
&\quad \left. + \sqrt{3}(\mathcal{D}_7C_{33} + C_{33} + 3C_{11}\mathcal{D}_7) \right) \mathcal{D}_8 + \\
&\quad \left. + C_{23} \left(\left(\sqrt{3}\mathcal{D}_4 + 3 \right) (\mathcal{D}_7 + 1) + \mathcal{D}_3 \left(6\mathcal{D}_4 + \sqrt{3}(\mathcal{D}_8 + 3) \right) \right) \right), \\
G_{44}^{[6]} &= \frac{9}{4} \left(3\sqrt{3}C_{33}\mathcal{D}_4^2 + 6 \left(C_{12} + \sqrt{3}C_{13} + C_{33} \right) \mathcal{D}_8\mathcal{D}_4 \right. \\
&\quad + \left(3\sqrt{3}C_{11} + 6C_{13} + \sqrt{3}C_{33} \right) \mathcal{D}_8^2 + \\
&\quad + C_{22} \left(\mathcal{D}_4 \left(\sqrt{3}\mathcal{D}_4 + 6 \right) + 3\sqrt{3} \right) + 6\sqrt{3}C_{12}\mathcal{D}_8 \\
&\quad \left. + 2C_{23} \left(3\mathcal{D}_4^2 + \sqrt{3}(\mathcal{D}_8 + 3)\mathcal{D}_4 + 3\mathcal{D}_8 \right) \right).
\end{aligned} \tag{A.16}$$

$$\begin{aligned}
G_{11}^{[7]} &= 9 \left(\mathcal{D}_1 \left(2\sqrt{3}C_{12} + 3C_{13} + \sqrt{3}C_{22}\mathcal{D}_1 + 3C_{23}\mathcal{D}_1 \right) \right. \\
&\quad \left. + C_{11} \left(3\mathcal{D}_5 + \sqrt{3} \right) + \right. \\
&\quad \left. + \mathcal{D}_5 \left(3\mathcal{D}_5C_{13} + 2\sqrt{3}C_{13} + 3C_{12}\mathcal{D}_1 \right. \right. \\
&\quad \left. \left. + 2\sqrt{3}C_{23}\mathcal{D}_1 + 3C_{33}\mathcal{D}_1 + \sqrt{3}C_{33}\mathcal{D}_5 \right) \right), \\
G_{12}^{[7]} &= \frac{9}{2} \left(2\sqrt{3}C_{12}\mathcal{D}_2 + 3C_{33}\mathcal{D}_5 + 3C_{11}\mathcal{D}_6 + \right. \\
&\quad \mathcal{D}_5 \left(3C_{12}\mathcal{D}_2 + 2\sqrt{3}C_{23}\mathcal{D}_2 + 3C_{33}\mathcal{D}_2 + 2\sqrt{3}C_{33}\mathcal{D}_6 \right) + \\
&\quad \left. + C_{13} \left(3\mathcal{D}_2 + 6\mathcal{D}_5\mathcal{D}_6 + 2\sqrt{3}\mathcal{D}_6 + 3 \right) \right. \\
&\quad \left. + \mathcal{D}_1 \left(2\sqrt{3}C_{22}\mathcal{D}_2 + 3(C_{12} + C_{33})\mathcal{D}_6 + C_{23} \left(6\mathcal{D}_2 + 2\sqrt{3}\mathcal{D}_6 + 3 \right) \right) \right), \\
G_{13}^{[7]} &= \frac{9}{2} \left(2\sqrt{3}C_{12}\mathcal{D}_3 + 3C_{11}\mathcal{D}_7 + \mathcal{D}_1 \left(2\sqrt{3}C_{22}\mathcal{D}_3 \right. \right. \\
&\quad \left. \left. + 3C_{12}\mathcal{D}_7 + 3C_{33}(\mathcal{D}_7 + 1) \right) + \right. \\
&\quad \left. + \mathcal{D}_5 \left(3(C_{12} + C_{33})\mathcal{D}_3 + 2\sqrt{3}C_{33}(\mathcal{D}_7 + 1) \right) \right. \\
&\quad \left. + 2C_{23} \left(\mathcal{D}_3 \left(3\mathcal{D}_1 + \sqrt{3}\mathcal{D}_5 \right) + \sqrt{3}\mathcal{D}_1(\mathcal{D}_7 + 1) \right) + \right. \\
&\quad \left. + C_{13} \left(3\mathcal{D}_3 + 2\sqrt{3}(\mathcal{D}_7 + 1) + \mathcal{D}_5(6\mathcal{D}_7 + 3) \right) \right), \\
G_{14}^{[7]} &= \frac{9}{2} \left(3C_{13}\mathcal{D}_4 + 6C_{23}\mathcal{D}_1\mathcal{D}_4 + 2\sqrt{3}C_{23}\mathcal{D}_5\mathcal{D}_4 \right. \\
&\quad \left. + 3C_{33}\mathcal{D}_5\mathcal{D}_4 + C_{22}\mathcal{D}_1 \left(2\sqrt{3}\mathcal{D}_4 + 3 \right) + \right. \\
&\quad \left. + 3C_{23}\mathcal{D}_5 + \left(3C_{11} + 2\sqrt{3}C_{13} + 2\sqrt{3}C_{23}\mathcal{D}_1 \right. \right. \\
&\quad \left. \left. + 3C_{33}\mathcal{D}_1 + 6C_{13}\mathcal{D}_5 + 2\sqrt{3}C_{33}\mathcal{D}_5 \right) \mathcal{D}_8 + \right. \\
&\quad \left. + C_{12} \left(3\mathcal{D}_5\mathcal{D}_4 + 2\sqrt{3}\mathcal{D}_4 + 3\mathcal{D}_1\mathcal{D}_8 + 3 \right) \right), \\
G_{22}^{[7]} &= 9 \left(\sqrt{3}C_{22}\mathcal{D}_2^2 + C_{23} \left(3\mathcal{D}_2 + 2\sqrt{3}\mathcal{D}_6 + 3 \right) \mathcal{D}_2 \right. \\
&\quad \left. + \mathcal{D}_6 \left(\sqrt{3}\mathcal{D}_6C_{33} + 3C_{33} + 3(C_{12} + C_{33})\mathcal{D}_2 + 3C_{13}\mathcal{D}_6 \right) \right), \\
G_{23}^{[7]} &= \frac{9}{2} \left(2\sqrt{3}C_{22}\mathcal{D}_2\mathcal{D}_3 + 3C_{12}\mathcal{D}_6\mathcal{D}_3 + 3C_{13}\mathcal{D}_6 + 3C_{12}\mathcal{D}_2\mathcal{D}_7 + 6C_{13}\mathcal{D}_6\mathcal{D}_7 \right. \\
&\quad \left. + C_{23} \left(\mathcal{D}_3 \left(6\mathcal{D}_2 + 2\sqrt{3}\mathcal{D}_6 + 3 \right) + \right. \right. \\
&\quad \left. \left. + 2\sqrt{3}\mathcal{D}_2(\mathcal{D}_7 + 1) \right) + C_{33} \left(3(\mathcal{D}_2 + 1)(\mathcal{D}_7 + 1) \right. \right. \\
&\quad \left. \left. + \mathcal{D}_6 \left(3\mathcal{D}_3 + 2\sqrt{3}(\mathcal{D}_7 + 1) \right) \right) \right),
\end{aligned}$$

$$\begin{aligned}
G_{24}^{[7]} &= \frac{9}{2} \left(C_{22} \mathcal{D}_2 \left(2\sqrt{3} \mathcal{D}_4 + 3 \right) + 3(C_{12} + C_{33}) \mathcal{D}_4 \mathcal{D}_6 \right. \\
&\quad + \left(3C_{12} \mathcal{D}_2 + 6C_{13} \mathcal{D}_6 + C_{33} \left(3\mathcal{D}_2 + 2\sqrt{3} \mathcal{D}_6 + 3 \right) \right) \mathcal{D}_8 + \\
&\quad \left. + C_{23} \left(3\mathcal{D}_6 + \mathcal{D}_4 \left(6\mathcal{D}_2 + 2\sqrt{3} \mathcal{D}_6 + 3 \right) + 2\sqrt{3} \mathcal{D}_2 \mathcal{D}_8 \right) \right), \\
G_{33}^{[7]} &= 9 \left(\sqrt{3} C_{22} \mathcal{D}_3^2 + C_{23} \left(3\mathcal{D}_3 + 2\sqrt{3} (\mathcal{D}_7 + 1) \right) \mathcal{D}_3 \right. \\
&\quad + 3\mathcal{D}_7 (\mathcal{D}_7 C_{13} + C_{13} + C_{12} \mathcal{D}_3) + \\
&\quad \left. + C_{33} (\mathcal{D}_7 + 1) \left(3\mathcal{D}_3 + \sqrt{3} (\mathcal{D}_7 + 1) \right) \right), \\
G_{34}^{[7]} &= \frac{9}{2} \left(C_{22} \mathcal{D}_3 \left(2\sqrt{3} \mathcal{D}_4 + 3 \right) + 3\mathcal{D}_4 (C_{33} + (C_{12} + C_{33}) \mathcal{D}_7) + 3C_{13} \mathcal{D}_8 + \right. \\
&\quad + \left(3C_{12} \mathcal{D}_3 + 6C_{13} \mathcal{D}_7 + C_{33} \left(3\mathcal{D}_3 + 2\sqrt{3} (\mathcal{D}_7 + 1) \right) \right) \mathcal{D}_8 + \\
&\quad \left. + C_{23} \left(3\mathcal{D}_7 + 2\mathcal{D}_4 \left(3\mathcal{D}_3 + \sqrt{3} (\mathcal{D}_7 + 1) \right) + 2\sqrt{3} \mathcal{D}_3 \mathcal{D}_8 + 3 \right) \right), \\
G_{44}^{[7]} &= 9 \left(C_{22} \mathcal{D}_4 \left(\sqrt{3} \mathcal{D}_4 + 3 \right) + \mathcal{D}_8 \left(3(C_{12} + C_{33}) \mathcal{D}_4 + 3C_{13} \mathcal{D}_8 + \sqrt{3} C_{33} \mathcal{D}_8 \right) + \right. \\
&\quad \left. + C_{23} \left(3\mathcal{D}_4^2 + 2\sqrt{3} \mathcal{D}_8 \mathcal{D}_4 + 3\mathcal{D}_8 \right) \right). \tag{A.17}
\end{aligned}$$

$$\begin{aligned}
G_{11}^{[8]} &= \frac{18}{\ell} (\mathcal{D}_1 M_{21}^* + \mathcal{D}_5 M_{31}^* + M_{11}^*), \\
G_{12}^{[8]} &= \frac{9}{\ell} (\mathcal{D}_1 M_{22}^* + \mathcal{D}_2 M_{21}^* + \mathcal{D}_5 M_{32}^* + \mathcal{D}_6 M_{31}^* + M_{12}^*), \\
G_{13}^{[8]} &= \frac{9}{\ell} (\mathcal{D}_1 M_{23}^* + \mathcal{D}_3 M_{21}^* + \mathcal{D}_5 M_{33}^* + \mathcal{D}_7 M_{31}^* + M_{13}^* + M_{31}^*), \\
G_{14}^{[8]} &= \frac{9}{\ell} (\mathcal{D}_1 M_{24}^* + \mathcal{D}_4 M_{21}^* + \mathcal{D}_5 M_{34}^* + \mathcal{D}_8 M_{31}^* + M_{14}^*), \\
G_{22}^{[8]} &= \frac{18}{\ell} (\mathcal{D}_2 M_{22}^* + \mathcal{D}_6 M_{32}^*), \\
G_{23}^{[8]} &= \frac{9}{\ell} (\mathcal{D}_2 M_{23}^* + \mathcal{D}_3 M_{22}^* + \mathcal{D}_6 M_{33}^* + \mathcal{D}_7 M_{32}^* + M_{32}^*), \\
G_{24}^{[8]} &= \frac{9}{\ell} (\mathcal{D}_2 M_{24}^* + \mathcal{D}_4 M_{22}^* + \mathcal{D}_6 M_{34}^* + \mathcal{D}_8 M_{32}^*), \\
G_{33}^{[8]} &= \frac{18}{\ell} (\mathcal{D}_3 M_{23}^* + \mathcal{D}_7 M_{33}^* + M_{33}^*), \\
G_{34}^{[8]} &= \frac{9}{\ell} (\mathcal{D}_3 M_{24}^* + \mathcal{D}_4 M_{23}^* + \mathcal{D}_7 M_{34}^* + \mathcal{D}_8 M_{33}^* + M_{34}^*), \\
G_{44}^{[8]} &= \frac{18}{\ell} (\mathcal{D}_4 M_{24}^* + \mathcal{D}_8 M_{34}^*) \tag{A.18}
\end{aligned}$$

$$\begin{aligned}
G_{11}^{[9]} &= \frac{9}{\ell} \left(\mathcal{D}_1 \left(M_{21}^* + \sqrt{3} M_{31}^* \right) + \sqrt{3} \mathcal{D}_5 M_{11}^* + \mathcal{D}_5 M_{31}^* + M_{11}^* \right), \\
G_{12}^{[9]} &= \frac{9}{2} \left(\mathcal{D}_1 M_{22}^* + \sqrt{3} (\mathcal{D}_1 M_{32}^* + M_{31}^*) + \mathcal{D}_2 \left(M_{21}^* + \sqrt{3} M_{31}^* \right) \right. \\
&\quad \left. + \sqrt{3} \mathcal{D}_5 M_{12}^* + \mathcal{D}_5 M_{32}^* + \mathcal{D}_6 \left(\sqrt{3} M_{11}^* + M_{31}^* \right) + M_{12}^* \right), \\
G_{13}^{[9]} &= \frac{9}{2\ell} \left(\mathcal{D}_1 M_{23}^* + \sqrt{3} \mathcal{D}_1 M_{33}^* + \mathcal{D}_3 M_{21}^* + \sqrt{3} \mathcal{D}_3 M_{31}^* \right. \\
&\quad \left. + \sqrt{3} \mathcal{D}_5 M_{13}^* + \mathcal{D}_5 M_{33}^* + \mathcal{D}_7 \left(\sqrt{3} M_{11}^* + M_{31}^* \right) + M_{13}^* + M_{31}^* \right), \\
G_{14}^{[9]} &= \frac{9}{2\ell} \left(\sqrt{3} (\mathcal{D}_1 M_{34}^* + \mathcal{D}_4 M_{31}^*) + \mathcal{D}_1 M_{24}^* + (\mathcal{D}_4 + \sqrt{3}) M_{21}^* \right. \\
&\quad \left. + \sqrt{3} \mathcal{D}_5 M_{14}^* + \mathcal{D}_5 M_{34}^* + \mathcal{D}_8 \left(\sqrt{3} M_{11}^* + M_{31}^* \right) + M_{14}^* \right), \\
G_{22}^{[9]} &= \frac{9}{\ell} \left(\mathcal{D}_2 M_{22}^* + \sqrt{3} (\mathcal{D}_2 + 1) M_{32}^* + \mathcal{D}_6 \left(\sqrt{3} M_{12}^* + M_{32}^* \right) \right), \\
G_{23}^{[9]} &= \frac{9}{2\ell} \left(\mathcal{D}_2 M_{23}^* + \sqrt{3} \mathcal{D}_2 M_{33}^* + \mathcal{D}_3 M_{22}^* + \sqrt{3} \mathcal{D}_3 M_{32}^* \right. \\
&\quad \left. + \mathcal{D}_6 \left(\sqrt{3} M_{13}^* + M_{33}^* \right) + \mathcal{D}_7 \left(\sqrt{3} M_{12}^* + M_{32}^* \right) + M_{32}^* + \sqrt{3} M_{33}^* \right), \\
G_{24}^{[9]} &= \frac{9}{2\ell} \left(\sqrt{3} (\mathcal{D}_2 M_{34}^* + \mathcal{D}_4 M_{32}^* + M_{34}^*) + \mathcal{D}_2 M_{24}^* + (\mathcal{D}_4 + \sqrt{3}) M_{22}^* \right. \\
&\quad \left. + \mathcal{D}_6 \left(\sqrt{3} M_{14}^* + M_{34}^* \right) + \mathcal{D}_8 \left(\sqrt{3} M_{12}^* + M_{32}^* \right) \right), \\
G_{33}^{[9]} &= \frac{9}{\ell} \left(\mathcal{D}_3 \left(M_{23}^* + \sqrt{3} M_{33}^* \right) + \mathcal{D}_7 \left(\sqrt{3} M_{13}^* + M_{33}^* \right) + M_{33}^* \right), \\
G_{34}^{[9]} &= \frac{9}{2\ell} \left(\mathcal{D}_3 M_{24}^* + \sqrt{3} \mathcal{D}_3 M_{34}^* + (\mathcal{D}_4 + \sqrt{3}) M_{23}^* + \sqrt{3} \mathcal{D}_4 M_{33}^* \right. \\
&\quad \left. + \mathcal{D}_7 \left(\sqrt{3} M_{14}^* + M_{34}^* \right) + \mathcal{D}_8 \left(\sqrt{3} M_{13}^* + M_{33}^* \right) + M_{34}^* \right), \\
G_{44}^{[9]} &= \frac{9}{\ell} \left((\mathcal{D}_4 + \sqrt{3}) M_{24}^* + \sqrt{3} \mathcal{D}_4 M_{34}^* + \mathcal{D}_8 \left(\sqrt{3} M_{14}^* + M_{34}^* \right) \right) \\
G_{11}^{[10]} &= \frac{3\sqrt{3}}{\ell^2} A_{11}^* + \frac{5}{8} \sqrt{3} \left(\mathcal{D}_5^2 (C_{11} + C_{33}) + C_{11} + 2C_{12} \mathcal{D}_1 \right. \\
&\quad \left. + 2\mathcal{D}_5 (\mathcal{D}_1 (C_{13} + C_{23}) + C_{13}) + \mathcal{D}_1^2 (C_{22} + C_{33}) \right), \\
G_{12}^{[10]} &= \frac{3\sqrt{3}}{\ell^2} A_{12}^* + \frac{5}{8} \sqrt{3} \left(\mathcal{D}_6 (C_{11} \mathcal{D}_5 + \mathcal{D}_1 (C_{13} + C_{23}) + C_{13}) \right. \\
&\quad \left. + \mathcal{D}_2 (C_{12} + \mathcal{D}_5 (C_{13} + C_{23}) + C_{22} \mathcal{D}_1) + C_{13} \mathcal{D}_5 + \right. \\
&\quad \left. + C_{33} (\mathcal{D}_1 \mathcal{D}_2 + \mathcal{D}_1 + \mathcal{D}_5 \mathcal{D}_6) \right),
\end{aligned} \tag{A.19}$$

$$\begin{aligned}
G_{13}^{[10]} &= \frac{3\sqrt{3}}{\ell^2} A_{13}^* + \frac{5}{8}\sqrt{3} (\mathcal{D}_7(\mathcal{D}_5(C_{11} + C_{33}) + \mathcal{D}_1(C_{13} + C_{23}) + C_{13}) \\
&\quad + C_{12}\mathcal{D}_3 + C_{13}\mathcal{D}_3\mathcal{D}_5 + C_{13} + \mathcal{D}_1\mathcal{D}_3(C_{22} + C_{33}) + \\
&\quad + C_{23}\mathcal{D}_1 + C_{23}\mathcal{D}_3\mathcal{D}_5 + C_{33}\mathcal{D}_5), \\
G_{14}^{[10]} &= \frac{3\sqrt{3}}{\ell^2} A_{14}^* + \frac{5}{8}\sqrt{3} (\mathcal{D}_8(C_{11}\mathcal{D}_5 + C_{13}\mathcal{D}_1 + C_{13} + C_{33}\mathcal{D}_5) \\
&\quad + C_{12}(\mathcal{D}_4 + \mathcal{D}_5) + C_{13}\mathcal{D}_4\mathcal{D}_5 + \mathcal{D}_1\mathcal{D}_4(C_{22} + C_{33}) + \\
&\quad + C_{23}(\mathcal{D}_1\mathcal{D}_8 + \mathcal{D}_1 + \mathcal{D}_4\mathcal{D}_5)), \\
G_{22}^{[10]} &= \frac{3\sqrt{3}}{\ell^2} A_{22}^* + \frac{5}{8}\sqrt{3} (\mathcal{D}_6(C_{11}\mathcal{D}_6 + 2(\mathcal{D}_2(C_{13} + C_{23}) + C_{13})) \\
&\quad + C_{22}\mathcal{D}_2^2 + C_{33}((\mathcal{D}_2 + 1)^2 + \mathcal{D}_6^2)), \\
G_{23}^{[10]} &= \frac{3\sqrt{3}}{\ell^2} A_{23}^* + \frac{5}{8}\sqrt{3} (C_{11}\mathcal{D}_6\mathcal{D}_7 + C_{13}(\mathcal{D}_2\mathcal{D}_7 + \mathcal{D}_3\mathcal{D}_6 + \mathcal{D}_7) \\
&\quad + C_{22}\mathcal{D}_2\mathcal{D}_3 + C_{23}(\mathcal{D}_2\mathcal{D}_7 + \mathcal{D}_2 + \mathcal{D}_3\mathcal{D}_6) + \\
&\quad + C_{33}(\mathcal{D}_2\mathcal{D}_3 + \mathcal{D}_3 + \mathcal{D}_6\mathcal{D}_7 + \mathcal{D}_6)), \\
G_{24}^{[10]} &= \frac{3\sqrt{3}}{\ell^2} A_{24}^* + \frac{5}{8}\sqrt{3} (\mathcal{D}_8(\mathcal{D}_6(C_{11} + C_{33}) + C_{13}(\mathcal{D}_2 + 1)) + C_{12}\mathcal{D}_6 \\
&\quad + \mathcal{D}_4(C_{13}\mathcal{D}_6 + C_{22}\mathcal{D}_2 + C_{33}\mathcal{D}_2 + C_{33}) + \\
&\quad + C_{23}(\mathcal{D}_2\mathcal{D}_8 + \mathcal{D}_2 + \mathcal{D}_4\mathcal{D}_6 + 1)), \\
G_{33}^{[10]} &= \frac{3\sqrt{3}}{\ell^2} A_{33}^* + \frac{5}{8}\sqrt{3} (C_{11}\mathcal{D}_7^2 \\
&\quad + 2\mathcal{D}_3\mathcal{D}_7(C_{13} + C_{23}) + \mathcal{D}_3(C_{22}\mathcal{D}_3 + 2C_{23}) + C_{33}(\mathcal{D}_3^2 + (\mathcal{D}_7 + 1)^2)), \\
G_{34}^{[10]} &= \frac{3\sqrt{3}}{\ell^2} A_{34}^* + \frac{5}{8}\sqrt{3} (\mathcal{D}_8(\mathcal{D}_7(C_{11} + C_{33}) + C_{13}\mathcal{D}_3 + C_{33}) \\
&\quad + C_{12}\mathcal{D}_7 + C_{13}\mathcal{D}_4\mathcal{D}_7 + \mathcal{D}_3\mathcal{D}_4(C_{22} + C_{33}) + \\
&\quad + C_{23}(\mathcal{D}_3\mathcal{D}_8 + \mathcal{D}_3 + \mathcal{D}_4\mathcal{D}_7 + \mathcal{D}_4)), \\
G_{44}^{[10]} &= \frac{3\sqrt{3}}{\ell^2} A_{44}^* + \frac{5}{8}\sqrt{3} (\mathcal{D}_8^2(C_{11} + C_{33}) + 2\mathcal{D}_8(C_{12} + \mathcal{D}_4(C_{13} + C_{23})) \\
&\quad + C_{22}\mathcal{D}_4^2 + C_{22} + 2C_{23}\mathcal{D}_4 + C_{33}\mathcal{D}_4^2).
\end{aligned} \tag{A.20}$$

Bibliography

- [1] H. Abdoul-Anziz and P. Seppecher. "Strain gradient and generalized continua obtained by homogenizing frame lattices". In: *Mathematics and Mechanics of Complex Systems* 6.3 (2018), pp. 213–250.
- [2] A. Askar and A.S. Cakmak. "A structural model of a micropolar continuum". In: *International Journal of Engineering Science* 6.10 (1968), pp. 583–589.
- [3] N. Auffray, R. Bouchet, and Y. Bréchet. "Strain gradient elastic homogenization of bidimensional cellular media". In: *International Journal of Solids and Structures* 47.13 (2010), pp. 1698–1710. ISSN: 0020-7683.
- [4] N. Auffray, J. Dirrenberger, and G. Rosi. "A complete description of bi-dimensional anisotropic strain-gradient elasticity". In: *International Journal of Solids and Structures* 69 (2015), pp. 195–206.
- [5] M. Bacca, D. Bigoni, F. Dal Corso, and D. Veber. "Mindlin second-gradient elastic properties from dilute two-phase Cauchy-elastic composites. Part I: Closed form expression for the effective higher-order constitutive tensor". In: *International Journal of Solids and Structures* 50.24 (2013), pp. 4010–4019.
- [6] M. Bacca, D. Bigoni, F. Dal Corso, and D. Veber. "Mindlin second-gradient elastic properties from dilute two-phase Cauchy-elastic composites Part II: Higher-order constitutive properties and application cases". In: *International Journal of Solids and Structures* (2013).
- [7] A. Bacigalupo. "Second-order homogenization of periodic materials based on asymptotic approximation of the strain energy: formulation and validity limits". In: *Meccanica* 49.6 (2014), pp. 1407–1425.
- [8] A. Bacigalupo and L. Gambarotta. "Computational two-scale homogenization of periodic masonry: characteristic lengths and dispersive waves". In: *Computer Methods in Applied Mechanics and Engineering* 213 (2012), pp. 16–28.
- [9] A. Bacigalupo and L. Gambarotta. "Second-gradient homogenized model for wave propagation in heterogeneous periodic media". In: *International Journal of Solids and Structures* 51.5 (2014), pp. 1052–1065.
- [10] A. Bacigalupo and L. Gambarotta. "Second-order computational homogenization of heterogeneous materials with periodic microstructure". In: *ZAMM-Journal of Applied Mathematics and Mechanics/Zeitschrift für Angewandte Mathematik und Mechanik* 90.10-11 (2010), pp. 796–811.
- [11] A. Bacigalupo and L. Gambarotta. "Simplified modelling of chiral lattice materials with local resonators". In: *International Journal of Solids and Structures* 83 (2016), pp. 126–141.
- [12] A. Bacigalupo and L. Gambarotta. "Wave propagation in non-centrosymmetric beam-lattices with lumped masses: Discrete and micropolar modeling". In: *International Journal of Solids and Structures* 118 (2017), pp. 128–145.

- [13] A. Bacigalupo, F. Paggi M. and Dal Corso, and D. Bigoni. "Identification of higher-order continua equivalent to a Cauchy elastic composite". In: *Mechanics Research Communications* (2017). ISSN: 0093-6413.
- [14] A.J. Beveridge, M.A. Wheel, and D.H. Nash. "The micropolar elastic behaviour of model macroscopically heterogeneous materials". In: *International Journal of Solids and Structures* 50.1 (2013), pp. 246–255. ISSN: 0020-7683.
- [15] D. Bigoni and W.J. Drugan. "Analytical derivation of Cosserat moduli via homogenization of heterogeneous elastic materials". In: *Journal of Applied Mechanics* 74.4 (2007), pp. 741–753.
- [16] M. Born and K. Huang. *Dynamical theory of crystal lattices*. Clarendon press, 1954.
- [17] P.M. Buechner and R.S. Lakes. "Size effects in the elasticity and viscoelasticity of bone". In: *Biomechanics and modeling in mechanobiology* 1.4 (2003), pp. 295–301.
- [18] A.L. Cauchy. "Sur l'équilibre et le mouvement d'un système de points matériels sollicités par forces d'attraction ou de répulsion mutuelle". In: *Ex. de Math.* (1828), 3:187—213.
- [19] F. Dal Corso and J.R. Willis. "Stability of strain-gradient plastic materials". In: *Journal of the Mechanics and Physics of Solids* 59.6 (2011), pp. 1251–1267.
- [20] A.R. Day, K.A. Snyder, E.J. Garboczi, and M.F. Thorpe. "The elastic moduli of a sheet containing circular holes". In: *Journal of the Mechanics and Physics of Solids* 40.5 (1992), pp. 1031–1051.
- [21] A. Genoese, A. Genoese, N. L. Rizzi, and Ginevra Salerno. "Force constants of BN, SiC, AlN and GaN sheets through discrete homogenization". In: *Meccanica* 53.3 (2018), pp. 593–611.
- [22] P.A. Gourgiotis and D. Bigoni. "Folding and faulting of an elastic continuum". In: *Proc.R.Soc.A* 472 (2016), p. 20160018.
- [23] P.A. Gourgiotis and D. Bigoni. "Stress channelling in extreme couple-stress materials Part II: Localized folding vs faulting of a continuum in single and cross geometries". In: *Journal of the Mechanics and Physics of Solids* 88 (2016), pp. 169–185.
- [24] P.N. Keating. "Effect of invariance requirements on the elastic strain energy of crystals with application to the diamond structure". In: *Physical Review* 145.2 (1966), p. 637.
- [25] J.G. Kirkwood. "The skeletal modes of vibration of long chain molecules". In: *The Journal of Chemical Physics* 7.7 (1939), pp. 506–509.
- [26] R.S. Lakes. "Experimental microelasticity of two porous solids". In: *International Journal of Solids and Structures* 22.1 (1986), pp. 55–63.
- [27] R.M. Latture, M.R. Begley, and F.W. Zok. "Design and mechanical properties of elastically isotropic trusses". In: *Journal of Materials Research* 33.3 (2018), pp. 249–263.
- [28] H. Le Dret and A. Raoult. "Homogenization of hexagonal lattices". In: *Networks and Heterogeneous Media* 8.2 (2013), pp. 541–572.
- [29] S.G. Lekhnitskii, P. Fern, J.J. Brandstatter, and E.H. Dill. "Theory of elasticity of an anisotropic elastic body". In: *Physics Today* 17 (1964), p. 84.

- [30] B. Loret and J.H. Prevost. "On the existence of solutions in layered elasto-(visco-) plastic solids with negative hardening". In: *European journal of mechanics. A. Solids* 10.6 (1991), pp. 575–586.
- [31] B. Loret and J.H. Prevost. "On the Occurrence of Unloading in 1D Elasto-(Visco-) plastic Structures with Softening". In: *European Journal of Mechanics. A. Solids* 12 (1993), pp. 757–772.
- [32] R.D. Mindlin. "Micro-structure in linear elasticity". In: *Archive for Rational Mechanics and Analysis* 16.1 (1964), pp. 51–78.
- [33] R.D. Mindlin and N.N. Eshel. "On first strain-gradient theories in linear elasticity". In: *International Journal of Solids and Structures* 4.1 (1968), pp. 109–124. ISSN: 0020-7683.
- [34] A. Needleman. "Material rate dependence and mesh sensitivity in localization problems". In: *Computer Methods in Applied Mechanics and Engineering* 67.1 (1988), pp. 69–85. ISSN: 0045-7825.
- [35] H.P. Neumann. "Equations of state and phase transitions for some plane-lattice models". In: *Physical Review A* 11.3 (1975), p. 1043.
- [36] M. Ostoja-Starzewski. "Lattice models in micromechanics". In: *Applied Mechanics Reviews* 55.1 (2002), pp. 35–60.
- [37] P. Seppecher, J.-J. Alibert, and F. Dell'Isola. "Linear elastic trusses leading to continua with exotic mechanical interactions". In: *Journal of Physics: Conference Series* 319 (Sept. 2011), pp. 109–124.
- [38] P. Shi G. and Tong. "The derivation of equivalent constitutive equations of honeycomb structures by a two scale method". In: *Computational Mechanics* 15.5 (1995), pp. 395–407.
- [39] L.J. Sluys, R. De Borst, and H.-B. Mühlhaus. "Wave propagation, localization and dispersion in a gradient-dependent medium". In: *International Journal of Solids and Structures* 30.9 (1993), pp. 1153–1171.
- [40] K.A. Snyder, E.J. Garboczi, and A. R. Day. "The elastic moduli of simple two-dimensional isotropic composites: Computer simulation and effective medium theory". In: *Journal of applied physics* 72.12 (1992), pp. 5948–5955.
- [41] A. Spadoni and M. Ruzzene. "Elasto-static micropolar behavior of a chiral auxetic lattice". In: *Journal of the Mechanics and Physics of Solids* 60.1 (2012), pp. 156–171. ISSN: 0022-5096.
- [42] A.S.J. Suiker, A.V. Metrikine, and R. De Borst. "Comparison of wave propagation characteristics of the Cosserat continuum model and corresponding discrete lattice models". In: *International Journal of Solids and Structures* 38.9 (2001), pp. 1563–1583.
- [43] W. E. Warren and E. Byskov. "Three-fold symmetry restrictions on two-dimensional micropolar materials". In: *European Journal of Mechanics-A/Solids* 21.5 (2002), pp. 779–792.
- [44] A. Waseem, A.J. Beveridge, M.A. Wheel, and D.H. Nash. "The influence of void size on the micropolar constitutive properties of model heterogeneous materials". In: *European Journal of Mechanics - A/Solids* 40 (2013), pp. 148–157. ISSN: 0997-7538.
- [45] M.A. Wheel, J.C. Frame, and P.E. Riches. "Is smaller always stiffer? On size effects in supposedly generalised continua". In: *International Journal of Solids and Structures* 67-68 (2015), pp. 84–92. ISSN: 0020-7683.

A second-gradient elastic material has been identified as the equivalent homogeneous material of an hexagonal lattice made up of three different orders of linear elastic bars (hinged at each junction). In particular, the material equivalent to the lattice exhibits: (i.) non-locality, (ii.) non-centrosymmetry, and (iii.) anisotropy (even if the hexagonal geometry leads to isotropy at first-order). A Cauchy elastic equivalent solid is only recovered in the limit of vanishing length of the lattice's bars. The identification of the second-gradient elastic material is complemented by analyses of positive definiteness and symmetry of the constitutive operators. Solutions of specific mechanical problems in which the lattice response is compared to the corresponding response of an equivalent boundary value problem for the homogeneous second-gradient elastic material are presented. These comparisons show the efficacy of the proposed identification procedure.